STUDY OF PHOTOINDUCED FERROMAGNETISM IN DILUTED MAGNETIC SEMICONDUCTOR (Ga,Mn)As

By

Chernet Amente Geffe

A **Dissertation** Submitted to
the **Department of Physics** Addis Ababa University

In Partial Fulfillment of the Requirements for the
Degree of Doctor of Philosophy in Physics

June 2010
Addis Ababa, Ethiopia

Addis Ababa University
Department of Physics

STUDY OF PHOTOINDUCED FERROMAGNETISM IN DILUTED MAGNETIC SEMICONDUCTOR (Ga,Mn)As

By
Chernet Amente Geffe

Approved by the Examination Committee

Chairman: _____
Dr. Mulugeta Bekele

External Examiner: _____
Prof. A. K. Rai

Internal Examiner: _____
Prof. Malnev V.

Advisor: _____
Prof. P. Singh

Acknowledgments

First of all I would like to thank God for his special guidance. I would like to express my deepest gratitude to my advisor **Prof. P. Singh** who have been guiding, assisting, supervising me and making critical reading of this dissertation. I appreciate him for his friendly approach, limitless and invaluable encouragement without any reservation during the whole period of the research work.

I am very much pleased to thank my wife **Dinkitu Wako** for her decision to take the responsibility of managing the family when I was supposed to join this program. The patience of my children: **Latera**, **Hika**, **Fedhi** and **Kena Chernet** during which I was away for more than seven years can not also be undermined.

I would also like to thank all staff members of the department of physics Addis Ababa University who have encouraged and assisted me morally and materially; especially those were **heads of the department during the time interval: Dr. Mulugeta Bekele, Dr. Tilahun Tesfaye, Dr. Gizaw Mengistu and Dr. Tesgera Bedhasa and also the secretary, W/ro Tsilat Adinew.**

My especial thanks goes to **Dr. Sintayehu Tesfa**, and **Dr. Lemi Demeyu** for their technical and material assistance.

Last but not least, it gives me great pleasure to thank **Oromiya Education bureau** and **Nekemte College of Teachers Education** for their support in sponsoring and offering me this opportunity.

Dedication

This Work is dedicated to :

My Father: **Dhugaasaa Fufaa Jalduu** (who is unlucky)

and

My mother: **Warqituu Guddataa Jafee** (lucky to see these good days)

Table of Contents

Acknowledgements i

Dedication ii

Table of Contents iii

List of Tables vi

List of Figures vii

Abstract ix

General Introduction 1

1. Review Literature 4
1.1 Introduction 4
1.2 Types of DMSs 6
1.2.1 The II-VI DMSs 7
1.2.2 The III-V DMSs 8
1.2.3 The group IV based DMSs 9
1.2.4 Other Types of DMSs 10
1.3 Origin of Ferromagnetism 10
1.4 The $(Ga_{1-x}, Mn_x)As$ DMS 13
1.4.1 Compositional Dependence of Lattice Constant of (Ga,Mn)As . 15
1.4.2 Exchange Energy and Carrier Concentration in (Ga,Mn)As . . . 16
1.4.3 Magnetization and Transition Temperature of the (Ga,Mn)As DMS 17
1.4.4 Factors Affecting Ferromagnetic Transition Temperature and Magnetization of the $(Ga, Mn)As$ 19
1.5 Photoinduced Ferromagnetism in DMSs 21
1.5.1 Effect of Photo-excitation on (II,Mn)VI Diluted Magnetic Semiconductors 21

1.5.2 Effect of Photo-excitation on (III,Mn)V Diluted Magnetic Semiconductors . . . 22

2. Mathematical Technique . . . 26
2.1 Introduction . . . 26
2.2 The double-time temperature dependent Green function . . . 27
2.3 The equation of motion of the Green Function . . . 30

3. Carrier Mediated Exchange Energy in (Ga,Mn)As DMS . . . 34
3.1 Introduction . . . 34
3.2 The exchange coupling constant . . . 35
3.2.1 The Ferromagnetic Transition Temperature of the $(Ga, Mn)As$ DMS . . . 42
3.3 Result and Discussion . . . 42

4. Exchange Coupling and Photoinduced Magnetic Ordering in $(Ga, Mn)As$ *DMS* 46
4.1 Introduction . . . 46
4.2 Formulation of the Problem . . . 46
4.3 Exchange Coupling energy of the Mn^{2+} spins in $(Ga, Mn)As$ DMS . . . 47
4.4 Result and Discussion . . . 51

5. Photo-excitation and Scattering Effects on Ferromagnetism of the $(Ga, Mn)As$ *DMS* . . . 54
5.1 Introduction . . . 54
5.2 Formulation of the Problem . . . 54
5.3 Magnon Dispersion and the Green Function Formalism . . . 56
5.4 Correlation Function and the Number of Magnons . . . 66
5.5 Magnetization and Ferromagnetic Transition Temperature of the $(Ga, Mn)As$ DMS . . . 68
5.6 Effect of photo-excitation and spin wave-scattering on magnon specific heat capacity of the $(Ga, Mn)As$ DMS . . . 70
5.7 Result and Discussion . . . 72

6. Summary and Conclusion . . . 80

Appendix 91

A. Appendix . . . 92
A.1 Evaluation of Cauchy Principal value . . . 92
A.2 Integrating on fermi surface . . . 94
A.3 The Curie Temperature, T_c . . . 95

B. Appendix . . . 100
B.1 Interaction of radiation with magnons . . . 100

C. Appendix 102
C.1 Magnon Dispersion 102
C.2 Calculating total number of magnons 103
C.3 Calculation of Magnon Energy 105

List of Tables

1.1 The most commonly used magnetic elements for doping purpose in DMSs. 6

5.1 Rough estimate of T_C with and without inclusion of the contribution of spin wave scattering and magnon-photon coupling constant α^2, for $x = 0.053$. 75

List of Figures

1.1 Different types of semiconductors: (a) nonmagnetic semiconductor, which contains no magnetic ions; (b) diluted magnetic semiconductor (DMS), i.e., a cross between a nonmagnetic semiconductor and a magnetic transition-metal (TM) element, in a paramagnetic state; (c) DMS with ferromagnetic order mediated by charge carriers (holes) 11

1.2 Direct exchange, in which the magnetic ions interact because their charge distributions overlap. 12

1.3 Super exchange, interaction in which magnetic ions with non-overlapping charge distributions interact because both have overlap with the same non-magnetic ion. 12

1.4 Indirect exchange, in which in the absence of overlap a magnetic interaction is mediated by interactions with the conduction electrons. . . . 13

1.5 Specific heat due to spin wave. 18

1.6 (a) Structure of the sample. An arrow also shows direction of light irradiation. (b) Band edge profile of (In,Mn)As/GaSb heterostructure. E_C, E_V, and E_F denote band edge of conduction band, valence band, and Fermi level, respectively [14]. 23

3.1 The oscillatory term, $F(2k_F R_{nm})$ and its second derivative, of the exchange energy Vs. the term containing spin separation, $2k_F R_{nm}$ is plotted. 43

3.2 The exchange energy, J_{nm}, and the term contributing to oscillatory $F(2k_F R_{nm})$ Vs. the term containing mean local spin separation, $2k_F R_{nm}$, is plotted. 44

4.1 Exchange coupling energy J_{nm} vs. frequency of the radiation field ω_q, for different half line width, ε. 52

4.2 Exchange coupling energy, J_{nm}, vs. frequency of radiation field, ω_q for $\varepsilon = 0.1\omega_{\sigma\sigma'}$. 53

5.1 Reduced magnetization vs temperature at impurity concentration $x = 0.053$, 0.06, 0.07 and 0.08 for magnon-photon coupling constant $\alpha^2 = 0$ (left panel) and $\alpha^2 = 10^{-16}$ (right panel) in the absence of scattering. . . 72
5.2 Reduced magnetization vs temperature at impurity concentration $x = 0.053$, 0.06, 0.07 and 0.08 for magnon-photon coupling constant $\alpha^2 = 0$ (left panel) and $\alpha^2 = 10^{-16}$ (right panel) in which spin wave scattering is considered. 73
5.3 Reduced magnetization vs. temperature for $x = 0.053$ without (left panel) and with (right panel) inclusion of spin wave scattering. 74
5.4 Reduced magnetization vs. temperature when $x = 0.053$ (left panel) and $x = 0.08$ (right panel) in the absence and presence of spin wave scattering. Graphs labeled by (a) are plotted for $\alpha^2 = 10^{-16}$, and (b) for $\alpha^2 = 0$. 74
5.5 Ferromagnetic transition temperature T_C vs. impurity concentration x, is plotted in the absence (left panel) and presence (right panel) of spin wave scattering. 75
5.6 Ferromagnetic transition temperature T_C vs. impurity concentration x 76
5.7 Magnon heat capacity vs. temperature for $x = 0.053$ without (left panel) and with (right panel) inclusion of spin wave scattering factor. 77
5.8 Magnon heat capacity vs. temperature for $x = 0.053$ (left panel) and $x = 0.08$ (right panel). 77
5.9 Magnon heat capacity vs. temperature for $\alpha^2 = 0$ (left panel) and $\alpha^2 = 10^{-16}$ (right panel) without inclusion of spin wave scattering factor. . . 78
5.10 Magnon heat capacity vs. temperature for $\alpha^2 = 0$ (left panel) and $\alpha^2 = 10^{-16}$ (right panel) with inclusion of spin wave scattering factor. 78

Abstract

Effects of photo-excitation and spin wave scattering on magnetism of the diluted magnetic semiconductor (DMS) (Ga,Mn)As is theoretically studied. The exchange coupling energy between Mn^{+2} spins local moments is computed starting with the zeeman energy. Its equivalence with the Rudermann-Kittel-Kasuya-Yosida (RKKY) exchange energy which is known to have an oscillatory characteristics and contributing to an indirect exchange, expressed based on the Zener model is described. This energy is shown to rise to maximum near/at resonance. Green function formalism is used to find expression for ferromagnetic transition temperature T_C, magnetization and magnetic specific heat C_{mag} starting with a model Hamiltonian consisting of magnons, photons and an interaction of magnons with photons. T_C is indicated for zero impurity concentration, $x = 0$. Unusual upturn in magnetization and negative magnon specific heat are observed at very low temperature values for larger magnon-photon coupling constant α, in which an increase in this coupling is found to decrease C_{mag}, and enhance the magnetization and the ferromagnetic ordering. There is no observed effect of spin wave scattering on C_{mag} at lower temperatures which, however, is found to rise faster exceeding scattering absence as temperature increases. Exchange coupling energy J_{nm}, magnetization $M(T)/M(0)$, ferromagnetic transition temperature T_C and magnon specific heat capacity C_{mag} are plotted and compared with available experimental observations.

General Introduction

Recently, there has been increasing interest of studying diluted magnetic semiconductors (DMS) both experimentally and theoretically [1, 2, 3]. It is not only the possibility of potential technological applications of the materials but also a very rich physics, which follows from the unique combination of magnetic and semiconductor properties coexisting in diluted magnetic semiconductors that motivated this interest [4, 5].

The importance of magnetism has been known since compass needles used by ancient peoples [6]. It is routinely used in devices such as motors, loud speakers, computer memory magnetic tapes, sound and video recording equipments, and computer disks. Magnetism and electricity exist together and can not be separated. For instance, while spinning on its own axis each electron revolve around nucleus in an atom contributing a circulating electric current like the current flowing through a coil producing a small magnetic field [7]. In atoms of most materials the electrons orbits are more or less random resulting in cancelation of the magnetic fields generated by individual electrons. Moreover, being paired the magnetic effects of spins also cancel each other. Furthermore, the thermal agitation in materials does not permit any possible alignment of magnetic moments and the vector moment of each magnetic ion would average to zero. In some solids, however, individual magnetic ions have non-vanishing average vector moments below a critical temperature T_C and known magnetically ordered where in the simplest ferromagnets all the local moments have the same magnitude and average direction. The incomplete $3d$ sub shell transition elements could also give a new feature on being doped into semiconductors resulting in novel spintronic devices [1].

Semiconductors are group of materials having conductivities between those of

metals and insulators [8]. GaAs is the most studied and useful semiconductor, especially, in producing optical devices due to its good optical properties and its application in which, for example, high speed is required [9]. Doping magnetic impurity, such as Mn, into this compound gives rise to diluted magnetic semiconductor (DMS) with both magnetic and semiconducting properties under certain critical temperature.

Today's semiconductors work by exploiting the electric charge attached to electrons. But electrons in solids have another fundamental property known as "spin," which makes them act like small magnets. Computer hard discs, which consist of layers of metals such as cobalt and copper, already tap this magnetic property to produce memory storage [6]. Scientists have long sought to merge this capability with the signal processing capability of microprocessors, a technology called magneto resistive random access memory, or M-RAM. This has been successfully shown by Laureates of the 2007 Nobel prize in physics, Albert Fert and Peter Grünberg, by their independent discovery [10, 11] of such system for use as magnetoresistance sensors.

Semiconductor-based magnetic memories would enable computers to be like a TV set where it has not to reload the operating systems. Achieving spintronic devices of such kind is a step towards a new breed of computer chips that will couple memory with information processing and photonic capabilities [5]. Such chips will retain data even when the computer is turned off, eliminating the time-consuming process of "booting up" information from hard drive to processor [12, 13]. In the long term, advances in spintronics may usher in vastly more powerful "quantum" computing. Besides eliminating long boot-up time, M-RAM chips are likely to require far less power because controlling the current flow by altering electronic spin may require only small voltages. It could significantly extend battery life in hand-held electronic devices such as mobile phones also. In addition, spin-based lasers and other light-emitters could transmit data that is encoded or labeled by the polarization of the light. Knowing how to capture and manipulate the spin of individual electrons will create quantum computers thousands of times faster than those of today's [10, 11].

Our objective is to study effect of photo-excitation on ferromagnetism of the diluted magnetic semiconductor $(Ga_{1-x}Mn_x)As$. It is known that when light is irradiated to such materials additional holes are excited [14, 15] and mediate ferromagnetism where the interaction is attributed to be RKKY type, as explained by the Dietl

model [2]. This is one of the mechanisms suggested that could enhance ferromagnetism of localized Mn spin doped into semiconductor $GaAs$ [16].

In the first chapter progress in the study of ferromagnetism of diluted magnetic semiconductors is reviewed. The second chapter introduces the mathematical technique of Green functions applicable to quantum field theory. The third chapter discusses the oscillatory character of the exchange energy making use of the Zener model [17, 18] and comparing it with the Dietl model [2]. In the forth chapter exchange coupling and magnetic ordering in photoinduced $(Ga, Mn)As$ DMS is studied, where the enhancement of exchange coupling due to excitation is described. Starting with a model Hamiltonian consisting of free photon, free magnons and magnon-photon interaction, the magnetization, the ferromagnetic transition temperature and magnon specific heat of the $(Ga_{1-x}Mn_x)As$ DMS are also studied in chapter five. In chapter six summary and conclusions are given.

1

Review Literature

1.1 Introduction

A newly emerging interest in the field of manipulating charge and spin of electrons in spintronics has been enhancing the study of magnetic impurity and semiconductor alloys. Such systems are classified into magnetic semiconductors (intrinsically) and diluted magnetic semiconductors (doped).

Magnetic semiconductors are materials possessing magnetic and semiconducting properties intrinsically. Typical examples are rare-earth chalcogenides in which Europium chalcogenides are widely studied [19, 20, 21] and Cr-spinels which are families of important AB_2X_4 oxide minerals, where A and B are metal ions and X=O, S, Se, Te. Chromium spinel oxides, ACr_2O_4, offer the opportunity to study magnetic frustration in the absence of charge and orbital effects. On the other hand, researches on europium chalcogenides EuX, with $X = O,\ \ S,\ \ Se,\ \ Te$, have been the subject of many studies for several years. The identification of EuO by Matthias et al. in 1961 [19], which was reported as truly ferromagnetic at $77K$ with saturation moment of close to 7 Bohr magnetons ($7\mu_0$), is the first rare earth oxide to be found to become ferromagnetic with true ferromagnetic coupling. This is the first motivation for further investigations of europium chalcogenides as magneto-optic memories in computers, and magneto-optic modulators [20].

However, the study on such magnetic semiconductor systems is ceased due to the complexity during the crystal growth while controlling magnetic spins and charges separately making the production of mono-crystalline europium chalcogenides on

the industrial scale very expensive also. At present, it is commonly accepted that there is no chance for any industrial application of these compounds, and the current interest in the use of magnetic semiconductors as light beam addressable memory system is focussed on mixed valence systems [20] known as diluted magnetic semiconductors.

In diluted magnetic semiconductors the cations of semiconductor materials are partially substituted with a transition-metal impurity, such as iron (Fe), chromium (Cr), cobalt (Co) and manganese (Mn) or with rare-earths [22, 23]. These magnetic impurities can be incorporated in the lattice up to large alloy fraction preserving the crystalline and band structure of the host semiconductor [24]. The most commonly used magnetic element for doping purpose is Manganese, Mn [3, 23] for its maximum number of $3d$ unpaired sub shell electrons. As a consequence of the exchange interaction between these unpaired d-shell electrons of the Mn^{2+} ions and the s-and p-like electrons in the conduction and valence band of the host lattice, the magneto-optical properties of the material will be affected.

These alloys are required for spintronics application and also sometimes referred to as doped magnetic semiconductors, for which the abbreviation DMS is used. These issues have recently attracted a great deal of attention [1, 25] for their potential in combining ferromagnetic and semiconductor properties. Integrated circuits for data processing use the charge of electrons in semiconductors, while data storage media such as hard disks use the spin of electrons in a magnetic material. It is of great technological importance to find DMS systems with Curie temperature T_c above room temperature having robust ferromagnetic order combining these information processing and storage functionalities in a single crystal material. Therefore, these material alloys are known to combine the two large branches in condensed matter physics; semiconductor and magnetism [3, 26, 27, 28].

Moreover, ferromagnetism in DMS occurs because of exchange interaction between magnetic ion local moments and itinerant hole or electron spins [29]. It has been established that the behavior of substitutional Mn element is particularly simple in many host semiconductors, because of a strong tendency toward well defined

$3d^5$, (half-field), S=5/2 and zero angular momentum (L=0), Mn^{2+} local moments following Hunds rule [30]. Therefore, we can say that DMSs are alloy systems with inherent positional disorder of Mn atoms [31].

The most commonly studied diluted magnetic semiconductors consist of Mn doped $II-VI$, $III-V$, ..., compound and IV elemental [29] non-magnetic semiconductors. Mn is intentionally doped so that systems more desirable than Eu- and Mn-chalcogenides and Cr-spinels, which exhibit ferromagnetic interaction and yet have antiparallel spins [32] having different crystal structure from common semiconductors, such as Si and GaAs [33], is produced. Hence, the basic model for DMS is of a magnetically inert (without magnetic property) host semiconductor doped with localized spins which may then be doped with carriers-electrons or holes. This is either through addition of another element, or, as is the case for Mn in III-V materials in which the magnetic ion can it self be an acceptor [34].

In this chapter a literature review of types of DMSs, magnetization and transition temperature of the $(Ga,Mn)As$, and photoinduced ferromagnetism in $(Ga,Mn)As$ and other DMSs is done.

1.2 Types of DMSs

In this section classes of diluted magnetic semiconductors known as transition metal doped compound and elemental semiconductors, and DMSs without transition metal impurity are discussed. The magnetic transition elements for doping purpose have been used to date are mainly; Mn, Cr,and Fe.

Tab. 1.1: The most commonly used magnetic elements for doping purpose in DMSs.

Element configuration	Cr^{24} $3d^5$ $4s^1$	Mn^{25} $3d^5$ $4s^2$	Fe^{26} $3d^6$ $4s^2$
Element configuration	Cr^{2+} $3d^4$	Mn^{2+} $3d^5$	Fe^{2+} $3d^6$
Element configuration			Fe^{3+} $3d^5$

Table 1.1 shows configuration why Mn^{2+} is more appropriate for doping. In Mn^{2+}

doped III-V DMSs, there is a valence mismatch between that of ($S = \frac{5}{2}$) Mn and the group-III element. In Cr^{2+} doped III-V the $3d$ electrons are less in number (4 per atom) and $S = 4 \times \frac{1}{2} = 2$ where less magnetic impurity spins per atom results in weak ordering in the compound compared to Mn. In Fe^{2+} the 3d electrons give rise to $S = 4 \times \frac{1}{2} = 2$ also and Fe^{3+} gives valence match with group III element just as Mn^{2+} does in II-VI DMSs, where holes can not be created resulting in antiferromganetic nearest neighbor interaction of the impurity spins. Therefore, Mn^{2+} with shorter nearest neighbor distance of $2.24A^0$ [8] is relatively more preferable for doping purpose in which high concentration of the 3d electrons is required and holes to mediate the RKKY type indirect exchange interaction is created in the valence band as in Dietl model [2]. On the other hand, the acceptor levels of Fe and Co are unlikely to lead to high valence band hole concentrations in arsenides and antimonides [35].

1.2.1 The II-VI DMSs

In 1980s, research in DMS focused mainly on II-VI semiconductors such as (Cd,Mn)Te and (Zn,Mn)Se [23, 36]. This class of DMSs is obtained by doping Mn^{2+} in to, non-magnetic semiconductors, ZnSe, ZnS, CdTe, CdSe, HgSe, ..., etc. Therefore the compounds are expressed as $(II_{1-x}Mn_x)VI$ which becomes $(Zn_{1-x}Mn_x)Se$, $(Cd_{1-x}Mn_x)Te$ [23, 37] and so on, where x is fraction of magnetic transition metal atoms typically Mn that substitutes the II element ion at cation site [24]. This makes possible the compound to achieve a high density of magnetic atoms where the provided local moments alter the host semiconductor valence and conduction bands very weakly. Because, the valence of Mn is the same as that of group II cation and not introduce any carrier unless another dopant with a different valence such as Nitrogen N, a p-type, is introduced. This otherwise, makes it difficult to dope to p- or n- type, hence, the magnetic interactions are dominated by antiferromagnetic direct exchange between the Mn atoms, resulting in paramagnetic, spin-glass, and ultimately long range antiferromagnetic behavior. However, recent progress in doping technology of II-VI materials shows carrier-mediated ferromagnetism is discovered in p-type II-VI DMS heterostructures, though at present this only occurs at very low temperatures; typically below $2.0K$ [33, 39].

On the other hand, Mn doped III-V DMSs appeared attractive to material scientists alternatively. It is due to the fact that, the density of holes required for mediation of the ferromagnetism of local moments is so small in Mn doped II-VI DMSs, hence, difficult to control conduction by doping and so attributed to be one of the major obstacles for the use as electronic materials in general.

1.2.2 The III-V DMSs

The mechanism used is doping Mn into III-V semiconductors (as host material); and are the most intensively studied [22, 31, 38, 40, 41]. These materials are expressed in the form of $III_{1-x}Mn_xV$, examples of which are $Ga_{1-x}Mn_xAs$, $In_{1-x}Mn_xAs$, $Ga_{1-x}Mn_xP$, $Ga_{1-x}Mn_xN$, and $Ga_{1-x}Mn_xSb$ where the carriers are typically holes [38, 40]. These DMS materials exhibit ferromagnetism and provide new degrees of freedom based on the magnetic cooperative phenomena in the semiconductor heterostructures used in transistors and lasers.

The III-V DMS materials differ from the II-VI DMS materials in that, in Mn^{2+} (valence-II Mn) doped III-V compound semiconductors, Mn has a different valence to group III elements (like Ga) and introduces a spin $S = 5/2$ moment, leading to both local moment formation (playing role of magnetic ions) and acts as an acceptor introducing valence band holes due to valence mismatch [31] (Mn^{2+} replacing Ga^{3+}) in semiconductor host [43]. These holes mediate interactions between the Mn moments correlating their orientations and making ferromagnetism possible [29, 34, 38, 42]. While this implies nominally equal concentrations of holes and local moment spins, experimentally it is found that the hole concentration is only $p = 10 - 30\%$ of Mn concentration. The compensation process(es) responsible for the removal of such a large fraction $(70 - 90\%)$ of the holes from the carrier band are not fully understood, but it is believed that an important role is played by antisites (like As antisite defects in the case of the $(Ga, Mn)As$ DMS) [43]. Such defects are created when group-V (like As) substitutes for group-III Ga, and removes two holes introduced by Mn impurities, thus effectively decreasing the hole concentration. Compensation is responsible not only for the substitutional decrease of the hole concentration,

but also leads to the appearance of charged compensation centers (As^{2+} for As antisites). The Coulomb potential created by these charged compensation centers may also play a role in the physics [44].

In these Mn doped $III-V$-based magnetic alloy semiconductors, there is a strong hybridization between the d orbital of incorporated Mn and the p orbital of host $III-V$ semiconductors resulting in the long range parallel alignment of Mn spins (ferromagnetism) accompanied by spin-polarized energy bands. This cooperative behavior opens way to control both magnetic and semiconductor properties by changing the carrier characteristics such as concentration and spin degrees of freedom [14, 16, 28].

The pioneering discovery of ferromagnetic properties in p-type (In,Mn)As [45] led to series of research works on Mn doped III-V DMS, specially, $Ga_{1-x}Mn_xAs$ and $Ga_{1-x}Mn_xN$. This is found to be suitable particularly for studying carrier-spin interaction due to the fact that carrier type and concentration can be controlled either by doping impurities and/or by changing the growth conditions.

Since the magnetic impurity equilibrium solubility of Mn in III-V semiconductors is low [3] under ordinary crystal growth conditions there is difficulty of introducing high density of magnetic atoms and is found to be the main barrier for fabrication. However, in order to have ferromagnetism in such DMS a sizeable amount of magnetic ions are needed and can only be done by means of non-equilibrium crystal growth technique-the low temperature molecular beam epitaxy (LT-MBE [28, 34]), with deposition temperature about 250^0c, for example, to prevent segregation of Mn and GaAs in $Ga_{1-x}Mn_xAs$ [3, 34]. Hence, the III-V DMS is believed to give an enhanced T_C ferromagnetism for spintronic application than impurity doped group IV (Ge) once and others.

1.2.3 The group IV based DMSs

The group-IV semiconductors, especially Ge [29], as host material based DMSs have also attracted research interest for practical applications. More recently, several groups reported the ferromagnetism of the $Ge_{1-x}Mn_x$ thin films grown by molecular beam epitaxy (MBE) and Cr, Fe-doped bulk Ge single crystal [46]. Dietl et al. [47, 48, 49] have

predicted that $Ge_{1-x}Mn_x$ have a lower Curie temperature at $x = 0.05$ than $(Ga, Mn)As$.

1.2.4 Other Types of DMSs

Other than those mentioned above, there are also ternary, such as, $Pb_{1-x-y}Mn_xSn_yTe$ DMSs [50] believed to be the pioneer experimental work of the topic. On the other hand, a new ferromagnetic material which does not contain transition metal elements have been theoretically designed recently. $CaAs$ is one of such materials with a distorted Zinc-blende structure [51]. Moreover, a new class of high T_c diluted magnetic semiconductor based on Si- or Ge doped K_2S without transition metal elements has been reported [52]. However, the mechanism of magnetic ordering in such systems is still not well known.

1.3 Origin of Ferromagnetism

Ferromagnetism in $(Ga, Mn)As$ and some other $(III, Mn)V$ ferromagnets originates from Mn local moments though Mn-doped phosphides and nitrides DMSs are less well understood.

Fig. 1.1 shows the mechanism of magnetic ordering in II-VI and III-V DMS where in II-VI DMS adding holes that mediate ferromagnetism is required. Moreover, different mechanisms of coupling localized spins in a solid have been identified [53]. These are Heisenberg's direct exchange, Kramer's super exchange, Zener's double exchange and Zener's kinetic exchange interactions [30].

- The origin of Heisenberg's [30, 54] direct exchange between two local spins is the difference between the Coulomb energy of a symmetric orbital wave function (antisymmetric singlet spin wave function) state and an antisymmetric orbital wave function (symmetric triplet spin wave function) state (see Fig 1.2).
- Kramers's [55] superexchange interaction applies to local moments that are separated by a non-magnetic atom (see Fig. 1.3). In a crystal environment, an electron can be transferred from the non-magnetic atom to an empty shell of the magnetic atom and interact, via direct exchange,

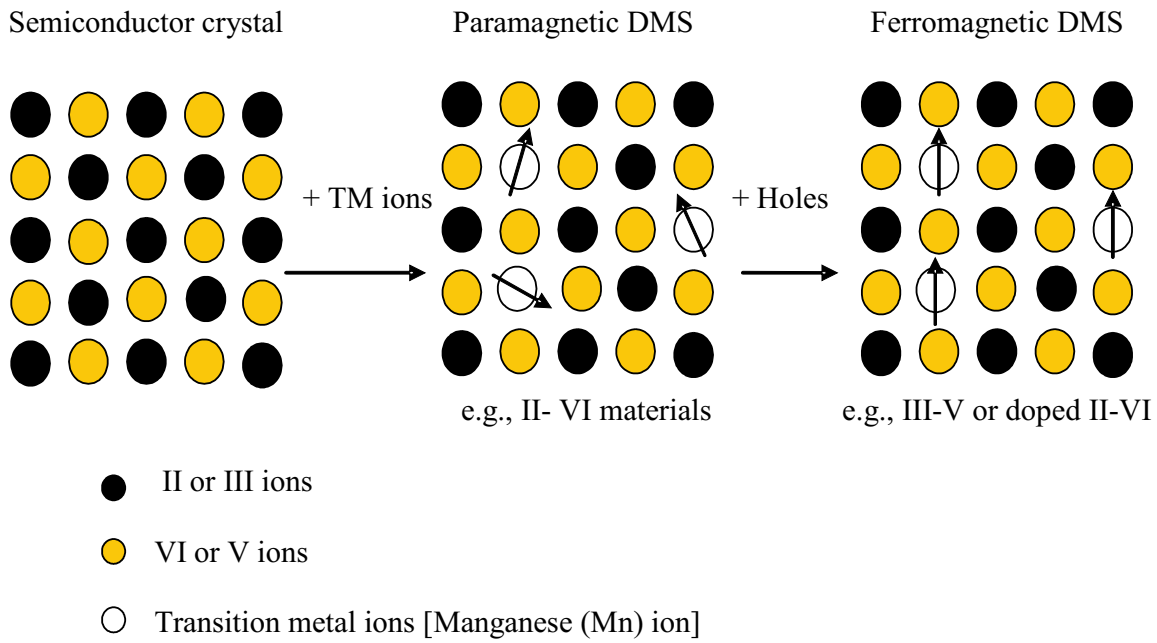

Fig. 1.1: Different types of semiconductors: (a) nonmagnetic semiconductor, which contains no magnetic ions; (b) diluted magnetic semiconductor (DMS), i.e., a cross between a nonmagnetic semiconductor and a magnetic transition-metal (TM) element, in a paramagnetic state; (c) DMS with ferromagnetic order mediated by charge carriers (holes)

with electrons forming its local moment. The non-magnetic atom is polarized and is coupled via direct exchange with all its magnetic neighbors. Whether the resulting superexchange interaction between local moments is ferromagnetic or antiferromagnetic depends on the relative sign of the two direct-exchange interactions [30]. In $(III, Mn)V$ materials, superexchange gives an antiferromagnetic contribution to the interaction between Mn moments located on neighboring cation sites.

- Zener's [17] double-exchange mechanism also assumes an intermediate nonmagnetic atom. In its usual form, this interaction occurs when the two isolated magnetic atoms have a different number of electrons in the magnetic shell and hoping through the intermediate nonmagnetic atom involves magnetic-shell electrons. Electrical conduction and Mn-Mn exchange coupling are both realized through hopping within an impurity

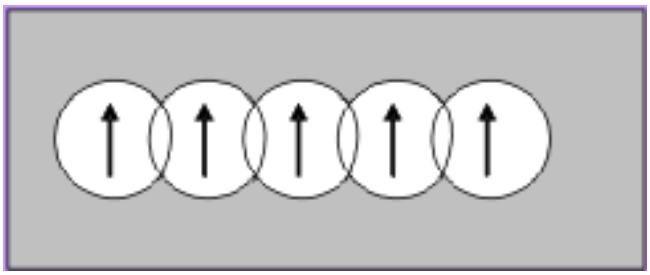

Fig. 1.2: Direct exchange, in which the magnetic ions interact because their charge distributions overlap.

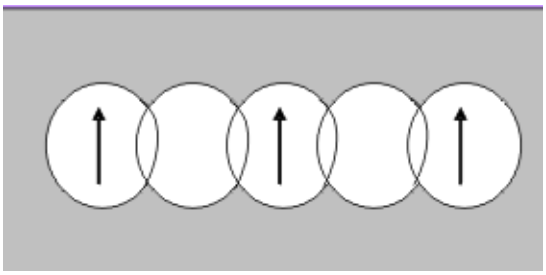

Fig. 1.3: Super exchange, interaction in which magnetic ions with non-overlapping charge distributions interact because both have overlap with the same non-magnetic ion.

band. The potential importance of double exchange is greater at lower Mn doping and in wider-gap $(III, Mn)V$ materials.

- Zener's [18] kinetic exchange or indirect-exchange interaction (see Fig. 1.4) arises in models with local, usually d-shell or f-shell, moments whose coupling is mediated by s- or p-band itinerant carriers. The local moments can have a ferromagnetic direct exchange interaction with band electrons on the same site and/or an antiferromagnetic interaction due to hybridization between the local moments and band electrons on neighboring sites. Polarization of band electrons due to the interaction at one site is propagated to neighboring sites. The range of this interaction can be long and interactions between separate local moments can be either ferromagnetic or antiferromagnetic and tends to vary in space on the length of the itinerant band's Fermi wavelength. Unlike the double-exchange case, magnetic order in this case does not lead to a significant change in the width of the conducting band. This type of mechanism certainly does play a role

in $(III, Mn)V$ ferromagnetism, likely dominating in the case of strongly metallic $(Ga, Mn)As$, $(In, Mn)As$, and Mn-doped antimonides. There is no sharp distinction between impurity-band double-exchange and kinetic-exchange interactions; the former is simply a strong-coupling, narrow-band limit of the latter.

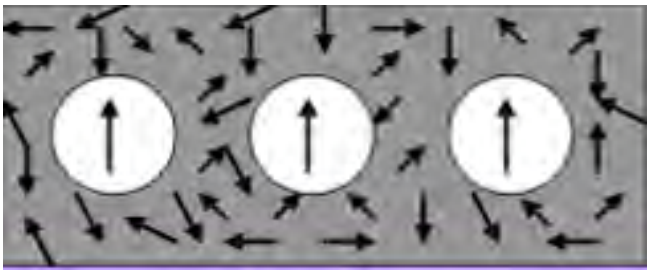

Fig. 1.4: Indirect exchange, in which in the absence of overlap a magnetic interaction is mediated by interactions with the conduction electrons.

1.4 The $(Ga_{1-x}, Mn_x)As$ DMS

The III-V compound semiconductors are used widely for high speed electronic as well as for optoelectronic devices as light emitting diodes, LEDs. If one wants an LED for which the wave-length doesn't matter, for remote control devices and so on, then $GaAs$ is a good material to use. This is due to the optical absorption involving excitation of electrons from a filled to an empty state. As GaAs is a semiconductor with direct band gap [8] light emission is very high during recombination.

GaAs crystal has zinc blende (ZnS) structure [9]. It is an example of the mixed ionic and covalent bonding [30]. The chemical bonding is interpreted as the superposition of these two extreme cases. In ionic bonding, an electron is transferred from Ga to As to give the ionic structure $Ga^{+}As^{-}$. In covalent bonding, with the displacement of an electron from As to Ga, the number of electrons in the outer shell of both Ga and As atoms becomes four resulting in sp^3 hybridization [30].

There is a well developed technology for the manufacture and processing of $GaAs$, and it is an efficient emitter. For many applications the fact that its out put is outside the visible range is advantageous. LEDs giving light of colors red through orange and

yellow to green can be made by using different composition of the three-element alloy, $GaAsP$.

Moreover, $GaAs$ is found important in preparing quantum dotes and manufacturing quantum wells and also found as an important substrate (like GaAs/GaAs(100)) for preparing diluted magnetic semiconductor materials as an epitaxial layer [22, 28, 40]. Hence, doping magnetic impurities to this compound gives a new and interesting phenomena in producing efficient spintronic devices. Therefore, $Ga_{1-x}Mn_xAs$ DMS would be the most studied III-V systems and has been established as the prototype displaying ferromagnetism mediated by delocalized carriers [56] in which the Mn ions substitutionally replace Ga at the cation sites [31, 38].

When Mn substitutes for the cation, it is nominally in the Mn^{3+} state with 4 electrons in its outer d-shell, which we denote as d^4. Up on bonding with the anion, the Mn may absorb an electron converting it to Mn^{2+} and producing a hole. Such holes are, therefore, believed to be created by the transfer of charge from the group-V element's p-orbital to Mn d-orbital. Similar to a non-magnetic impurity the hole will experience a Coulomb attraction to the Mn creating an acceptor level. Hence, the strength of the exchange between the holes and the local moments is proportional to the overlap of these orbitals. This mixing of local Mn and extended group-V element states is generally referred to as p-d hybridization[57].

In 1996, Ohno et al. [28] have reported the discovery of $(Ga, Mn)As$ DMS for the first time, in which the technique of molecular beam epitaxy (MBE) is used with the semi-insulating (001) GaAs as a substrate. They could observe ferromagnetic ordering, and anomalous Hall effect in this sample layer by magnetization and magneto-transport measurements, respectively. Boeck et al. 1996 [58] have also studied magnetism of the material using the same process where the matrix is GaMn and the precipitates are ferromagnetic MnAs. They described the feasibility of fabricating MnAs-rich magnetic layers that reveal room-temperature ferromagnetic behavior using a 2-step process (MBE + annealing). Although the equilibrium solubility of Mn atoms in GaAs is quite low, ($\sim 10^{19} cm^{-3}$), $Ga_{1-x}Mn_xAs$ film with x up to 0.078 were grown at $200 - 300^0_C$ under As rich condition. Furthermore, all samples grown for $x =$

$0.005 - 0.078$ show p-type conduction with the hole concentration of $3.8 \times 10^{17} cm^{-3} - 2.58 \times 10^{20} cm^{-3}$. However, no ferromagnetic behavior was observed at room temperature [59].

1.4.1 Compositional Dependence of Lattice Constant of (Ga,Mn)As

Using density-functional calculations Mašek et al. 2003 [60] have studied the compositional dependence of the lattice constant of (Ga,Mn)As containing various native defects, and suggested that the lattice constant of perfect mixed crystals does not depend much on the concentration of Mn. The lattice parameter increases if some Mn atoms occupy interstitial positions and the same happens if As antisite defects are present, where it is correlated with the degree of compensation: the materials with low compensation should have lattice constants close to the lattice constant of a GaAs crystal. They started with ideal mixed crystals $(Ga_{1-x}Mn_x)As$, where all Mn atoms are in the substitutional positions and calculated lattice constants for a series of materials with x=0.01, 0.02, 0.03, 0.04, 0.05, and 0.10. Their result shows that lattice constant might depend linearly on the concentration of the impurity for values up to x=0.10, and could be explained by the mathematical relation

$$a(x) = a_0 + 0.02x(A^0). \tag{1.4. 1}$$

This is in good agreement with the Vegard law that the lattice parameters of all known DMS ternary alloys obey very closely; applied to $(Ga_{1-x}Mn_x)As$ [41, 60]. This calculated lattice constant of GaAs crystal, $a_0 = 5.569A^0$, is smaller than the observed value $a_0^{exp} = 5.653A^0$.

Additionally, Van Esch et al. have given an explanation to the dependence of the lattice constant of $(Ga, Mn)As$ on the lattice constant of $MnAs$ and expressed as:

$$a_{GaMnAs} = (1 - x)a_{LT-GaAs} + xa_{MnAs} \tag{1.4. 2}$$

where $a_{LT-GaAs} = 5.6572A^0$ and $a_{MnAs} = 6.014A^0$ is the lattice parameter of the zinc-blende $MnAs$ [41]. From these one can understand that increase in lattice parameter with increase in Mn interstitials and As antisite defects would decrease magnetization of the system reducing density of local moments by taking Ga position.

1.4.2 Exchange Energy and Carrier Concentration in (Ga,Mn)As

The exchange between the Mn local moments and the carriers they produce plays a key role in the physics of $III - V$ DMS. In fact, it is this exchange that enables the carriers to mediate the ferromagnetism between the diluted moments.

In their experimental results of detailed magneto-transport study of ferromagnetic p-type (Ga,Mn)As layers Matsukura et al., 1998 [40] reported Curie temperature as high as $110K$ with the hole density $N_h = 10^{18} - 10^{20} cm^{-3}$. They have also measured and determined the p-d exchange between carrier spin and Mn spin $J_{pd} \simeq 150 eVA^{0^3}$ in which the origin of ferromagnetism is shown, quantitatively, to be the RKKY interaction via J_{pd}. This could be understood as the strong p-d hybridization between the Mn d levels and the valence-band p state of GaAs leads to strong kinetic exchange coupling between hole spins and Mn spins [38, 42].

Das Sarma et al. 2003 [38] have also determined the basic parameters such as the density of magnetically active dopants N_d, the hole density N_h and the local effective exchange coupling between the holes and the magnetic impurities which revealed that increasing N_h/N_d does lead to enhanced magnetization. They argued that the ferromagnetism in (Ga,Mn)As could be widely accepted due to anti-ferromagnetic exchange between itinerant (mobile) holes and d-electrons localized on the Mn sites. The itinerant nature of the holes, thus, leads to an effective ferromagnetic coupling between Mn spins, overwhelming the anti-ferromagnetic Mn-Mn supper exchange interaction.

It is also assumed that the Mn spins are strongly localized and their magnetic local exchange coupling is given by, J_{nm}, of the form,

$$J_{nm} = J_0 |\phi_m(R_n)|^2 = J_0 e^{\frac{-2|R_n - R_m|}{a_B}}, \tag{1.4. 3}$$

which is proportional to the charge density at the n^{th} Mn site due to the carrier in the hydrogenic orbital around the m^{th} Mn site [34]. In this expression $J_0 \propto J_{pd}^2$ and a_B is the Bohr radius ($a_B \sim \ell$), where ℓ is the mean free path. Accordingly, effective pair exchange interactions for (Ga,Mn)As alloys depend on the distance between the

Mn atoms. These alloys show ferromagnetic characteristics exhibiting half-metallic behavior with filled minority sub bands where the exchange interactions between the Mn atoms are ferromagnetic for distances larger than the average nearest Mn-Mn distance. The calculated exchange interactions exhibit oscillatory character and are exponentially damped in the presence of compensating defects where as, for the isolated Mn impurities in the semiconductor host with the same number of valence holes exhibit an undamped RKKY-type [42].

1.4.3 Magnetization and Transition Temperature of the (Ga,Mn)As DMS

It is now understandable that in $(III_{1-x}Mn_x)V$ and $Ge_{1-x}Mn_x$ DMS materials the carrier (p)-local moment(d) (kinetic or p-d) exchange coupling, eventually leads to a global ferromagnetic ordering of impurity local moment (i.e Mn) for $T < T_c$ over coming any direct antiferromagnetic (supper exchange) interaction between the local moment spins themselves [38]. Unlike II-VI DMSs the III-V DMSs show ferromagnetism with relatively high Curie temperature. The highest value obtained to date is for $(Ga, Mn)N$, which is about $940K$ with Mn composition $x = 0.03 - 0.05$ [34]. However, since for nitrides and phosphides the ionization energy of the acceptor levels is higher and the Mn impurity level is not deep in the valence band, contrary to that in arsenides, the d-charge fluctuations cannot be neglected. Moreover, magnetization measurements confirmed that the electronic configuration of Mn impurity in this compounds has not yet been conclusively established, and these claims have not yet been widely confirmed [35].

On the other hand, $(Ga_{1-x}Mn_x)As$ is found to be ferromagnetic with Curie temperature as high as $T_c = 10 - 110K$ for $x = 0.01 - 0.07$ where x corresponding to the highest T_c is 0.053 [38, 40]. A recent report on its improvement to $T_C \sim 173K$ [61] at $x \sim 8\%$ Mn impurity, however, indicates that there could be possibility of reaching room temperature value.

For their electronic calculations Kudrnovsky et al., 2004 [42] have utilized an expression,

$$K_B T_c^{MFA} = \frac{2}{3} x \sum_{i(i\neq 0)} \overline{J}_{0i}^{Mn,Mn} \qquad (1.4.\ 4)$$

to estimate Curie temperature of exchange interactions in (Ga,Mn)As, where the sum extends over all sites occupied by Mn atoms on the Ga sublattice for $(Ga_{1-x}Mn_x)As$ alloys. Similarly, Matsukura et al. [40] have estimated and compared to their experimental results an expression given by,

$$T_c = \frac{1}{3}xS(S+1)\sum_r Z_r J_{nm}(r), \tag{1.4. 5}$$

where Z_r is the number of r^{th} nearest neighbor sites and gave a generalization, $T_c \cong 2000xK$ up to $x = 0.053$ Mn concentration in the sample. They also argued and suggested that the origin of ferromagnetic ordering in (Ga,Mn)As, not at very low density of carriers [62], is Rudermann-Kittel-Kasuya-Yosida (RKKY) interaction [40] .

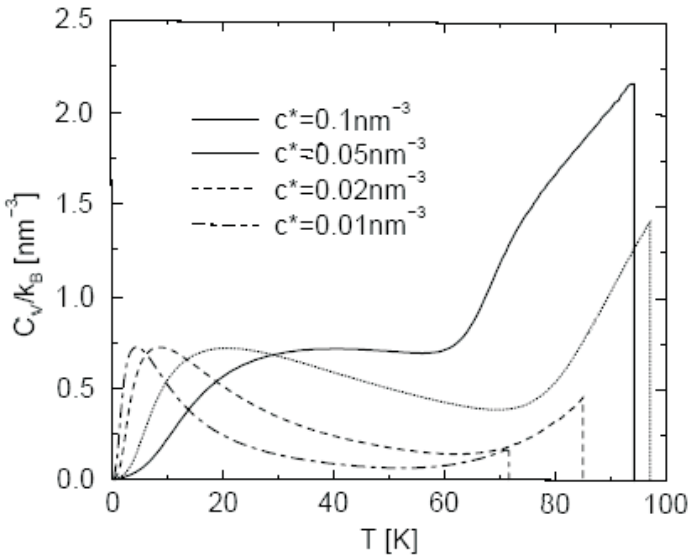

Fig. 1.5: Specific heat due to spin wave.

Moreover, J$\ddot{u}$rgen K$\ddot{o}$nig et al. [63] have calculated a specific heat of magnetic ions for a self consistent spin wave approach and found it proportional to $T^{3/2}$ at low temperature. Accordingly, the heat capacity is shown to have a jump at the transition temperature where the jump is 15% of the lattice specific heat when $T_c \rightsquigarrow 100K$. As one can see from Fig. 1.5, C_{mag} decreases with impurity concentration at lower temperature values. However, this could not describe the situation in high temperature ferromagnetism, and requires new mechanism of understanding.

1.4.4 Factors Affecting Ferromagnetic Transition Temperature and Magnetization of the $(Ga, Mn)As$

It is known that $(Ga, Mn)As$ is one of the III-V magnetic alloy semiconductors. The starting point for modeling the ferromagnetism of, specially, this compound is mean field theory in which the magnetization of both carriers and Mn ions are considered to be uniform in space. (Ga, Mn)As is a very promising material since it is compatible with the existing technology. Being placed at cation sites of the zinc-blende lattice, Mn ions generate free holes in the valence band due to valence difference of Mn^{2+} and Ga^{3+}. These free carriers couple antiferromagnetically to the local spins of Mn, through a strong p-d interaction, as mentioned earlier and gives rise to carrier-mediated ferromagnetic coupling between the Mn ions. However, some factors are known to reduce/favor magnetization and Curie temperature of the $(Ga, Mn)As$ DMS. These factors include anisotropy, As antisite defects, Mn interstitials, (Mn_I) and disorder [31, 44, 64, 65, 66, 67].

i. Magnetic anisotropy

Ferromagnetic p-type (Ga, Mn)As thin films are known to be prepared by molecular beam epitaxy on GaAs/GaAs(001) substrates. But, compressive strain caused by the lattice mismatch between a $(Ga, Mn)As$ epilayer and a GaAs substrate results in the in-plane magnetic anisotropy [16] which is demonstrated to be perpendicular magnetic anisotropy (PMA) in some special cases [68]. Therefore, anisotropic exchange interactions are one possibility which can lead to a reduction in the saturation magnetization at low temperatures. However, carrier mediated nature of the ferromagnetism suggests that anisotropy is may be important for transport; especially in the insulating phase where hopping between sites will be preferred when the Mn spins have similar orientations [69].

ii. Antisites

Studies revealed that [43], in low-temperature molecular beam epitaxy grown (Ga,Mn)As, hole concentration is usually much smaller than Mn concentration and there will be

a compensation. This is largely due to the excess of arsenic incorporated as As antisites, As_{Ga}, where As_{Ga} are the largest source of electron donors which compensate the number of holes available for mediating the ferromagnetic interaction between substitutional Mn impurities. For instance, for $(Ga_{1-x}Mn_x)As$ with $x = 0.053$ and $(N_{Mn} = 1.3 \times 10^{21} cm^{-3})$, T_c is found to be about $110^0 c$ [40]. In this case the hole concentration has been carefully measured to be $N_h(p) = 3.5 \times 10^{20} cm^{-3}$. Assuming that As_{Ga} is the only source of compensation, there has been obtained concentration of $4.2 \times 10^{20} cm^{-3}$ in such a sample. Moreover, there is a prediction for the existence of metastable As interstitial-Ga vacancy $(As_i - V_{Ga})$ pair in $(Ga, Mn)As$ [43] though the corresponding regeneration temperature is very similar to that of GaAs. Upon illumination As_{Ga} undergoes a structural transition to an As $(As_i - V_{Ga})$ pair, which is obtained by moving As_{Ga} along the $< 111 >$ direction. It is crucial to observe that the $(As_i - V_{Ga})$ pair is not electronically active in GaAs, since its only state in the band gap is completely filled. It has also been explained that there is no metastable $(Mn_i - V_{Ga})$ pair and the ferromagnetic order in $(Ga, Mn)As$ is unaffected by the presence of $(As_i - V_{Ga})$ pairs. Finally it is proposed that illumination of $(Ga, Mn)As$ should be able to enhance the hole concentration, and in turn strengthen the ferromagnetic coupling due to this optically induced transition of the As_{Ga} antisites to metastable $(As_i - V_{Ga})$ pairs. Such pairs are electronically inactive and reduce the hole compensation caused by the As_{Ga} antisites. The effect suggested here constitutes a valuable way to tune the hole concentration in $(Ga, Mn)As$ without changing either the Mn concentration or its microscopic distribution. However, the mechanism fails since the As_{Ga} regenerate for higher temperatures, and can not be used to obtain high $T_C's$ required for technological applications. Therefore, it is understandable that upon elimination of such defects without affecting the Mn concentration, part of the compensation will be removed and very large hole concentration can be reached.

iii. Spin-orbit coupling

It was proposed recently that spin-orbit coupling leads to frustration in the magnetic ordering [70]. It is one of the factors that reduce the spin polarization by mixing different spin states in the valence bands [64].

iV. Disorder

The word disorder is very general and includes for example, i) the dilution of magnetic atoms in a non-magnetic matrix, ii) substitution of a non-magnetic atom by another one which has a different radius or/and valency as in manganites $A_{1-x}B_xMnO_3$ where $A = La$, Pr and $B = Sr,\ Ca,\ Ba$ for example, iii) intrinsic defects which may appear during the growth of the material, for instance vacancies in "d^0" of compound ZrO_2, HfO_2 or TiO_2 [71]. It is thought to enhance the ferromagnetic transition temperature for metallic densities not too far from the metal-insulator transition leading to large effects on the hole carriers which form impurity bands as well as hybridizing with the valence band [31, 44, 64].

1.5 Photoinduced Ferromagnetism in DMSs

Optical control of magnetic properties has emerged and attracted considerable attention recently [3, 14, 15, 53, 72, 73]. A new impetus to this field has been given by discoveries of materials in which photoinduced magnetic phenomena coexisted with cooperative magnetic behavior and/or magnetic order in which irradiation of DMSs, such as $(II, Mn)VI$ and $(III, Mn)V$, promised room temperature application of spintronic devices.

1.5.1 Effect of Photo-excitation on (II,Mn)VI Diluted Magnetic Semiconductors

It has been understood that Mn has the same valence as the element at the cation site in $II - VI$ DMSs. This requires means of introducing carriers/holes that mediate ferromagnetism of the localized spins, where photo-excitation has shown the prospect.

Ferna'ndez-Rossier et al. [72] have predicted ferromagnetism in undoped (II,Mn)VI DMSs illuminated by intense sub-band gap laser radiation following the pioneer work of Koshihara et al. [14]. Accordingly, the coherence between conduction and valence

bands induced by light leads to an optical exchange interaction that could be explained as a result of the formation of a meta-stable state, stabilized by a lattice distortion, in which exchange interaction is locally enhanced. In line with this, the exchange interaction between two electron spins in separate dots for a typical semiconductor quantum dot (QD) systems have also been studied by Piermarocchi et al. [74]. The mechanism is by virtual excitation of delocalized exciton states in the host material, which interact with the electrons in both dots. This is a time-dependent effective interaction which is driven by the external laser field and is, thus, controllable. Hence, an indirect exchange analogous to RKKY interaction between two magnetic impurities mediated by conduction electrons or exciton, is produced by the external light. Photo-excitation is, thus, broadly studied for the case of $(III, Mn)V$ DMSs, especially (Ga,Mn)As which is central to this research work.

1.5.2 Effect of Photo-excitation on (III,Mn)V Diluted Magnetic Semiconductors

Due to the appearance of ferromagnetism in p-type layers in III-V based magnetic alloy semiconductors the mechanism of manipulating coupled spins by the external stimulations, such as light and an electric field, is found interesting [3, 14, 15, 53, 73]. In contrast to the paramagnetic II-VI DMSs, they have ferromagnetic spin exchange coupling between magnetic ions inherently. Thus, optical spin injection to these III-V magnetic alloy semiconductors may cause novel cooperative phenomena, which are inaccessible by the paramagnetic II-VI DMSs [16].

Koshihara et al. [14, 15, 73] have demonstrated effects of photo-excitation in III-V based DMSs in their primary work of this topic. The experiment was carried out on (In,Mn)As/GaSb heterostructures as a sample using GaAs/GaAs(100) substrate. The investigation was done by properly adjusting the growth condition setting the hole concentration slightly below the value necessary to induce ferromagnetism, and the sample was irradiated by light to generate extra amount of holes. They thought that

type II band alignment in which extra holes are transferred and stored in the magnetic layer to strengthen the ferromagnetic interaction among Mn ions is the important contriviance [14]. Hence, the inducement of a ferromagnetic order by photogenerated carriers in this novel III-V based magnetic semiconductor heterostructure P-(In,Mn)As/GaSb grown by molecular beam epitaxy was shown. The sample is seen to preserve ferromagnetic order and persistent conductivity even after the light is switched off at low temperature $(< 35K)$. The results were explained in terms of hole transfer from GaSb to (In,Mn)As in the heterostructure. Moreover, n-type (In,Mn)As exhibit paramagnetic characteristics where as p-type layers and related heterostructures, p-(In,Mn)As/(Ga,Al)Sb, show various types of ferromagnetic order at low temperatures. These facts suggest that holes can change the strength of spin exchange among Mn ions.

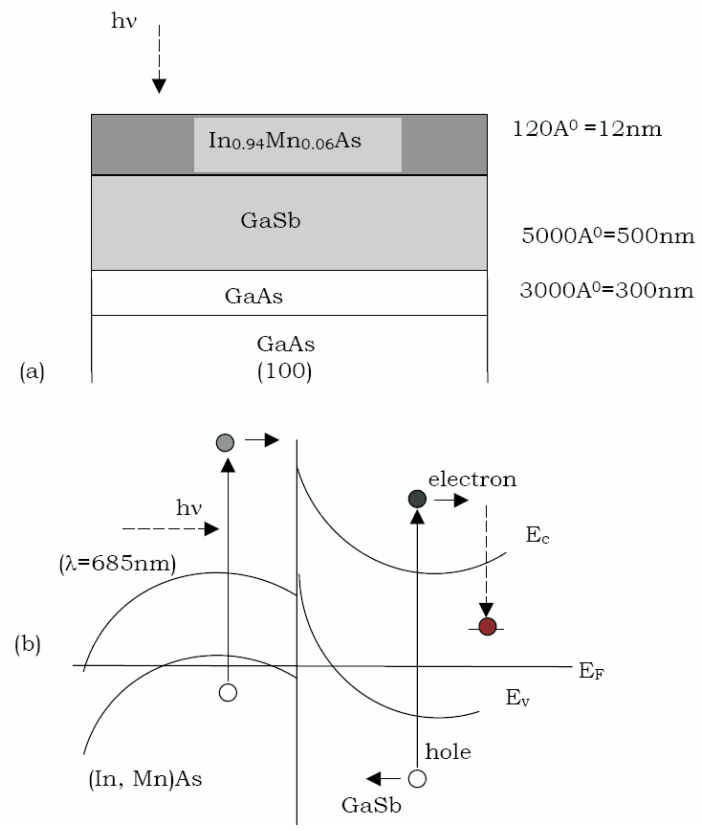

Fig. 1.6: (a) Structure of the sample. An arrow also shows direction of light irradiation. (b) Band edge profile of (In,Mn)As/GaSb heterostructure. E_C, E_V, and E_F denote band edge of conduction band, valence band, and Fermi level, respectively [14].

This experimental study revealed the occurrence of magnetization due to sample irradiation and could be understood as, holes generated in a GaSb layer are transferred effectively to a thin p-type (In,Mn)As layer due to large bending across the heterostructure.

Fig. 1.6 shows (In,Mn)As/GaSb heterostructure which most likely consists a broken-gap type-II band alignment similar to that of InAs/GaSb [75]. Accordingly, electrons are believed to drift towards the opposite direction so that holes do not recombine immediately with electrons when the light is switched off. Holes thus transferred to the p-(In,Mn)As layer are thought to enhance the ferromagnetic spin exchange among Mn ions and induce observed enhancement in magnetization and phase change. Gradual increase in both magnetization and conductivity during the irradiation could be explained in terms of the existence of carrier trapping centers in GaSb and (In,Mn)As layers, and/or the (In,Mn)As/GaSb heterointerface [14, 15]. Photon energy larger than the band gap of GaSb (0.8eV) was used for illumination which turned the paramagnetic sample without remanent magnetization in to a ferromagnetic with a clear hysteresis at 5K. It appears that the interface electric field separates photo-holes and photo-electrons. The former being accumulated in the (In, Mn)As layer, which triggers the ferromagnetism. It is shown that there is a change in hole concentration after illumination revealing the change in magnetization is purely electronic, and is not accompanied by any photoinduced and/or heat-induced structural or chemical changes [14].

GaAs has direct-gap which is closely below the energy range of visible radiation. This makes (Ga,Mn)As suitable for the fabrication of efficient optical devices [16] where the phenomena is controlled by spin interactions in the system. In such diluted magnetic semiconductors, hole-spin and Mn spin subsystems are believed to couple through p-d exchange, hence, alteration of either of these two subsystems cause significant influence on the entire system. This can be achieved by the carrier spin injection through the adequate inter-band optical excitation where in (Ga,Mn)As optical-absorption is known to occur in the visible range. However, to what extent the injected carrier spins modify the strength of p-d exchange interaction is the most

inspiring question currently [53, 76].

It has been understood that, spin-polarized carriers(holes) generated by the circularly polarized light change orientation of ferromagnetically coupled Mn spins depending on the light ellipticity. These coupled spin moments induce large perpendicular magnetization without the application of a magnetic field [77]. Due to the fact that the memorization effect has also been found as a trace after the photoinduced magnetization, the spin flipped Mn spins develop into collective rotation and yield reversed magnetic domains. Moreover, the photo-induced perpendicular magnetization is negligibly small when the photon energy is smaller than the band gap energy, E_g, of $(Ga, Mn)As$ eventually very close to that of $GaAs$. When photon energy is increased and becomes higher than the band gap, the induced magnetization increases steeply. However, with further increase in excitation energy it is seen to decrease gradually. This is probably due to the fact that the spin states in the valence band could mixup by the spin-orbit coupling for $k \neq 0$.

According to careful comparison of temporal profile of the photoinduced reflectivity change study of dynamics of photoinduced magnetization in ferromagnetic p-(Ga,Mn)As [78], rotation of ferromagnetically coupled Mn spins is induced by photogenerated hole spins within the excitation pulse width of a $100fs$. Hole and Mn spins are suggested to rotate and relax together upon optical excitation and their relaxation takes place in tens of picoseconds as a result of strong damping. This would be a different type of excitation (coupled hole-Mn spin complex) appearing in the hole-mediated ferromagnetic systems.

In this research we theoretically study the effect of photo-excitation when light is impinged on a diluted magnetic semiconductor system, (Ga,Mn)As, which is intended to remain ferromagnetic below certain critical temperature.

2

Mathematical Technique

2.1 Introduction

In this chapter, the Green function formalism used in subsequent chapters based on quantum field theory is discussed briefly. Quantum field theory (QFT) is the theory of fields providing theoretical framework widely used in particle physics and condensed matter physics, in formulating consistent quantum theories of many-particle systems, especially in situations where particles may be created and destroyed. It is originated in the problem of computing the energy radiated by an atom when dropped from one quantum state to another of lower energy providing us with an efficient method of solving a given problem in terms of some approximation. The real many-body problem begins with a system of particles that interact with one another where we can no longer consider the particles to act independently but must take into account the enormously complicated influence that each particle has on the behavior of all the others. Moreover, the theory utilizes the methods of second quantization where the inter particle interactions are represented in terms of particle creation and annihilation operators that the Hamiltonian describing the system requires [79].

In quantum field theory the Green functions are the so-called *propagators*. This name is based on the idea that, in order to find the important physical properties of a system, it is essential to know, not the detailed behavior of each particle in the system, but rather just the average behavior of one or two typical particles. The quantities

that describe this average behavior are called the one-particle and two-particle propagators, respectively. The single-particle propagator $G(\mathbf{r}_2, t_2; \mathbf{r}_1, t_1)$, gives the probability amplitude that, if we put a particle into the interacting system at point $\mathbf{r}_1$ at time t_1 and let it collide with the other particles for a while (i.e., propagate through the system), it will be observed at point $\mathbf{r}_2$ at time t_2. The propagator G yields directly the energies and life times of the quasi-particles. It also gives the momentum distribution, the spin, and the particle density and can be used as well to calculate the ground state energy. All these properties may be obtained at finite temperatures by using the finite-temperature version of G. The two particle propagator G_2 gives the probability amplitude for observing one particle at $(\mathbf{r}_3, t_3)$ and another at $(\mathbf{r}_4, t_4)$ if the first particle was put into the system at $(\mathbf{r}_1, t_1)$ and the second at $(\mathbf{r}_2, t_2)$. G_2 also gives directly the energies and life times of the collective excitations, as well as the magnetic susceptibility, the electrical conductivity, and other non-equilibrium properties at all temperatures.

2.2 The double-time temperature dependent Green function

The method of the double-time temperature dependent Green functions [80] in statistical mechanics are the appropriate generalizations of the correlation functions. They are useful in calculating the average of dynamical quantities, and they have great advantages when equations are framed and solved.

The retarded and advanced Green functions $G_r(t, t')$ and $G_a(t, t')$ for the double-time temperature-dependent Green function $\ll A(t); B(t') \gg$ involving two Heisenberg operators $A(t)$ and $B(t')$ is defined by

$$\begin{aligned} G_r(t, t') &\equiv \ll \mathbf{A}(t); \mathbf{B}(t') \gg_r \\ &= -i\theta(t - t') < [\mathbf{A}(t), \mathbf{B}(t')] >_r \end{aligned} \tag{2.2. 1}$$

and

$$\begin{aligned} G_a(t, t') &\equiv \ll \mathbf{A}(t); \mathbf{B}(t') \gg_a \\ &= i\theta(t - t') < [\mathbf{A}(t), \mathbf{B}(t')] >_a, \end{aligned} \tag{2.2. 2}$$

where $\ll \ldots \gg_{r,a}$ are the abbreviated notations for the corresponding Green functions, the square brackets $[..,..]$ denote a commutator or anticommutator, single-pointed brackets $< \ldots >$ denote a thermal average over a canonical ensemble which is appropriate since the number of particles is not constant, and $\theta(t-t')$ is heaviside, a step function with the value unity when $t > t'$ and the value zero when $t < t'$ and can be shortly written as

$$\theta(t) = \begin{cases} 0, & (t-t')<0 \\ \\ 1, & (t-t')>0 \end{cases}. \tag{2.2. 3}$$

These Heisenberg representations operators, $\mathbf{A}(t)$ and $\mathbf{B}(t')$ can be expressed as the product of the quantized field operators, i.e.,

$$\mathbf{A}(t) = e^{iHt}\mathbf{A}(0)e^{-iHt}, \;\; \hbar = 1 \tag{2.2. 4}$$

and

$$\mathbf{B}(t') = e^{iHt'}\mathbf{B}(0)e^{-iHt'}, \;\; \hbar = 1. \tag{2.2. 5}$$

Moreover, a commutator or anticommutator $[\mathbf{A}(t), \mathbf{B}(t)]$ will have an expression of the form

$$[\mathbf{A}(t), \mathbf{B}(t)] = \mathbf{AB} - \eta\mathbf{BA} \qquad \eta = \pm 1, \tag{2.2. 6}$$

where the sign of η is positive if **A** and **B** are both Bose operators and negative if they are Fermi operators. In general, **A** and **B** are neither Bose nor Fermi operators since products of operators can satisfy more complicated commutation relations. The sign of η is chosen by considering what is most convenient for the problem.

Substituting Eq. (2.2. 6), into both Eq. (2.2. 1) and (2.2. 2) gives

$$G_r(t,t') = -i\theta(t-t')[< \mathbf{A}(t)\mathbf{B}(t') > -\eta < \mathbf{B}(t')\mathbf{A}(t) >] \tag{2.2. 7}$$

and

$$G_a(t,t') = i\theta(t-t')[< \mathbf{A}(t)\mathbf{B}(t') > -\eta < \mathbf{B}(t')\mathbf{A}(t) >]. \tag{2.2. 8}$$

We note from (2.2. 7) and (2.2. 8) that $G_r(t,t') \neq 0$ when $t' < t$, $G_r(t,t') = 0$ when $t' > t$, and $G_r(t,t')$ is not defined when $t = t'$, because of the discontinuity of $\theta(t-t')$ at $t-t' = 0$. Similar considerations apply to $G_a(t,t')$, hence, $G_{r,a}(t,t')$ depends only on the difference $(t-t')$ in the case of statistical equilibrium. This property is utilized in finding the "spectral representation" of the Green function, which is, in fact, a Fourier integral representation. This fact is verified as follows:

Using Eq. (2.2. 4) and (2.2. 5),

$$\begin{aligned}\mathbf{A}(t)\mathbf{B}(t') &= e^{iHt}\mathbf{A}(0)e^{-iHt}e^{iHt'}\mathbf{B}(0)e^{-iHt'} \\ &= e^{iHt}e^{-iHt'}\mathbf{A}(0)e^{-iHt}e^{iHt'}\mathbf{B}(0)e^{-iHt'}e^{iHt'} \\ &= e^{iH(t-t')}\mathbf{A}(0)e^{-iH(t-t')}\mathbf{B}(0). \end{aligned} \tag{2.2. 9}$$

Similarly,

$$\mathbf{B}(t')\mathbf{A}(t) = e^{iH(t'-t)}\mathbf{B}(0)e^{-iH(t'-t)}\mathbf{A}(0). \tag{2.2. 10}$$

Substituting Eq. (2.2. 9) and (2.2. 10) into (2.2. 7),

$$\begin{aligned}G_r(t,t') = &-i\theta(t-t')Z^{-1}Tr[e^{H[i(t-t')-\beta]}\mathbf{A}(0)e^{-iH(t-t')}\mathbf{B}(0)] \\ &+ i\eta\theta(t-t')Z^{-1}Tr[e^{H[i(t-t')-\beta]}\mathbf{B}(0)e^{-iH(t-t')}\mathbf{A}(0)], \end{aligned} \tag{2.2. 11}$$

where the process $< ... >$ in quantum mechanics is defined by

$$< \rho >= \frac{1}{Z}Tr\left(\rho e^{-\beta H}\right) \tag{2.2. 12}$$

with

$$Z = \sum_n e^{-\beta E_n} = Tr(e^{-\beta H}) \tag{2.2. 13}$$

and

$$\rho = A(t)B(t') \quad or \quad B(t')A(t), \tag{2.2. 14}$$

where

$$\beta = \frac{1}{\kappa_B T}. \tag{2.2. 15}$$

Eq (2.2. 11) shows that

$$G_r(t,t') = G_r(t-t'). \tag{2.2. 16}$$

Similarly,

$$G_a(t,t') = G_a(t-t'). \tag{2.2. 17}$$

The average over the statistical ensemble of the product of operators in the Heisenberg representation of the kind

$$F_{AB}(t,t') =< A(t)B(t') > \tag{2.2. 18}$$

and

$$F_{BA}(t,t') =< B(t')A(t) > \tag{2.2. 19}$$

are important in statistical mechanics and are called the time-correlation functions. When the times are different ($t \neq t'$), these averages yield the time-correlation functions which are essential for transport processes. Just like the Green functions in statistical equilibrium, these time-correlation functions also depend on $(t-t')$, i.e.,

$$F_{BA}(t,t') = F_{BA}(t-t') \tag{2.2. 20}$$

and

$$F_{AB}(t,t') = F_{AB}(t-t'), \tag{2.2. 21}$$

as can be verified easily. This fact helps in finding a spectral representation (the Fourier transform of $F_{AB}(t,t')$ and $F_{BA}(t,t')$ that relates them to the Green functions.

2.3 The equation of motion of the Green Function

We now derive the equation of motion of the Green function. It is known that $A(t)$ and $B(t)$ satisfy equations of the form

$$i\frac{dA}{dt} = [A,H]. \tag{2.3. 1}$$

We now differentiate the Green functions given by Eq. (2.2. 1) and (2.2. 2) where G denotes both G_r and G_a and obtain

$$\begin{aligned} i\frac{dG}{dt} &= i\frac{d}{dt} \ll \mathbf{A}(t); \mathbf{B}(t') \gg \\ &= \frac{d}{dt}\{\theta(t-t') < [A(t)B(t') - \eta B(t')A(t)] >\} \\ &= \frac{d}{dt}\theta(t-t') < [A(t)B(t') - \eta\theta(t-t')B(t')A(t)] > \\ &+ i\theta(t-t') < \left[i\frac{dA(t)}{dt}B(t') - \eta B(t')i\frac{dA(t)}{dt}\right] > \\ &= \frac{d}{dt}\theta(t-t') < [A(t), B(t')] > + < T\frac{dA(t)}{dt}, B(t') > \\ &= \frac{d}{dt}\theta(t-t') < [A(t), B(t')] > + \ll i\frac{dA(t)}{dt}, B(t') \gg . \end{aligned} \tag{2.3. 2}$$

Since

$$\frac{d\theta(t-t')}{dt} = -\frac{d\theta(t-t')}{dt} \tag{2.3. 3}$$

and

$$\theta(t-t') = \int_{-\infty}^{t} \delta(t-t')dt. \tag{2.3. 4}$$

one can verify that,

$$\frac{d\theta(t-t')}{dt} = \delta(t-t'). \tag{2.3. 5}$$

Hence, making use of Eq. (2.3. 1) and (2.3. 5), Eq. (2.3. 2) can be written as,

$$i\frac{dG}{dt} = \delta(t-t') < [A(t), B(t')] > + \ll [A(t), H(t)]; B(t') \gg \tag{2.3. 6}$$

or

$$i\frac{dG}{dt} = \delta(t-t') < [A, B]_{-\eta} > + \ll [A, H]_{-}\,; B \gg . \tag{2.3. 7}$$

Substituting for the Green function which is given by

$$G(t-t') = \int_{-\infty}^{\infty} dE G(E) e^{-iE(t-t')} \tag{2.3. 8}$$

and the delta function by

$$\delta(t-t') = \frac{1}{2\pi}\int_{-\infty}^{\infty} e^{-iE(t-t')}dE, \tag{2.3. 9}$$

and multiplying both sides of Eq. (2.3. 7) by i gives

$$E\int_{-\infty}^{\infty} dEG(E)e^{-iE(t-t')} = \frac{1}{2\pi}\int_{-\infty}^{\infty} e^{-iE(t-t')}dE < [A,B]_{-\eta} > +\theta(t-t') < \left[i\frac{dA(t)}{dt}, B(t')\right] > . \tag{2.3. 10}$$

The Fourier transform of Eq. (2.3. 10) can be obtained by multiplying its both sides by

$$\frac{1}{2\pi}\int_{-\infty}^{\infty} dte^{i\omega(t-t')}, \tag{2.3. 11}$$

hence,

$$E\int_{-\infty}^{\infty} dEG(E)\frac{1}{2\pi}\int_{-\infty}^{\infty} dte^{i(\omega-E)(t-t')} = \frac{1}{2\pi}\int_{-\infty}^{\infty} dE\frac{1}{2\pi}\int_{-\infty}^{\infty} e^{i(\omega-E)(t-t')}dt < [A,B]_{-\eta} > + \; F.T.of \;\; \theta(t-t') < \left[i\frac{dA(t)}{dt}, B(t')\right] >, \tag{2.3. 12}$$

which could be rewritten as

$$E\int_{-\infty}^{\infty} G(E)\delta(\omega-E)dE = \frac{1}{2\pi}\int_{-\infty}^{\infty} \delta(\omega-E)dE < [A,B]_{-\eta} > + \ll \left[A,H\right], B \gg \tag{2.3. 13}$$

and in its more simplified form,

$$EG(E) = \frac{1}{2\pi} < [A,B]_{-\eta} > + \ll [A,H], B \gg, \tag{2.3. 14}$$

where

$$\frac{1}{2\pi}\int_{-\infty}^{\infty} e^{i(\omega-E)(t-t')}dt = \delta(\omega-E) \tag{2.3. 15}$$

and

$$\delta(\omega-E)dE = 1 \quad at\,\omega = E. \tag{2.3. 16}$$

Hence,

$$EG(E) = \frac{1}{2\pi} < [A(t), B(t')] > + \ll [A(t), H(t)]_- ; B(t') \gg . \qquad (2.3.\ 17)$$

Since $G(E)$ is Fourier transform of $G(t-t')$, we can write $G(E) = \ll A(t), B(t') \gg$ so that Eq. (2.3. 17) becomes

$$E \ll A(t); B(t') \gg = \frac{1}{2\pi} < [A(t), B(t')] > + \ll [A(t), H(t)]_- ; B(t') \gg, \qquad (2.3.\ 18)$$

where $[\quad]_-$ means a commutator. Eq. (2.3. 17) follows since the Fourier transform of the δ function is $\frac{1}{2\pi}$, and E represents the dispersion of a system, magnon, like what we are studying.

For future use we write Eq. (2.3. 18) in the form

$$E \ll A, B \gg_E = \frac{1}{2\pi} < [A, B]_- > + \ll [A, H]_-; B \gg_E . \qquad (2.3.\ 19)$$

The only other equation which we shall require from Green function theory is that defining the relationship between $\ll A(t); B(t') \gg_E$ if it is denoting the Fourier transform of the Green function involving operators $A(t)$ and $B(t')$ and its related correlation function $< B(t')A(t) >$. This may be written as

$$< B(t')A(t) > = \lim_{\varepsilon \to +0} i \int_{-\infty}^{\infty} \frac{\ll A; B \gg_{E+i\varepsilon} - \ll A; B \gg_{E-i\varepsilon}}{e^{\beta\hbar E} - 1} e^{-iE(t-t')} dE. \qquad (2.3.\ 20)$$

However, there are cases where the second term on the right-hand side in Eq. (2.3. 19) is a higher order Green function. Hence, one can construct equations of the same form which entails still higher order functions obtaining a hierarchy of coupled equations; as will be seen in chapter five. Moreover, as yet, no method to find the exact solution of such a set of coupled equations, an approximate method of decoupling chain of equations reducing it to a finite set of equations is used which then can be solved. It is to be noted that the success of the Green function method lies in the handling of the coupled chain of equations [79, 82, 83, 84].

we have also used the well known Dirac identity [79]

$$\frac{1}{x \pm i\varepsilon} = \wp \frac{1}{x} \mp i\pi\delta(x) \qquad (2.3.\ 21)$$

in treating the singularities, where $\wp$ is the principal part of the function.

3

Carrier Mediated Exchange Energy in (Ga,Mn)As DMS

3.1 Introduction

In magnetic impurity doped semiconductors, enhancement of the ferromagnetic transition temperature is required for spintronic devices to operate at room temperature. This temperature is described through exchange coupling energy of localized spins from a transition metal, incomplete, d-shells mediated by carriers (holes) from the semiconductor valence band [2].

Zener and Heisenberg models have been used to describe such systems in analytical calculation of exchange energy, magnetization, transition temperature and other parameters, and also for comparison of experimental results with theoretical works [40]. However, the two models are described differently in such a way that in the former case the ferromagnetic coupling between the unfilled adjacent d shells is via the conduction electrons and hence is of long-range type where as in the latter case the ferromagnetic coupling is due to the short-range type. Therefore, in Zener's theory the outer s electrons of the isolated atoms become conduction electrons in the metallic state and contribute quite appreciably to the total exchange energy. The exchange interaction between the conduction s electrons and d electrons will therefore be ferromagnetic in nature. It is with the assumption that, each individual conduction electrons tend to align the spins of the incomplete d shell in a direction parallel to its own spin. Usually there are as many conduction electrons with up spin as with down spin, so that their net effect on the spin of the incomplete d electrons is zero. According to Zener, the exchange interactions responsible for ferromagnetism are to

be found mainly between the $3d$ and $4s$ electrons rather than between the $3d$ electrons; the $3d-4s$ coupling is also strongly ferromagnetic that it dominates the $3d-3d$ interaction, which he assumes to be antiferromagnetic [17, 18, 79].

In early 2000's [2]dietl proposed a model that considers interaction of holes with localized spins and has similarity to that of Zener's model in that for n-doped materials the exchange is due to ferromagnetic s-d coupling, while for p-doped ones it is due to antiferromagnetic p-d coupling. In both cases, the free carriers are believed to mediate an effective ferromagnetic coupling between the Mn spins, which is typically stronger than the shorter-range antiferromagnetic direct exchange coupling present in undoped system. It is due to the fact that in indirect exchange interaction the distances between magnetic atoms with incomplete d electronic shells are much larger than the shell radii so that direct exchange cannot account for their observed magnetic properties; one has to invoke the idea of an indirect exchange interaction to explain their magnetism.

In this chapter, we estimate the exchange energy between the localized spins from which ferromagnetic transition temperature can also be estimated. The maximum value of this energy depends on the density of holes required to mediate the ferromagnetism. The Heisenberg type expression for the Zener model valuably used to describe the Dietl model [2] is applied to explain the ferromagnetism of the diluted magnetic semiconductor $(Ga, Mn)As$ in the absence of application of radiation.

3.2 The exchange coupling constant

The indirect exchange interaction between two local spins could be obtained from the second order energy correction. The Hamiltonian describing the system is of the form given by Kasuya [85] and Mitchell [86] for the s-d type interaction. It is based on the mechanism of polarizing conduction electrons by the exchange interaction with the d-electrons of the paramagnetic ions proposed by Zener [18]. This model Hamiltonian is written as,

$$H_{exch} = -\frac{1}{N}\sum_{kk'n} J(|k-k'|)e^{i(k-k')\cdot R_n}\{(c^+_{k\uparrow}c_{k'\uparrow} - c^+_{k\downarrow}c_{k'\downarrow})S^z_n + c^+_{k\uparrow}c_{k'\downarrow}S^-_n + c^+_{k\downarrow}c_{k'\uparrow}S^+_n\}, \tag{3.2. 1}$$

where N is the number of magnetic lattice points in a unit volume, R_n represents the position of the Mn ion, S_n represents its spin operator, and k and k' are the wave vectors of conduction electrons/holes, $c^+_{k\sigma}$ and $c^+_{k'\sigma'}$ are the creation and annihilation operators for the electrons/holes with wave vector **k** and spin $\sigma = \uparrow, \downarrow$.

The exchange integral, between a conduction electron and the d electron spin of the Mn ion in Zener model and between hole and the d core electron spin of the Mn ion in Dietl model [2, 47, 49], is given by Kasuya and yosida [85, 87] as,

$$J(|k-k'|) = N \int d\tau_{12} \phi^*_{k'}(r_1)\phi^*_d(r_2 - R_n)\frac{e^2}{r_{12}}\phi_k(r_2)\phi_d(r_1 - R_n)e^{i(k'-k)\cdot\mathbf{R}_n}. \quad (3.2.\ 2)$$

where

$$\phi_k = |k> = \frac{1}{\sqrt{\Omega_V}} e^{i\mathbf{k}\cdot\mathbf{r}} u_k(r) \quad (3.2.\ 3)$$

is Bloch function, where $u_k(r)$ is its periodic part, and Ω_V is the volume.

$$\phi_d(r - R_n) = \frac{1}{\sqrt{N}} \sum_k e^{-ik.R_n}\phi_k(r) = \frac{1}{\sqrt{N}} \sum_k e^{ik.(r-R_n)} u_k(r) \quad (3.2.\ 4)$$

is a Wannier function localized within cell (Brillouin zone) and are peaked around the lattice sites. R_n is a lattice point, r is any vector in the volume of crystal and k is a plane wave vector. To find the exchange coupling constant we start with substituting equation Eq. (3.2. 1) into the second order energy correction, since the second order process gives rise to the effective spin-spin interaction between the unfilled shell electrons, while the first order process gives rise to the resistivity, according to Kasuya [85]:

$$E^{(2)}_k = \sum_{k'\sigma\sigma'} \frac{< k\sigma \mid H_{ex} \mid k'\sigma' >< k'\sigma' \mid H_{ex} \mid k\sigma >}{E_{k\sigma} - E_{k'\sigma'}} \quad (3.2.\ 5)$$

as in reference [88].

Following Kasuya [85] we get,

$$E_k^{(2)} = \frac{1}{N^2}\sum_{k'nm}\left[\frac{|J(k-k')|^2 e^{i(k-k').(R_n-R_m)}}{E_k - E_{k'}}\right] \times [n_{k\uparrow}(1-n_{k'\uparrow}) + n_{k\downarrow}(1-n_{k'\downarrow})]S_n^z S_m^z + n_{k\uparrow}(1-n_{k'\downarrow})S_n^- S_m^+ + n_{k\downarrow}(1-n_{k'\uparrow})S_n^+ S_m^- \quad (3.2.\ 6)$$

as in Yosida paper [87], where $n_{k\uparrow}$ and $n_{k\downarrow}$ are the Fermi distribution function of up and down spin electrons, respectively, and the $k' = k$ is excluded from the summation.

Let us replace $\mathbf{k} - \mathbf{k}'$ by $\mathbf{q}$ and $\mathbf{R}_n - \mathbf{R}_m$ by $\mathbf{R}_{nm}$ so that,

$$E_k^{(2)} = \frac{1}{N^2}\sum_{k'nm}\left[\frac{J^2(q)e^{i\mathbf{q}.\mathbf{R}_{nm}}}{E_k - E_{k'}}\right] \times [n_{k\uparrow}(1-n_{k'\uparrow}) + n_{k\downarrow}(1-n_{k'\downarrow})]S_n^z S_m^z + n_{k\uparrow}(1-n_{k'\downarrow})S_n^- S_m^+ + n_{k\downarrow}(1-n_{k'\uparrow})S_n^+ S_m^-, \quad (3.2.\ 7)$$

which can be alternatively written as,

$$\begin{aligned} E_k^{(2)} = \frac{1}{N^2}\sum_{k'nm}&\left[\frac{J^2(q)e^{i\mathbf{q}.\mathbf{R}_{nm}}}{E_k - E_{k'}}\right] \\ &\times [n_{k\uparrow} + n_{k\downarrow}]S_n^z S_m^z + n_{k\uparrow}S_n^- S_m^+ + n_{k\downarrow}S_n^+ S_m^- \\ &- \{[n_{k\uparrow}n_{k'\uparrow} + n_{k\downarrow}n_{k'\downarrow}]S_n^z S_m^z + n_{k\uparrow}n_{k'\downarrow}S_n^- S_m^+ + n_{k\downarrow}n_{k'\uparrow}S_n^+ S_m^-\}. \end{aligned} \quad (3.2.\ 8)$$

The term in square bracket in the right hand side of Eq. (3.2. 8) is of higher order term which can be ignored. Hence,

$$E_k^{(2)} = \frac{1}{N^2}\sum_{k'nm}{}'\left[\frac{J^2(q)e^{i\mathbf{q}.\mathbf{R}_{nm}}}{E_k - E_{k'}}\right][n_{k\uparrow} + n_{k\downarrow}]S_n^z S_m^z + n_{k\uparrow}S_n^- S_m^+ + n_{k\downarrow}S_n^+ S_m^-. \quad (3.2.\ 9)$$

In the sprit of second quantization, taking $n_{k\uparrow} = n_{k\downarrow} = n_k$ following Kasuya [85], $(n_{k\uparrow} + n_{k\downarrow})/2 = n_k$ is the average distribution function, which leads Eq. (3.2. 9) to

$$E_k^{(2)} = \frac{1}{N^2}\sum_{qk'nm}\left[\frac{J^2(q)e^{i\mathbf{q}.\mathbf{R}_{nm}}}{E_k - E_{k'}}\right] 2n_k[S_n^z S_m^z + \frac{1}{2}(S_n^- S_m^+ + S_n^+ S_m^-)]. \quad (3.2.\ 10)$$

Last expression can be reduced to

$$E_k^{(2)} = \frac{1}{N^2} \sum_{qk'nm} \left[\frac{J^2(q) e^{i\mathbf{q}.\mathbf{R}_{nm}}}{E_k - E_{k'}} \right] 2n_k \mathbf{S}_n \cdot \mathbf{S}_m, \tag{3.2. 11}$$

where

$$\mathbf{S}_n \cdot \mathbf{S}_m = S_n^z S_m^z + \frac{1}{2}(S_n^- S_m^+ + S_n^+ S_m^-). \tag{3.2. 12}$$

Hence,

$$E^{(2)} = \frac{1}{N^2} \sum_{k'} \sum_{nm} \left[\frac{J^2(q)}{\varepsilon_k - \varepsilon_{k'}} e^{i(q)\cdot R_{nm}} \right] 2n_k \mathbf{S}_n \cdot \mathbf{S}_m. \tag{3.2. 13}$$

Taking the fermi-dirac distribution function at very low temperature $T \to 0$ and investigating the occupancy of states whose energies are less than ϵ_F and greater than ϵ_F, so that

$$f(\epsilon),\ \epsilon < \epsilon_F = n_f = \frac{1}{e^{(\epsilon-\epsilon_F)/k_B T} + 1} = \frac{1}{e^{-\infty} + 1} = 1. \tag{3.2. 14}$$

and

$$f(\epsilon),\ \epsilon > \epsilon_F = n_f = \frac{1}{e^{(\epsilon-\epsilon_F)/k_B T} + 1} = \frac{1}{e^{\infty} + 1} = 0. \tag{3.2. 15}$$

If we neglect q-dependence of $J(q)$ [87] Eq. (3.2. 13) reduces to

$$E^{(2)} = \frac{4m^* J^2}{N^2} \sum_{k'} \sum_{nm} \left[\frac{1}{k^2 - k'^2} e^{i(k-k')\cdot R_{nm}} \right] \mathbf{S}_n \cdot \mathbf{S}_m. \tag{3.2. 16}$$

Or

$$E^{(2)} = \frac{4m^* J^2}{N^2} \sum_{k'} \sum_{nm} \left[\frac{1}{k^2 - k'^2} e^{-ik'\cdot R_{nm}} e^{ik\cdot R_{nm}} \right] \mathbf{S}_n \cdot \mathbf{S}_m. \tag{3.2. 17}$$

This can be further reduced to

$$E^{(2)} = \frac{4m^* J^2}{(2\pi)^3 N^2} \sum_{nm} \int_0^\infty d^3k' \frac{e^{-i\mathbf{k}'\cdot\mathbf{R}_{nm}}}{k^2 - k'^2} e^{i\mathbf{k}\cdot\mathbf{R}_{nm}} \mathbf{S}_n \cdot \mathbf{S}_m \tag{3.2. 18}$$

Using Eqs. (A.1. 15) and (A.1. 14) (derivation is given in the appendix), Eq. (3.2. 18) becomes

$$E_k^2 = \frac{4m^* J^2}{(2\pi)^3 N^2} \sum_{nm} \frac{-2\pi}{iR_{nm}} [\pi i cosk R_{nm}] e^{i\mathbf{k}\cdot\mathbf{R}_{nm}} \mathbf{S}_n \cdot \mathbf{S}_m. \tag{3.2. 19}$$

Making same rearrangements,

$$E_k^{(2)} = -\frac{4m^*J^2}{4\pi R_{nm}N^2}\sum_{nm} coskR_{nm}e^{i\mathbf{k}\cdot\mathbf{R}_{nm}}\mathbf{S}_n\cdot\mathbf{S}_m. \tag{3.2. 20}$$

For the effective energy, summing the last expression over the ground state fermi sea total electrons is required. Hence,

$$E^{(2)} = \sum_k E_k^{(2)}, \tag{3.2. 21}$$

which gives

$$E^{(2)} = -\frac{4m^*J^2}{4\pi R_{nm}N^2}\sum_{nm}\sum_k coskR_{nm}e^{i\mathbf{k}\cdot\mathbf{R}_{nm}}\mathbf{S}_n\cdot\mathbf{S}_m. \tag{3.2. 22}$$

Now, we convert the sum over k into integration:

$$E^{(2)} = -\frac{4m^*J^2}{(2\pi)^3 4\pi R_{nm}N^2}\sum_{nm}\int_0^{2\pi} d\varphi\int_0^{\pi} sin\theta d\theta\int_0^{k_F} dkk^2 coskR_{nm}e^{i\mathbf{k}\cdot\mathbf{R}_{nm}}\mathbf{S}_n\cdot\mathbf{S}_m \tag{3.2. 23}$$

or

$$E^{(2)} = -\frac{2\pi m^*4J^2}{(2\pi)^3 4\pi R_{nm})N^2}\sum_{nm}\int_0^{k_F} dkk^2 coskR_{nm}\int_0^{\pi} sin\theta d\theta e^{ikR_{nm}cos\theta}\mathbf{S}_n\cdot\mathbf{S}_m. \tag{3.2. 24}$$

From expression (A.2. 6) (For the detail derivation see the appendix)

$$E^{(2)} = \frac{4m^*J^2(2k_F)^4}{8N^2(2\pi)^3}\sum_{nm}\left(\frac{ycosy - siny}{y^4}\right)\mathbf{S}_n\cdot\mathbf{S}_m, \tag{3.2. 25}$$

If we make use of $y = 2k_F R_{nm}$, $R_{nm}^4 = \frac{y^4}{(2k_F)^4}$.
Let $\frac{ycosy-siny}{y^4} = F(2k_F R_{nm})$

$$E^{(2)} = \frac{2m^*4J^2k_F^4}{N^2(2\pi)^3}\sum_{nm} F(2k_F R_{nm})\mathbf{S}_n\cdot\mathbf{S}_m. \tag{3.2. 26}$$

Since the number of ground state fermi electron is given by

$$n = \frac{k_F^3}{6\pi^2} = \sum_0^{k_F} = \frac{1}{(2\pi)^3}\int_0^{k_F} d^3k, \tag{3.2. 27}$$

where

$$\frac{1}{(2\pi)^3}\int_0^{k_F} d^3k = \int_0^{2\pi} d\varphi \int_0^{\pi} sin\theta d\theta \int_0^{k_F} k^2 dk, \tag{3.2. 28}$$

Eq. 3.2. 26 becomes

$$E^{(2)} = \frac{4k_F^3}{6\pi^2}\left[\frac{6\pi^2}{k_F^3}\frac{2m^* J^2 k_F^4}{N^2(2\pi)^3}\right]\sum_{nm} F(2k_F R_{nm})\mathbf{S}_n \cdot \mathbf{S}_m. \tag{3.2. 29}$$

or

$$E^{(2)} = n\left[\frac{3m^* 4J^2 k_F}{2N^2\pi}\right]\sum_{nm} F(2k_F R_{nm})\mathbf{S}_n \cdot \mathbf{S}_m. \tag{3.2. 30}$$

Again, ground state fermi energy is given by, $\varepsilon_F = \frac{\hbar^2 k_F^2}{2m^*}$ and $m^* = \frac{\hbar^2 k_F^2}{2\varepsilon_F}$, hence substituting for m^* in Eq. (3.2. 30),

$$E^{(2)} = n\left[\frac{k_F^3}{\varepsilon_F}\frac{3J^2}{N^2\pi}\right]\sum_{nm} F(2k_F R_{nm})\mathbf{S}_n \cdot \mathbf{S}_m. \tag{3.2. 31}$$

Since $k_F^3 = 6\pi^2 n,$ the last equation can be rewritten as

$$E^{(2)} = n\left[\frac{6\pi^2 n}{\varepsilon_F}\frac{3J^2}{N^2\pi}\right]\sum_{nm} F(2k_F R_{nm})\mathbf{S}_n \cdot \mathbf{S}_m \tag{3.2. 32}$$

or

$$E^{(2)} = \frac{2\pi J^2}{\varepsilon_F}\left(\frac{3n}{N}\right)^2\sum_{nm} F(2k_F R_{nm})\mathbf{S}_n \cdot \mathbf{S}_m \tag{3.2. 33}$$

We now assume that Mn ions randomly occupy only Ga sites in the $GaAs$ zinc-blende lattice (fcc) with a lattice constant a. We operate in the (weekly) metallic limit and assume the carrier mediated effective Mn-Mn indirect exchange interaction to be of RKKY-type. However, with DMS systems being at best poor or bad metals with a mean free path typically of the order of $1 - 2A^0$, which is less than a, it is important to include the effects of a finite carrier mean free path; we do this by introducing a cutoff $\ell(\lesssim a)$ in the range of the RKKY function. The large value $(S = 5/2)$ of the impurity moment spins allows a treatment of the Mn spins as classical Heisenberg spins [89]. Hence, the Hamiltonian will reduce to

$$E^{(2)} = \sum_{nm} J_{nm} \mathbf{S}_n \cdot \mathbf{S}_m \tag{3.2. 34}$$

or

$$H = \sum_{nm} J_{nm} \mathbf{S}_n \cdot \mathbf{S}_m. \tag{3.2. 35}$$

The last expression shows the analogy of the Zener indirect exchange energy to the Heisenberg direct exchange energy that Dietl used in describing DMS systems.

From Eq. (3.2. 34) the exchange energy constant between spins of magnetic impurities localized at sites n and m is generally given by:

$$J_{nm} = \frac{2\pi J^2}{\varepsilon_F} \left(\frac{3n}{N}\right)^2 F(2k_F R_{nm}) \tag{3.2. 36}$$

or

$$J_{nm} = J_0 F(2k_F R_{nm}) e^{-\frac{R_{nm}}{\ell}}, \tag{3.2. 37}$$

where ℓ is carrier mean free path, k_F is the Fermi wave vector, $J_0 = \frac{2\pi J^2}{\varepsilon_F}\left(\frac{3n}{N}\right)^2$ which can be related to the local Zener coupling $J = J_{pd}$ between the Mn local moments and hole spins, and $J_0 \; \alpha \; J_{pd}^2$. This energy couples magnetic spins ferromagnetically depending on their separation and looks to show an oscillatory characteristics that can be described by the function $F(2k_F R_{nm})$. As the value of the expression $2k_F R_{nm}$ varies the value of this oscillatory function changes giving either positive or negative value and hence, the interaction in the system can be ferromagnetic or antiferromagnetic. The finally obtained results will be utilized to describe the ferromagnetic transition temperature in the next section. Moreover, in the case of ferromagnetic semiconductors there can be both electrons (due to s-d exchange in the conduction band) and holes (due to p-d exchange in the valence band) mediated exchange coupling of magnetic moments of the impurity Mn atoms/ions.

3.2.1 The Ferromagnetic Transition Temperature of the $(Ga, Mn)As$ DMS

The ferromagnetic transition temperature due to an indirect exchange interaction, being the temperature of transition from ferromagnetism to paramagnetism, is calculated for diluted magnetic semiconductors starting with mean (or molecular) field theory which gives a grossly inadequate picture of the critical region, and fails to predict spin waves at low temperatures [30]. Hence, making use of equations Eqs. (A.3. 17), (A.3. 19) and (A.3. 35) we obtain, (detailed derivation is given in the appendix)

$$\begin{aligned} T_C &= \gamma C \\ &= \frac{ZJ_{nm}}{Ng^2\mu_B^2} \cdot \frac{N_{Mn}g^2\mu_B^2 S(S+1)}{3\kappa_B}. \end{aligned} \tag{3.2. 38}$$

Which further reduces to

$$T_C = \frac{N_{Mn}ZJ_{nm}S(S+1)}{3N\kappa_B}. \tag{3.2. 39}$$

J_{nm} is the exchange coupling obtained as in expression Eq. (3.2. 33) expressed in terms of $J = J_{pd}$ which is the interaction energy of the orbital containing holes and localized d-shell electrons. $N_{Mn} = \frac{4x}{a^3}$ is the Mn_{Ga} density in $(Ga_{1-x}Mn_x)As$ with a lattice constant a, (or, the concentration of magnetic impurity is given by $x = \frac{N_{imp}}{N}$, where $N_{imp} = N_{Mn}$ is the number of magnetic impurities randomly distributed on lattice of N sites) [65, 71]. Hence, from the last expression, we can write the ferromagnetic transition temperature T_C as

$$T_C = \frac{xZJ_{nm}S(S+1)}{3\kappa_B}. \tag{3.2. 40}$$

where

$$J_{nm} = J_0 F(2k_F R_{nm}). \tag{3.2. 41}$$

3.3 Result and Discussion

Eq. (3.2. 41) is obtained from Eq. (3.2. 37) with the assumption that the carrier mean free path $\ell \gg R_{nm}$. Therefore, it is possible to make plot of J_{nm} and $F(2k_F R_{nm})$ vs. $(2k_F R_{nm})$ based upon this feature.

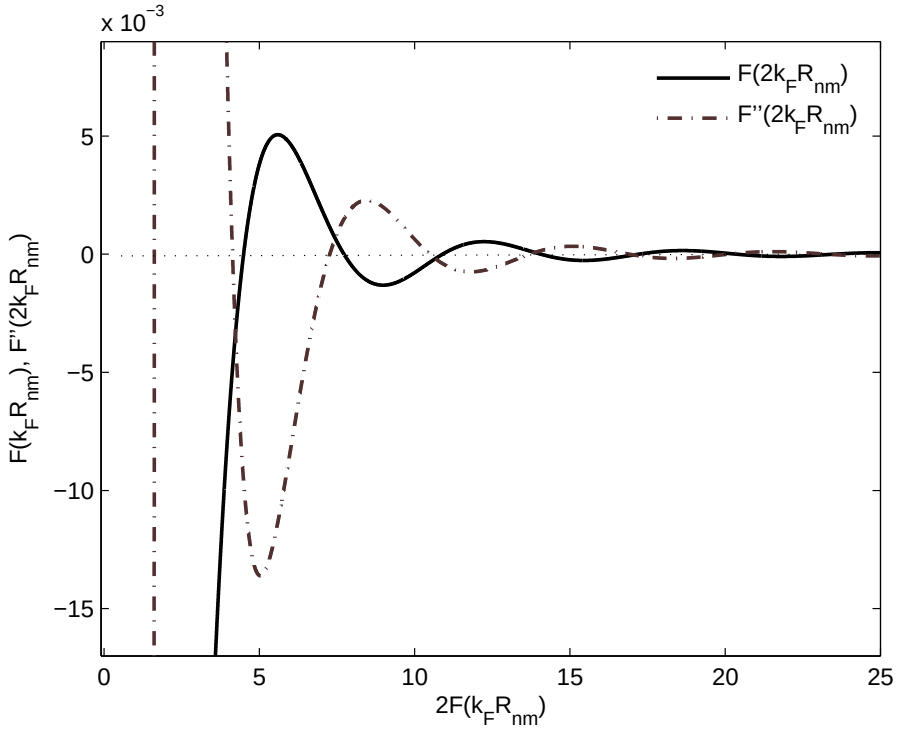

Fig. 3.1: The oscillatory term, $F(2k_FR_{nm})$ and its second derivative, of the exchange energy Vs. the term containing spin separation, $2k_FR_{nm}$ is plotted.

Fig. 3.1 summarizes relation between $F(2k_FR_{nm})$ and the product k_FR_{nm} containing Fermi wave vector k_F and distance R_{nm} between spins localized at n and m. The term determines the nature of the coupling energy which is shown to give negative value for smaller $2k_FR_{nm}$ and attributed to result in antiferromagnetic interaction between the localized spins overcoming any effect of holes. Beyond the maximum value of $F(2k_FR_{nm})$, i e., as $2k_FR_{nm}$ increases, it also decreases showing damping oscillations and seems to give rise to scattering where the localized spins are supposed to orient arbitrarily giving rise to paramagnetism or any other effects regardless of their interaction with holes. The two graphs are plotted for comparison where the second one is the second derivative of the first whose minima corresponds to the maximum of the localized spins exchange coupling energy.

The average $Mn_{Ga} - Mn_{Ga}$ separation in a $(Ga, Mn)As$ random alloy for spins at sites n and m can be estimated using expression $R_{nm} = 2(3/4\pi N_{Mn})^{1/3}$. Moreover, if

the spin-orbit interaction and band warping (distorting) are neglected, the top of the valence band is formed by six degenerate parabolic bands with $k_F = (\pi^2 N_h)^{1/3}$ [65] from which ε_F can be determined. From detailed microscopic calculations in non-magnetic GaAs with hole densities $N_h \sim 10^{18} - 10^{20} cm^{-3}$ one might expect $N_h \approx N_{Mn}$ since Mn is divalent. However N_h is 15% of Mn concentration N_{Mn}, at most. This may be due to compensation of Mn acceptors by deep donors such as the As antisite known to be present with high concentration in low-temperature grown GaAs [90].

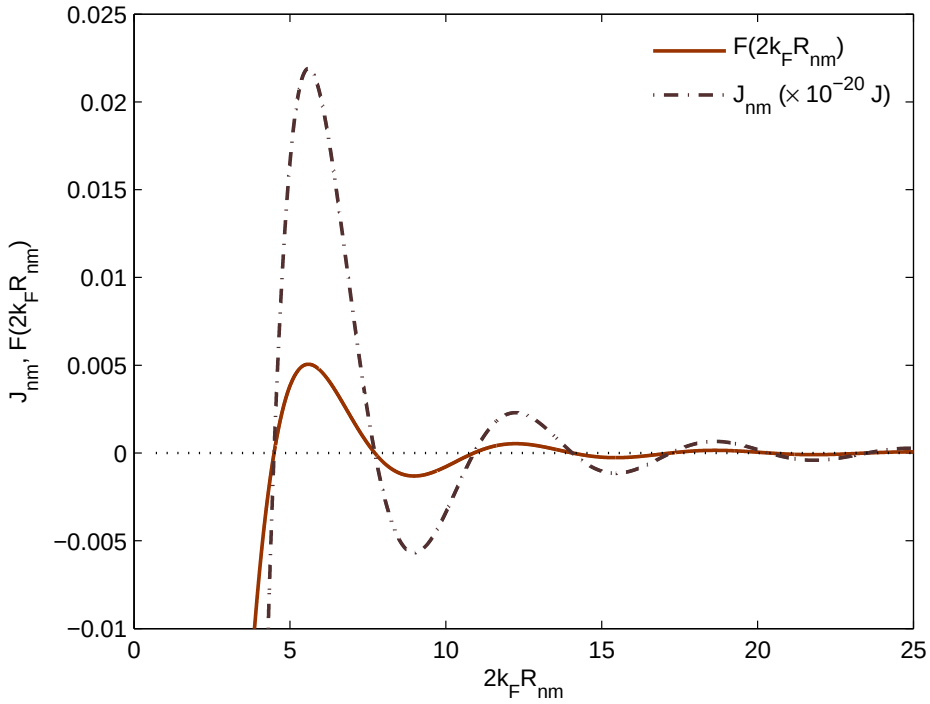

Fig. 3.2: The exchange energy, J_{nm}, and the term contributing to oscillatory $F(2k_F R_{nm})$ Vs. the term containing mean local spin separation, $2k_F R_{nm}$, is plotted.

Fig. 3.2 is plotted using Eq. (3.2. 41), from which the maximum value of J_{nm} can be estimated and could be approximated to of the order of $10^{-22} J \cong 130 meV$. In this estimation, $N_h = 15\% N_{Mn}$ at approximate value of $2k_F R_{nm} \approx 5.612$ where the maximum value of $F(2k_F R_{nm}) \approx 0.00505818$, $\varepsilon_F \approx 100 meV$ calculated assuming spherical fermi surface by first calculating N_h from $N_{Mn} = 2.3 \times 10^{27} m^{-3}$, thus, $N_h = 1.5 \times 10^{20} cm^{-3}$ [40] and $J_{pd} = 15 meV$ as discussed by Berciu and Bhatt [31] is considered. Accordingly, the

exchange coupling is shown to increase and become strong as the distance between localized impurity spins decrease until its maximum value is acquired. This coupling energy is found to depend on, and also increase with increase in hole density that might be described via k_F. Its decrease with increase in Fermi energy indicates that the exchange interaction could take place more by valence band subsystem where ϵ_F may shift towards the top of the valence band nearing the acceptor level, hence, the localized spins interact with holes created in the band due to excitation of electrons. Furthermore, using estimated value of exchange coupling, the maximum value of the ferromagnetic transition temperature T_C for a particular impurity concentration x can be estimated.

4

Exchange Coupling and Photoinduced Magnetic Ordering in $(Ga, Mn)As$ DMS

4.1 Introduction

In this chapter, photoinduced coupling of the magnetic moments of Mn^{2+} spins is studied theoretically. It is believed that the magnetic moments of Mn d shell electrons in a diluted magnetic semiconductor $(Ga, Mn)As$ interact with the spins of carriers induced by photon irradiation [14, 15, 73] in both conduction and valence bands [2, 17, 18] through exchange coupling energy. It is argued that this energy could be extremely large near or at ferromagnetic (FMR) and spin wave resonances (SWR). It is suggested that these resonances could be employed to establish the validity of the model calculation made.

4.2 Formulation of the Problem

The Hamiltonian describing the interaction of radiation with matter (spins) can be written as

$$H_I = g\mu_B \mathbf{H}_x \mathbf{S}_x, \tag{4.2. 1}$$

where g is the g-factor, μ_B-is the Bohr magneton ($\simeq 9.2741 \times 10^{-24} J.T^{-1}$), $\mathbf{H}_x$-is magnetic field part of the radiation taken to be along the x-axis and $\mathbf{S}_x$-is spin of the localized Mn d-shell electrons.

The magnetic field H_x is expressed in the second quantized form as

$$H_x = i \sum_{n,q} \left(\frac{\hbar}{2\epsilon_0 \omega_q V} \right)^{\frac{1}{2}} \left[\hat{d}_q(t) e^{i\mathbf{q}\cdot\mathbf{R}_n} - \hat{d}_q^+(t) e^{-i\mathbf{q}\cdot\mathbf{R}_n} \right] (\mathbf{q} \times \hat{\mathbf{e}}), \tag{4.2. 2}$$

where d_q and d_q^+ are time dependent annihilation and creation operators for photon, respectively, $\mathbf{q} \equiv (\mathbf{q}_x, \mathbf{q}_y, \mathbf{q}_z)$ is the wave vector of photon, V is the volume in which the radiation field is confined, $\hat{e}_q$ is a unit polarization vector. The spin operator S_x can be written as

$$S_x = \frac{S^+ + S^-}{2}. \tag{4.2. 3}$$

Substituting Eq. (4.2. 2) and (4.2. 3) into Eq. (4.2. 1) gives

$$H_I = i \sum_{n,q} \eta_q \left[\hat{d}_q e^{-i\omega_q t} e^{i\mathbf{q}\cdot\mathbf{R}_n} - \hat{d}_q^+ e^{i\omega_q t} e^{-i\mathbf{q}\cdot\mathbf{R}_n} \right] \left[\frac{S_n^+ + S_n^-}{2} \right], \tag{4.2. 4}$$

where $\eta_q = g\mu_B \left(\frac{\mu_0 \omega_q}{2V} \right)^{\frac{1}{2}}$ is momentum dependent photon-matter coupling constant, $|\mathbf{q} \times \hat{\mathbf{e}}| = q$ due to transversality condition, $\omega_q = cq$ is frequency of the electromagnetic radiation, c is speed of light ($\simeq 3 \times 10^8 m/s$ in free space), and μ_0 is magnetic permeability of vacuum ($\simeq 10^{-7} Tm/A$).

4.3 Exchange Coupling energy of the Mn^{2+} spins in $(Ga, Mn)As$ DMS

The exchange coupling energy of the indirect exchange interaction in ferromagnetic metals and alloys contains oscillatory term that vary as $F(k_F R_{nm})$, where $F(k_F R_{nm})$ is the Ruderman function and R_{nm} is separation between localized spins, as in Eq. (3.2. 37), in which the p-d exchange energy J_{pd} is found to play the important role. This parameter has been utilized in explaining the ferromagnetic transition temperature T_C of the DMSs. However, the estimated T_C for $(Ga, Mn)As$ DMS to date remain far below room temperature due to the inadequacy of the density of holes required for ferromagnetic mediation. On the other hand, recent experimental observations of the enhancement of T_C by photo excitation [14, 15] give the hope of enhancing T_C possibly to room temperature value. To calculate the exchange coupling resulting from radiation effect we use the second order energy correction using time dependent perturbation theory. This enables us to find the indirect exchange interaction between two localized spins [85] mediated by carriers from accepter doping and electrons/holes created due to excitation of electrons from the valence band. This energy is written, using Eq. (4.2. 1), as

$$E^{(2)} = \sum_{n}\sum_{m}\sum_{q}\sum_{q'}\sum_{\sigma'} \frac{< n_q, \sigma|H_I|n_{q'}, \sigma' >< n_{q'}, \sigma'|H_I|n_q, \sigma >}{\omega_q - \omega_{\sigma\sigma'}}, \tag{4.3. 1}$$

where $\omega_{\sigma\sigma'} = \frac{E_\sigma - E_{\sigma'}}{\hbar}$ is transition frequency due to Zeeman splitting that could be from $-\frac{1}{2}\hbar$ (down) to $\frac{1}{2}\hbar$ (up) spin state and/or dictated by selection rule.

Now, it is usual to write

$$\begin{aligned} | < n_q, \sigma|H_I|n_{q'}, \sigma' > |^2 =& < n_q, \sigma|H_I|n_{q'}, \sigma' >< n_{q'}, \sigma'|H_I|n_q, \sigma > \\ =& < n_q, \sigma|H_I|n_{q'}, \sigma' > (< n_q, \sigma|H_I|n_{q'}, \sigma' >)^*, \end{aligned} \tag{4.3. 2}$$

where

$$\begin{aligned} < n_q, \sigma|H_I|n_{q'}, \sigma' > = i \sum_{n,q,q',\sigma'} \eta_q \Big[& < n_q|\hat{d}_q|n_{q'} > e^{-i\omega_q t} e^{i\mathbf{q}\cdot\mathbf{R}_n} \\ & - < n_q|\hat{d}_q^+|n_{q'} > e^{i\omega_q t} e^{-i\mathbf{q}\cdot\mathbf{R}_n} \Big] < \sigma| \left[\frac{S_n^+ + S_n^-}{2} |\sigma' > \right], \end{aligned} \tag{4.3. 3}$$

and $< \sigma|S_n^+ + S_n^-|\sigma' >=< \sigma|S_n^+|\sigma' > + < \sigma|S_n^-|\sigma' >$.

Hence,

$$\begin{aligned} < n_q, \sigma|H_I|n_{q'}, \sigma' > = i \sum_{n}\sum_{q}\sum_{q'}\sum_{\sigma'} \eta_q \Big[& \sqrt{n_q + 1} < n_q + 1|n_{q'} > e^{-i\omega_q t} e^{i\mathbf{q}\cdot\mathbf{R}_n} \\ & - \sqrt{n_q} < n_q - 1|n_{q'} > e^{i\omega_q t} e^{-i\mathbf{q}\cdot\mathbf{R}_n} \Big] \\ & \times \frac{1}{2}(< \sigma|S_n^+|\sigma' > + < \sigma|S_n^-|\sigma' >), \end{aligned} \tag{4.3. 4}$$

and its hermitian conjugate is

$$\begin{aligned} (< n_q, \sigma|H_I|n_{q'}, \sigma' >)^* = -i \sum_{m}\sum_{q}\sum_{q'}\sum_{\sigma'} \eta_q \Big[& \sqrt{n_q + 1} < n_{q'}|n_q + 1 > e^{i\omega_q t} e^{-i\mathbf{q}\cdot\mathbf{R}_m} \\ & - \sqrt{n_q} < n_{q'}|n_q - 1 > e^{-i\omega_q t} e^{i\mathbf{q}\cdot\mathbf{R}_m} \Big] \\ & \times \frac{1}{2}(< \sigma'|S_m^-|\sigma > + < \sigma'|S_m^+|\sigma >). \end{aligned} \tag{4.3. 5}$$

Substituting Eq. (4.3. 4) and (4.3. 5) into Eq. (4.3. 2),

$$
\begin{aligned}
|<n_q|H_I|n_{q'}>|^2 = \sum_n \sum_m \sum_q \sum_{q'} \sum_{\sigma'} \eta_q^2 \Big[& (n_q+1) < n_q+1|n_{q'}>< n_{q'}|n_q+1> e^{i\mathbf{q}\cdot(R_n-R_m)} \\
& - \sqrt{n_q}\sqrt{n_q+1} < n_q-1|n_{q'}>< n_{q'}|n_q+1> e^{2i\omega_q t} e^{-i\mathbf{q}\cdot(R_n-R_m)} \\
& - \sqrt{n_q+1}\sqrt{n_q} < n_q+1|n_{q'}>< n_{q'}|n_q-1> e^{-2i\omega_q t} e^{i\mathbf{q}\cdot(R_n+R_m)} \\
& + n_q < n_q-1|n_{q'}>< n_{q'}|n_q-1> e^{-i\mathbf{q}\cdot(R_n-R_m)} \Big] \\
& \times \frac{1}{4}(<\sigma|S_n^+|\sigma'> + <\sigma|S_n^-|\sigma'>) \\
& \times (<\sigma'|S_m^-|\sigma> + <\sigma'|S_m^+|\sigma>). \qquad (4.3.\ 6)
\end{aligned}
$$

Similarly, substituting expression Eq. (4.3. 6) in to (4.3. 1),

a) when $n_{q'} = n_q + 1$, gives

$$
\begin{aligned}
E^{(2)} = \frac{1}{4} \sum_n \sum_m \sum_q \sum_{\sigma'} & \frac{\eta_q^2 (n_q+1)}{\omega_q - \omega_{\sigma\sigma'}} e^{i\mathbf{q}\cdot(R_n-R_m)} (<\sigma|S_n^+|\sigma'> + <\sigma|S_n^-|\sigma'>) \\
& \times (<\sigma'|S_m^-|\sigma> + <\sigma'|S_m^+|\sigma>), \qquad (4.3.\ 7)
\end{aligned}
$$

and

b) when $n_{q'} = n_q - 1$,

$$
\begin{aligned}
E^{(2)} = \frac{1}{4} \sum_n \sum_m \sum_q \sum_{\sigma'} & \frac{\eta_q^2 n_q}{\omega_q - \omega_{\sigma\sigma'}} e^{-i\mathbf{q}\cdot(R_n-R_m)} (<\sigma|S_n^+|\sigma'> + <\sigma|S_n^-|\sigma'>) \\
& \times (<\sigma'|S_n^+|\sigma> + <\sigma'|S_n^-|\sigma>). \qquad (4.3.\ 8)
\end{aligned}
$$

Adding both Eq. (4.3. 7) and (4.3. 8) gives the total expression that would be written as,

$$
\begin{aligned}
E^2 = \frac{1}{4} \sum_m \sum_n \sum_q \sum_{\sigma'} & \frac{\eta_q^2}{\omega_q - \omega_{\sigma\sigma'}} \Big((n_q+1) e^{i\mathbf{q}\cdot\mathbf{R}_{nm}} + n_q e^{-i\mathbf{q}\cdot\mathbf{R}_{nm}} \Big) \\
& \times (<\sigma|S_n^+|\sigma'>< \sigma'|S_m^-|\sigma> + <\sigma|S_n^+|\sigma>< \sigma'|S_m^+|\sigma> \\
& + <\sigma|S_n^-|\sigma'>< \sigma'|S_m^-|\sigma> + <\sigma|S_n^-|\sigma'>< \sigma'|S_m^+|\sigma>). \qquad (4.3.\ 9)
\end{aligned}
$$

In spin waves spins can not rise or lower at the same time, hence, terms $S_n^+ S_m^-$ and $S_n^- S_m^+$ should be retained. Therefore,

$$E^2 = \frac{1}{4}\sum_m \sum_n \sum_q \sum_{\sigma'} \frac{\eta_q^2}{\omega_q - \omega_{\sigma\sigma'}} \left((n_q + 1)e^{i\mathbf{q}\cdot\mathbf{R}_{nm}} + n_q e^{-i\mathbf{q}\cdot\mathbf{R}_{nm}} \right)$$
$$\times (< \sigma|S_n^+|\sigma' >< \sigma'|S_m^-|\sigma > + < \sigma|S_n^-|\sigma' >< \sigma'|S_m^+|\sigma >). \quad (4.3.\ 10)$$

Considering the commutation relation for the spin state S,

$$[S_n^+, S_m^-] = S_n^+ S_m^- - S_m^- S_n^+ = -2iS^z \delta_{nm}. \quad (4.3.\ 11)$$

Since the spin wave is not due to a spin flip at a site but due to wave propagation the two spins being at different sites, $n \neq m$, the delta function vanishes so that $S_m^- S_n^+ = S_n^+ S_m^-$ and in terms of one of these,

$$E^{(2)} \cong \frac{1}{2}\sum_{n,m,q} \frac{\eta_q^2}{\omega_q - \omega_{\sigma\sigma'}} \left[(n_q + 1)e^{i\mathbf{q}\cdot\mathbf{R}_{nm}} + n_q e^{-i\mathbf{q}\cdot\mathbf{R}_{nm}} \right] S_n^+ S_m^-. \quad (4.3.\ 12)$$

This energy operator can be expressed as,

$$\hat{H}' \cong \sum_{nm} J_{nm} S_n^+ S_m^-, \quad (4.3.\ 13)$$

which has resemblance of the Heisenberg type of Hamiltonian. Hence, the exchange coupling energy is given by,

$$J_{nm} = \sum_q \frac{g^2 \mu_B^2 \frac{\mu_0 \omega_q}{4V}}{\omega_q - \omega_{\sigma\sigma'}} \left[(n_q + 1)e^{i\mathbf{q}\cdot\mathbf{R}_{nm}} + n_q e^{-i\mathbf{q}\cdot\mathbf{R}_{nm}} \right]. \quad (4.3.\ 14)$$

For number (intensity) of photons $n_q \gg 1$, and $qR_{nm} << 1$, the exchange coupling energy could be written as,

$$J_{nm} \cong \sum_q \frac{g^2 \mu_B^2 \frac{\mu_0 \omega_q}{2V}}{\omega_q - \omega_{\sigma\sigma'}} n_q \quad (4.3.\ 15)$$

Using the identity

$$\frac{1}{\omega_q - \omega_{\sigma\sigma'} + i\varepsilon} = \wp\left(\frac{1}{\omega_q - \omega_{\sigma\sigma'}}\right) - i\pi\delta(\omega_q - \omega_{\sigma\sigma'}), \quad (4.3.\ 16)$$

in Eq. (4.3. 15), we can write

$$J_{nm} \cong g^2\mu_B^2\frac{\mu_0}{2V}n_q\left[\wp\sum_q\frac{\omega_q}{\omega_q-\omega_{\sigma\sigma'}}-i\pi\sum_q\delta(\omega_q-\omega_{\sigma\sigma'})\right] \tag{4.3. 17}$$

where the first term in the right hand side is the principal ($\wp$). Eq. (4.3. 17) can be written as

$$J_{nm} \cong \chi + i\gamma \tag{4.3. 18}$$

where χ denotes the shift in energy as a result of photo-excitation and γ represents the line broadening. At resonance γ will be a delta function.

The plot of this function is shown in the next section, where ε can be associated with the resonance line broadening.

One can also write T_C by substituting Eq. (4.3. 17) into (3.2. 40), as

$$T_C = \frac{xS(S+1)ZJ_{nm}}{3\kappa_B}, \tag{4.3. 19}$$

where $Z = 12$ for fcc lattice structure, $S = 5/2$. J_{nm} could be estimated to the order of $10^{-22}J$, hence, T_C which to our understanding can be significantly large at or near FMR and/or SWR.

4.4 Result and Discussion

The interaction of radiation with Mn^{2+} spins can give rise to exchange coupling between magnetic moments of Mn^{2+}. It appears that the photon exchange between Mn^{2+} spins does the same job as do the electrons and/or holes in metals and semiconductors. For better numerical estimate we considered intensity of polarized excitation pulse due to the irradiated photon (n_q) of the order of $\sim 10^{15} photons/pulse/cm^2$, if one can make adjustment to experiment done as in reference [73] for a system assumed to be confined in a volume $V = 0.01nm^3$. Hence, using Eq. (4.3. 17) the photon assisted exchange coupling energy could be shown to be of the order of $10^{-22}J$ and is equivalent to the result obtained by Geonnenwein et al., [91]. This energy is understood as responsible for the indirect exchange interaction of the localized spins in analogy with the RKKY expression of a kind shown in Eq. (3.2. 41). It is argued that in

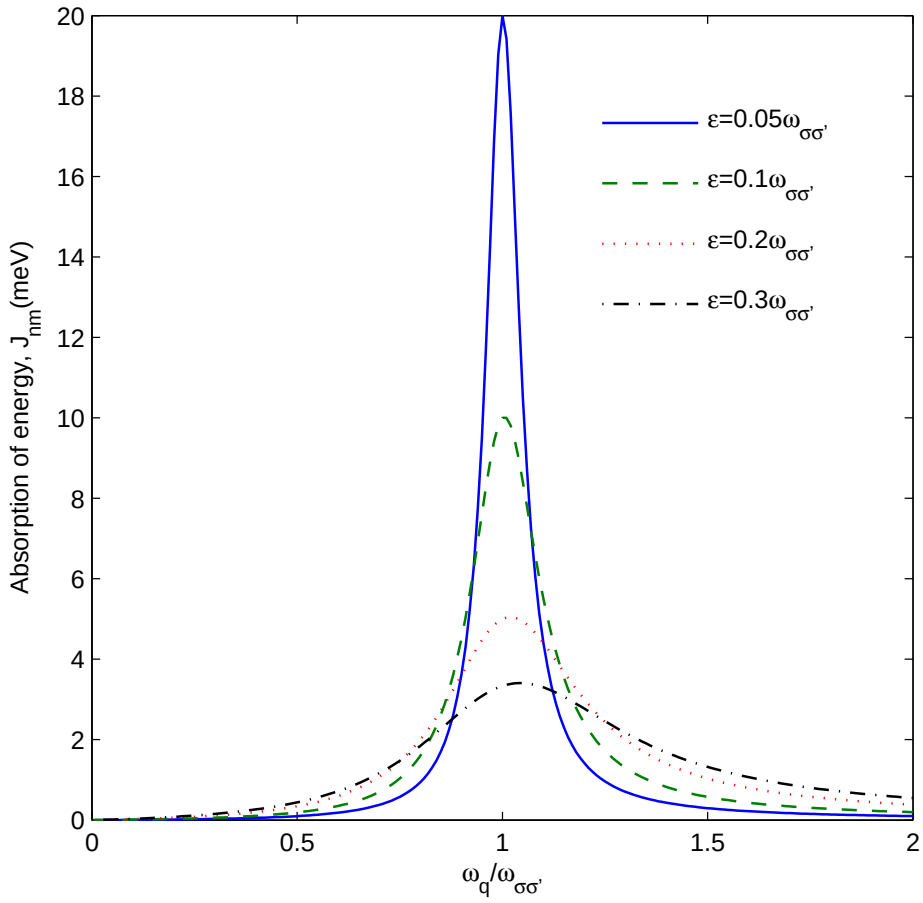

Fig. 4.1: Exchange coupling energy J_{nm} vs. frequency of the radiation field ω_q, for different half line width, ε.

addition to electron and/or hole exchange coupling we have photo exchange doing the same and hence leading to further enhancement of T_C.

Figs. 4.1 show increase in exchange coupling energy with source frequency that would rise to maximum near resonance. The line broadening of the absorption can be seen from Fig. 4.1 and 4.2 as a function of ε, and shown to decrease the energy revealing that the light frequency far from the resonance value would create less amount of holes required to mediate ferromagnetism. This is shown by plotting based on Eq. (4.3. 17), in which the imaginary part is responsible for absorption.

The increase in intensity of the irradiated photon (n_q) would also enhance ferromagnetism as J_{nm} will be enhanced. As the radiation field enters only a small layer,

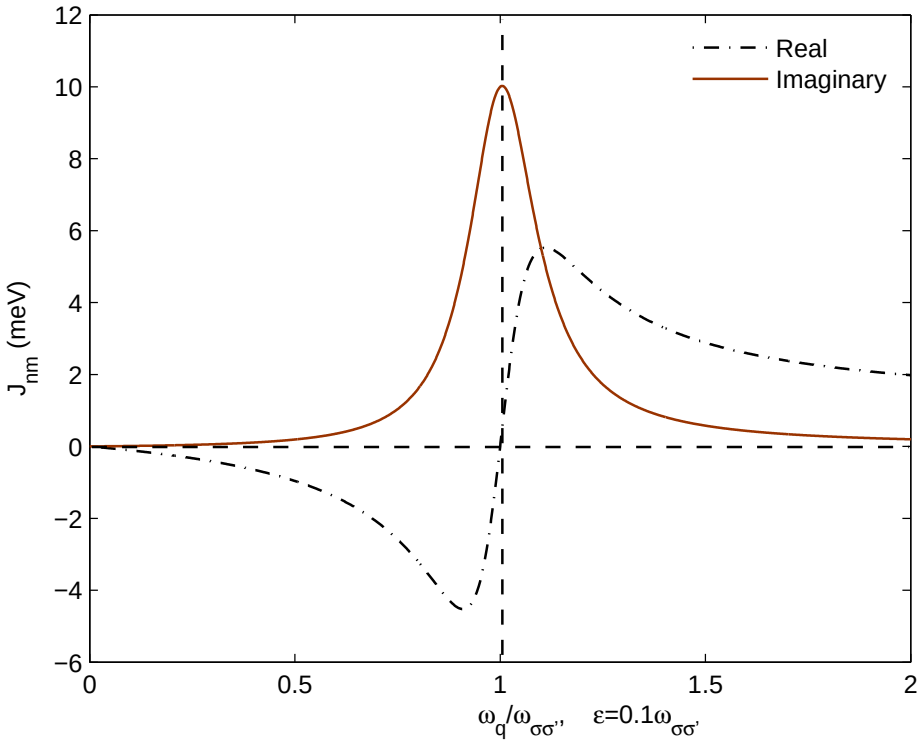

Fig. 4.2: Exchange coupling energy, J_{nm}, vs. frequency of radiation field, ω_q for $\varepsilon = 0.1\omega_{\sigma\sigma'}$.

the spins in the layer only experience ferromagnetic resonance where the others do not participate. So $k = 0$ mode that corresponds to ferromagnetic resonance may be partially excited along with other spin wave modes. In spin wave resonance the local moments are no longer parallel inside the sample and restoring torques due to exchange interaction resulting in effects in $k \neq 0$ excitations. The ferromagnetic and spin wave resonance experiments can be used to see the validity of the above suggested spin exchange interaction. It is argued that the irradiation mechanism can contribute to the enhancement of ferromagnetic transition temperature T_C at or near resonance. It is suggested that experiments with photo-excitation on ferromagnetic DMSs, such as (Ga,Mn)As, with finite T_C value be performed so as to further investigate the role of photo-excitation in this important class of semiconductors.

5

Photo-excitation and Scattering Effects on Ferromagnetism of the $(Ga, Mn)As$ DMS

5.1 Introduction

In this chapter we study effects of photon excitation and magnon-scattering on magnetization and ferromagnetic transition temperature T_C, of the diluted magnetic semiconductor $(Ga, Mn)As$. The Hamiltonian describing the system is constructed based on the standard models. The method of double-time temperature dependent Green function [80] which is appropriate generalization of the correlation function is employed in calculating the average of dynamical quantities. This approach is considered in a view that the particles in the system interact with one another. Applying this formalism the dispersion and mean number of magnons are calculated, which leads to determine magnetization, ferromagnetic transition temperature T_C and magnon specific heat capacity C_{mag}.

5.2 Formulation of the Problem

The system Hamiltonian is written as

$$H = H_{mag} + H_{phot} + H_{mag-phot}, \tag{5.2. 1}$$

where

$$H_{mag} = \sum_k \omega_k b_k^+ b_k + ZxJ_{nm}\xi(k_1, k_2, k_3, k_4). \tag{5.2. 2}$$

The first term in the right hand side of Eq. (5.2. 2) represents free magnon energy and the second term magnon scattering energy. $\omega_k = 2xJ_{nm}Sa^2k^2 + g\mu_B B$ represents the

free magnon dispersion where J_{nm} is the exchange integral between spins localized at sites n and m, S represents localized spins per atom, a is the separation between localized spins, $\boldsymbol{k}$ is magnon wave vector, g is the Landé g-factor, μ_B is the Bohr magneton, B is magnitude of applied field, $b_k^+(b_k)$ denotes the magnon creation (annihilation) operator, Z represents the number of nearest neighbor atoms considered for fcc atomic structure, x is percentage of impurity concentration replacing part of the element which is at the cation site. This concentration, x, is given by $x = \frac{N_{imp}}{N}$, where N_{imp} is number of impurities randomly distributed on lattice of N sites [65, 71] and expressed together with the representation of the impurity spins in terms of Holstein-Primakoff (HP) bosons [92], where by coarse graining the spin density S_n (spin at site n) can be replaced by a smooth function using bosonic fields,

$$S_n^+ = (\sqrt{2xS - a_n^+ a_n})a_n, \tag{5.2. 3}$$

$$S_n^- = a_n^+(\sqrt{2xS - a_n^+ a_n}), \tag{5.2. 4}$$

and

$$S_n^z = xS - a_n^+ a_n, \tag{5.2. 5}$$

which can be substituted in to $\sum_{nm} J_{nm}\mathbf{S}_n.\mathbf{S}_m$ with inclusion of the term involving external field $\mathbf{B}$ (i.e., $g\mu_B\mathbf{B}\sum_n S_n^z$) resulting in the Heisenberg type expression. Since the spin deviations are not localized to a particular lattice site but propagates throughout, it is necessary to use fourier variables, which are given by

$$a_n = \frac{1}{\sqrt{N}}\sum_k e^{-i\mathbf{k}.\mathbf{r}_n} b_k; \;\; a_n^+ = \frac{1}{\sqrt{N}}\sum_k e^{i\mathbf{k}.\mathbf{r}_n} b_k^+, \tag{5.2. 6}$$

where the Fourier transformation variables also satisfy the bosonic relations $[b_k, b_{k'}^+] = \delta_{kk'}$, hence, used in writing the Hamiltonian. On the other hand, the second term on the right hand side of Eq. (5.2. 2),

$$\xi(k_1,k_2,k_3,k_4) = \frac{1}{4N}\sum_{k_1,k_2,k_3,k_4}\Delta(k_1+k_2-k_3-k_4)b_{k_1}^+ b_{k_2}^+ b_{k_3} b_{k_4}\Big[\gamma_{1+2-3} + \gamma_1 + \gamma_{2-3-4} + \gamma_{-4} - 4\gamma_{1-4}\Big] \tag{5.2. 7}$$

is responsible for spin wave scattering, where $\gamma_k = \frac{1}{Z}\sum_\delta e^{\mathbf{k}\cdot\delta} = (1 - \frac{k^2\delta^2}{6})$ with $\gamma_1 = \gamma_{k_1} = (1 - \frac{k_1^2\delta^2}{6})$, $\gamma_{1-4} = \gamma_{k_1}\gamma_{-k_4}$ and so on, taking into consideration $k\delta << 1$. δ is supposed to join the central atom to its nearest neighbors. The second term in the right hand side of Eq. (5.2. 1),

$$H_{Phot} = \sum_k \lambda_k d_k^+ d_k \tag{5.2. 8}$$

represents free photon energy obtained from quantization of the electromagnetic radiation, $d_k^+(d_k)$ is photon creation (annihilation) operator, and $\lambda_k = ck$ is dispersion of photon where c is speed of light in free space. The third term in the right hand side of Eq. (5.2. 1),

$$H_{mag-Phot} = \sum_k \chi_k(d_{-k}^+ b_k + d_{-k} b_k^+) \tag{5.2. 9}$$

represents the magnon-photon interaction energy in which magnon and photon are supposed to propagate in opposite directions. $\chi_k = g\mu_\beta(\frac{S\mu_0 ck}{4V})^{\frac{1}{2}}$ in this expression is momentum dependent magnon-photon coupling strength, μ_0 is permeability of free space, and V is volume of the radiation field cavity.

5.3 Magnon Dispersion and the Green Function Formalism

Now, it is essential to find the average number of magnons and dispersion of the system under study employing the Green function formalism. This could be done starting with, substituting Eq. (5.2. 1) into Eq. (2.3. 19). Hence,

$$\epsilon_k \ll b_k; b_{k'}^+ \gg = \frac{< [b_k, b_{k'}^+] >}{2\pi} + \ll [b_k, H]; b_{k'}^+ \gg . \tag{5.3. 1}$$

The commutation relation can be solved substituting Eq. (5.2. 1) into (5.3. 1). The subscript k in H is substituted by p to avoid confusion, thus, the bosonic commutation relation

$$\begin{aligned}
[b_k, H] &= [b_k, \sum_p \omega_p b_p^+ b_p + \sum_p \lambda_p d_p^+ d_p + \sum_p \chi_p (d_{-p}^+ b_p + d_{-p} b_p^+) \\
&+ \frac{1}{4N} x Z J_{nm} \sum_{k_1,k_2,k_3,k_4} \Delta(k_1 + k_2 - k_3 - k_4) b_{k_1}^+ b_{k_2}^+ b_{k_3} b_{k_4} \\
&\times (\gamma_{1+2-3} + \gamma_1 + \gamma_{2-3-4} + \gamma_{-4} - 4\gamma_{1-4})] \\
&= \sum_p \omega_p \delta_{k,p} b_p + \sum_p \chi_p \delta_{k,p} d_{-p} + \frac{1}{4N} x Z J_{nm} \sum_{k_1,k_2,k_3,k_4} \Delta(k_1 + k_2 - k_3 - k_4) \\
&\times \delta_{k,k_1} b_{k_2}^+ b_{k_3} b_{k_4} (\gamma_{1+2-3} + \gamma_1 + \gamma_{2-3-4} + \gamma_{-4} - 4\gamma_{1-4}) \\
&+ \frac{1}{4N} x Z J_{nm} \sum_{k_1,k_2,k_3,k_4} \Delta(k_1 + k_2 - k_3 - k_4) \delta_{k,k_2} b_{k_1}^+ b_{k_3} b_{k_4} \\
&\times (\gamma_{1+2-3} + \gamma_1 + \gamma_{2-3-4} + \gamma_{-4} - 4\gamma_{1-4}), \qquad (5.3.\ 2)
\end{aligned}$$

where $\delta_{k,p} = 1$ only when $p = k$, $k_1 = k$ and $k_2 = k$ and zero otherwise by the property of delta function. Making use of these conditions Eq. (5.3. 2) can be rewritten as

$$\begin{aligned}
[b_k, H] &= \omega_k b_k + \chi_k d_{-k} + \frac{1}{4N} x Z J_{nm} \sum_{k_2,k_3,k_4} \Delta(k + k_2 - k_3 - k_4) b_{k_2}^+ b_{k_3} b_{k_4} \\
&\times (\gamma_{k+2-3} + \gamma_k + \gamma_{2-3-4} + \gamma_{-4} - 4\gamma_{k-4}) \\
&+ \frac{1}{4N} \sum_{nm} J_{nm} \sum_{k_1,k_3,k_4} \Delta(k_1 + k - k_3 - k_4) b_{k_1}^+ b_{k_3} b_{k_4} \\
&\times (\gamma_{1+k-3} + \gamma_1 + \gamma_{k-3-4} + \gamma_{-4} - 4\gamma_{1-4}). \qquad (5.3.\ 3)
\end{aligned}$$

Substituting Eq. (5.3. 3) into (5.3. 1) for $[b_k, H]$, we obtain

$$\epsilon_k \ll b_k; b_{k'}^+ \gg = \frac{< [b_k, b_{k'}^+] >}{2\pi}$$
$$+ \ll \omega_k b_k + \chi_k d_{-k} + \frac{1}{4N} \sum_{nm} J_{nm} \sum_{k_2,k_3,k_4} \Delta(k + k_2 - k_3 - k_4) b_{k_2}^+ b_{k_3} b_{k_4}$$
$$\times (\gamma_{k+2-3} + \gamma_k + \gamma_{2-3-4} + \gamma_{-4} - 4\gamma_{k-4})$$
$$+ \frac{1}{4N} xZJ_{nm} \sum_{k1,k3,k4} \Delta(k_1 + k - k_3 - k_4) b_{k_1}^+ b_{k_3} b_{k_4}$$
$$\times (\gamma_{1+k-3} + \gamma_1 + \gamma_{k-3-4} + \gamma_{-4} - 4\gamma_{1-4}); b_{k'}^+ \gg . \quad (5.3.\ 4)$$

Making same rearrangements, Eq. (5.3. 4) can be rewritten as

$$\epsilon_k \ll b_k; b_{k'}^+ \gg = \frac{< [b_k, b_{k'}^+] >}{2\pi} + \omega_k \ll b_k; b_{k'}^+ \gg + \chi_k \ll d_{-k}; b_{k'}^+ \gg$$
$$+ \frac{1}{4N} \sum_{nm} J_{nm} \sum_{k_2,k_3,k_4} \Delta(k + k_2 - k_3 - k_4) \ll b_{k_2}^+ b_{k_3} b_{k_4}; b_{k'}^+ \gg$$
$$\times (\gamma_{k+2-3} + \gamma_k + \gamma_{2-3-4} + \gamma_{-4} - 4\gamma_{k-4})$$
$$+ \frac{1}{4N} xZJ_{nm} \sum_{k_1,k_3,k_4} \Delta(k_1 + k - k_3 - k_4) \ll b_{k_1}^+ b_{k_3} b_{k_4}; b_{k'}^+ \gg$$
$$\times (\gamma_{1+k-3} + \gamma_1 + \gamma_{k-3-4} + \gamma_{-4} - 4\gamma_{1-4}), \quad (5.3.\ 5)$$

which can also be written using decoupling mechanism as

$$\epsilon_k \ll b_k; b_{k'}^+ \gg = \frac{< [b_k, b_{k'}^+] >}{2\pi}$$
$$+ \omega_k \ll b_k; b_{k'}^+ \gg + \chi_k \ll d_{-k}; b_{k'}^+ \gg$$
$$+ \frac{1}{4N} \sum_{nm} J_{nm} \sum_{k_2,k_3,k_4} \Delta(k + k_2 - k_3 - k_4)(< b_{k_2}^+ b_{k_3} > \ll b_{k_4}; b_{k'}^+ \gg$$
$$+ < b_{k_2}^+ b_{k_4} > \ll b_{k_3}; b_{k'}^+ \gg)(\gamma_{k+2-3} + \gamma_k + \gamma_{2-3-4} + \gamma_{-4} - 4\gamma_{k-4})$$
$$+ \frac{1}{4N} xZJ_{nm} \sum_{k_1,k_3,k_4} \Delta(k_1 + k - k_3 - k_4)(< b_{k_1}^+ b_{k_3} > \ll b_{k_4}; b_{k'}^+ \gg$$
$$+ < b_{k_1}^+ b_{k_4} > \ll b_{k_3}; b_{k'}^+ \gg)(\gamma_{1+k-3} + \gamma_1 + \gamma_{k-3-4} + \gamma_{-4} - 4\gamma_{1-4}). \quad (5.3.\ 6)$$

Collecting like terms, Eq. (5.3. 6) can also be written as

$$\epsilon_k \ll b_k; b_{k'}^+ \gg = \frac{< [b_k, b_{k'}^+] >}{2\pi} + \omega_k \ll b_k; b_{k'}^+ \gg + \chi_k \ll d_{-k}; b_{k'}^+ \gg$$
$$+ \frac{1}{4N} x Z J_{nm} \sum_{k_2,k_3,k_4} \Delta(k + k_2 - k_3 - k_4) < b_{k_2}^+ b_{k_3} > \ll b_{k_4}; b_{k'}^+ \gg$$
$$\times (\gamma_{k+2-3} + \gamma_k + \gamma_{2-3-4} + \gamma_{-4} - 4\gamma_{k-4})$$
$$+ \frac{1}{4N} x Z J_{nm} \sum_{k_2,k_3,k_4} \Delta(k + k_2 - k_3 - k_4) < b_{k_2}^+ b_{k_4} > \ll b_{k_3}; b_{k'}^+ \gg$$
$$\times (\gamma_{k+2-3} + \gamma_k + \gamma_{2-3-4} + \gamma_{-4} - 4\gamma_{k-4})$$
$$+ \frac{1}{4N} x Z J_{nm} \sum_{k_1,k_3,k_4} \Delta(k_1 + k - k_3 - k_4) < b_{k_1}^+ b_{k_3} > \ll b_{k_4}; b_{k'}^+ \gg$$
$$\times (\gamma_{1+k-3} + \gamma_1 + \gamma_{k-3-4} + \gamma_{-4} - 4\gamma_{1-4})$$
$$+ \frac{1}{4N} x Z J_{nm} \sum_{k_1,k_3,k_4} \Delta(k_1 + k - k_3 - k_4) < b_{k_1}^+ b_{k_4} > \ll b_{k_3}; b_{k'}^+ \gg$$
$$\times (\gamma_{1+k-3} + \gamma_1 + \gamma_{k-3-4} + \gamma_{-4} - 4\gamma_{1-4}), \quad (5.3.\ 7)$$

which can be simplified to

$$\epsilon_k \ll b_k; b_{k'}^+ \gg = \frac{< [b_k, b_{k'}^+] >}{2\pi} + \omega_k \ll b_k; b_{k'}^+ \gg + \chi_k \ll d_{-k}; b_{k'}^+ \gg$$
$$+ \frac{1}{4N} x Z J_{nm} \sum_{k_2,k_3,k_4} \Delta(k + k_2 - k_3 - k_4) < n_{23} > \delta_{23} \ll b_{k_4}; b_{k'}^+ \gg$$
$$\times (\gamma_{k+2-3} + \gamma_k + \gamma_{2-3-4} + \gamma_{-4} - 4\gamma_{k-4})$$
$$+ \frac{1}{4N} x Z J_{nm} \sum_{k_2,k_3,k_4} \Delta(k + k_2 - k_3 - k_4) < n_{24} > \delta_{24} \ll b_{k3}; b_{k'}^+ \gg$$
$$\times (\gamma_{k+2-3} + \gamma_k + \gamma_{2-3-4} + \gamma_{-4} - 4\gamma_{k-4})$$
$$+ \frac{1}{4N} x Z J_{nm} \sum_{k_1,k_3,k_4} \Delta(k_1 + k - k_3 - k_4) < n_{13} > \delta_{13} \ll b_{k_4}; b_{k'}^+ \gg$$
$$\times (\gamma_{1+k-3} + \gamma_1 + \gamma_{k-3-4} + \gamma_{-4} - 4\gamma_{1-4}))$$
$$+ \frac{1}{4N} x Z J_{nm} \sum_{k_1,k_3,k_4} \Delta(k_1 + k - k_3 - k_4) < n_{14} > \delta_{14} \ll b_{k_3}; b_{k'}^+ \gg$$
$$\times (\gamma_{1+k-3} + \gamma_1 + \gamma_{k-3-4} + \gamma_{-4} - 4\gamma_{1-4}). \quad (5.3.\ 8)$$

in which by the property of Kronecker delta function, $\delta_{23} = 1$ for $k_3 = k_2$, $\delta_{24} = 1$ for $k_4 = k_2$, $\delta_{14} = 1$ for $k_4 = k_1$, $\delta_{13} = 1$ for $k_3 = k_1$ and zero otherwise where $< b_{k_1}^+ b_{k_3} > = <$

$n_{13} > \delta_{13} =< b^+_{k_1} b_{k_1} >=< n_1 >$, $< b^+_{k_2} b_{k_3} >=< n_{23} > \delta_{23} =< b^+_{k_2} b_{k_2} >=< n_2 >$ and so on. Hence, Eq. (5.3. 8) can be more simplified into

$$\begin{aligned}
\epsilon_k \ll b_k; b^+_{k'} \gg &= \frac{< [b_k, b^+_{k'}] >}{2\pi} + \omega_k \ll b_k; b^+_{k'} \gg + \chi_k \ll d_{-k}; b^+_{k'} \gg \\
&+ \frac{1}{4N} x Z J_{nm} \sum_{k_2,k_4} \Delta(k-k_4) < n_2 > \ll b_{k_4}; b^+_{k'} \gg (\gamma_k + \gamma_k + \gamma_{-4} + \gamma_{-4} - 4\gamma_{k-4}) \\
&+ \frac{1}{4N} x Z J_{nm} \sum_{k_2,k_3} \Delta(k-k_3) < n_2 > \ll b_{k_3}; b^+_{k'} \gg (\gamma_{k+2-3} + \gamma_k + \gamma_3 + \gamma_{-2} - 4\gamma_{k-2}) \\
&+ \frac{1}{4N} x Z J_{nm} \sum_{k_1,k_4} \Delta(k-k_4) < n_1 > \ll b_{k_4}; b^+_{k'} \gg (\gamma_k + \gamma_1 + \gamma_{k-1-4} + \gamma_{-4} - 4\gamma_{1-4}) \\
&+ \frac{1}{4N} x Z J_{nm} \sum_{k_1,k_3} \Delta(k-k_3) < n_1 > \ll b_{k_3}; b^+_{k'} \gg (\gamma_{1+k-3} + \gamma_1 + \gamma_{k-3-1} + \gamma_{-1} - 4\gamma_0),
\end{aligned} \tag{5.3. 9}$$

where $\Delta(k-k_3) = 1$ when $k_3 = k$, $\Delta(k-k_4) = 1$ when $k_4 = k$ and zero otherwise, hence,

$$\begin{aligned}
\epsilon_k \ll b_k; b^+_{k'} \gg &= \frac{< [b_k, b^+_{k'}] >}{2\pi} + \omega_k \ll b_k; b^+_{k'} \gg + \chi_k \ll d_{-k}; b^+_{k'} \gg \\
&+ \frac{1}{4N} x Z J_{nm} < n_2 > \sum_{k_2} \ll b_k; b^+_{k'} \gg (\gamma_k + \gamma_k + \gamma_{-k} + \gamma_{-k} - 4\gamma_0) \\
&+ \frac{1}{4N} x Z J_{nm} < n_2 > \sum_{k_2} \ll b_k; b^+_{k'} \gg (\gamma_2 + \gamma_k + \gamma_k + \gamma_{-2} - 4\gamma_{k-2}) \\
&+ \frac{1}{4N} x Z J_{nm} < n_1 > \sum_{k_1} \ll b_k; b^+_{k'} \gg (\gamma_k + \gamma_1 + \gamma_{-1} + \gamma_{-k} - 4\gamma_{1-k}) \\
&+ \frac{1}{4N} x Z J_{nm} < n_1 > \sum_{k_1} \ll b_k; b^+_{k'} \gg (\gamma_1 + \gamma_1 + \gamma_{-1} + \gamma_{-1} - 4\gamma_0).
\end{aligned} \tag{5.3. 10}$$

Collecting like terms, the last equation can also be written as

$$\epsilon_k \ll b_k; b_{k'}^+ \gg = \frac{< [b_k, b_{k'}^+] >}{2\pi} + \omega_k \ll b_k; b_{k'}^+ \gg + \chi_k \ll d_{-k}; b_{k'}^+ \gg$$
$$+ \frac{1}{4N} x Z J_{nm} \sum_{k_2} < n_2 > \ll b_k; b_{k'}^+ \gg (4\gamma_k - 4\gamma_0)$$
$$+ \frac{1}{4N} x Z J_{nm} \sum_{k_2} < n_2 > \ll b_k; b_{k'}^+ \gg (2\gamma_2 + 2\gamma_k - 4\gamma_{k-2})$$
$$+ \frac{1}{4N} x Z J_{nm} \sum_{k_1} < n_1 > \ll b_k; b_{k'}^+ \gg (2\gamma_k + 2\gamma_1 + -4\gamma_{1-k})$$
$$+ \frac{1}{4N} x Z J_{nm} \sum_{k_1} < n_1 > \ll b_k; b_{k'}^+ \gg (4\gamma_1 - 4\gamma_0). \quad (5.3.\ 11)$$

Taking n out of the summation,

$$\epsilon_k \ll b_k; b_{k'}^+ \gg = \frac{< [b_k, b_{k'}^+] >}{2\pi} + \omega_k \ll b_k; b_{k'}^+ \gg + \chi_k \ll d_{-k}; b_{k'}^+ \gg$$
$$+ \frac{1}{4N} x Z J_{nm} < n_2 > \sum_{k_2} \ll b_k; b_{k'}^+ \gg (4\gamma_k - 4\gamma_0)$$
$$+ \frac{1}{4N} x Z J_{nm} < n_2 > \sum_{k_2} \ll b_k; b_{k'}^+ \gg (2\gamma_2 + 2\gamma_k - 4\gamma_{k-2})$$
$$+ \frac{1}{4N} x Z J_{nm} < n_1 > \sum_{k_1} \ll b_k; b_{k'}^+ \gg (2\gamma_k + 2\gamma_1 + -4\gamma_{1-k})$$
$$+ \frac{1}{4N} x Z J_{nm} < n_1 > \sum_{k_1} \ll b_k; b_{k'}^+ \gg (4\gamma_1 - 4\gamma_0). \quad (5.3.\ 12)$$

Following similar procedure we can write the equation of motion for $\ll d_{-k}; b_{k'}^+ \gg$, as

$$\ll d_{-k}; b_{k'}^+ \gg = \frac{\chi_k}{(\epsilon_k - \lambda_{-k})} \ll b_k; b_{k'}^+ \gg, \quad (5.3.\ 13)$$

where

$$\epsilon_k \ll d_{-k}; b_{k'}^+ \gg = \frac{< [d_{-k}, b_{k'}^+] >}{2\pi} \ll [d_{-k}, H]; b_k^+ \gg . \quad (5.3.\ 14)$$

Making substitution for H in Eq. 5.3. 14 and solving the commutation relation leads

Eq. (5.3. 12) to

$$\begin{aligned}\epsilon_k \ll b_k; b_{k'}^+ \gg &= \frac{< [b_k, b_{k'}^+] >}{2\pi} + \omega_k \ll b_k; b_{k'}^+ \gg + \chi_k \frac{\chi_k}{(\epsilon_k - \lambda_{-k})} \ll b_k; b_{k'}^+ \gg \\ &+ \frac{1}{4N} xZJ_{nm} < n_2 > \sum_{k_2} \ll b_k; b_{k'}^+ \gg (4\gamma_k - 4\gamma_0) \\ &+ \frac{1}{4N} xZJ_{nm} < n_2 > \sum_{k_2} \ll b_k; b_{k'}^+ \gg (2\gamma_2 + 2\gamma_k - 4\gamma_{k-2}) \\ &+ \frac{1}{4N} xZJ_{nm} < n_1 > \sum_{k_1} \ll b_k; b_{k'}^+ \gg (2\gamma_k + 2\gamma_1 + -4\gamma_{1-k}) \\ &+ \frac{1}{4N} xZJ_{nm} < n_1 > \sum_{k_1} \ll b_k; b_{k'}^+ \gg (4\gamma_1 - 4\gamma_0). \end{aligned} \tag{5.3. 15}$$

Collecting like terms,

$$\begin{aligned}\epsilon_k \ll b_k; b_{k'}^+ \gg &= \frac{< [b_k, b_{k'}^+] >}{2\pi} + \Bigg\{ \omega_k + \chi_k \frac{\chi_k}{(\epsilon_k - \lambda_{-k})} \\ &+ \frac{1}{4N} xZJ < n_2 > \sum_{k_2} (4\gamma_k - 4\gamma_0) + \frac{1}{4N} < n_2 > \sum_{k_2} (2\gamma_2 + 2\gamma_k - 4\gamma_{k-2}) \\ &+ \frac{1}{4N} xZJ < n_1 > \sum_{k_1} (2\gamma_k + 2\gamma_1 - 4\gamma_{1-k}) + \frac{1}{4N} xZJ < n_1 > \sum_{k_1} (4\gamma_1 - 4\gamma_0) \Bigg\} \ll b_k; b_{k'}^+ \gg . \end{aligned} \tag{5.3. 16}$$

or

$$\begin{aligned}\epsilon_k \ll b_k; b_{k'}^+ \gg &= \frac{< [b_k, b_{k'}^+] >}{2\pi} + \Bigg\{ \omega_k + \chi_k \frac{\chi_k}{(\epsilon_k - \lambda_{-k})} \\ &+ \frac{1}{4N} xZJ < n_2 > \sum_{k_2} (4\gamma_k - 4\gamma_0 + 2\gamma_2 + 2\gamma_k - 4\gamma_{k-2}) \\ &+ \frac{1}{4N} xZJ < n_1 > \sum_{k_1} (2\gamma_k + 2\gamma_1 - 4\gamma_{1-k} + 4\gamma_1 - 4\gamma_0) \Bigg\} \ll b_k; b_{k'}^+ \gg, \end{aligned} \tag{5.3. 17}$$

where

$$\gamma_k = \left(1 - \frac{k^2\delta^2}{6}\right). \tag{5.3. 18}$$

For a lattice with a center of symmetry at each spin and using the definition of the $\gamma' s$ the terms in Eq. (5.3. 17) can be approximated to

$$6\gamma_k - 4\gamma_0 + 2\gamma_2 - 4\gamma_{k-2} \cong -4\frac{k^2\delta^2}{6}\frac{k_2^2\delta^2}{6} = -4\frac{k^2 k_2^2 \delta^4}{36}, \tag{5.3. 19}$$

and

$$2\gamma_k + 6\gamma_1 - 4\gamma_{1-k} - 4\gamma_0 \cong -4\frac{k_1^2\delta^2}{6}\frac{k^2\delta^2}{6} = -4\frac{k_1^2k^2\delta^4}{36}. \tag{5.3. 20}$$

Substituting Eq. (5.3. 19) and (5.3. 20) into (5.3. 17) gives

$$\epsilon_k \ll b_k; b_{k'}^+ \gg = \frac{< [b_k, b_{k'}^+] >}{2\pi} + \left\{\omega_k + \frac{\chi_k^2}{(\epsilon_k - \lambda_{-k})} - \frac{1}{N}xZJ_{nm} < n_1 > \sum_{k_1}\frac{k_1^2k^2\delta^4}{36}\right.$$
$$\left. - \frac{1}{N}xZJ_{nm} < n_2 > \sum_{k_2}\frac{k^2k_2^2\delta^4}{36}\right\} \ll b_k; b_{k'}^+ \gg . \tag{5.3. 21}$$

For $k' = k$

$$\left[\epsilon_k - \omega_k - \frac{\chi_k^2}{(\epsilon_k - \lambda_{-k})} + \frac{1}{N}xZJ_{nm} < n_1 > \sum_{k_1}\frac{k_1^2k^2\delta^4}{36} + \frac{1}{N}xZJ_{nm} < n_2 > \sum_{k_2}\frac{k^2k_2^2\delta^4}{36}\right]$$
$$\times \ll b_k; b_k^+ \gg = \frac{1}{2\pi}. \tag{5.3. 22}$$

This can be rewritten as

$$\left[\epsilon_k - \frac{xZJ_{nm}Sa^2k^2}{6} + \frac{1}{N}xZJ_{nm} < n_1 > \sum_{k_1}\frac{k_1^2k^2\delta^4}{36} + \frac{1}{N}xZJ_{nm} < n_2 > \sum_{k_2}\frac{k^2k_2^2\delta^4}{36}\right.$$
$$\left. - \frac{\chi_k^2}{(\epsilon_k - \lambda_{-k})} - g\mu_B B\right] \ll b_k; b_k^+ \gg = \frac{1}{2\pi}, \tag{5.3. 23}$$

where

$$\omega_k = \frac{xZJ_{nm}Sa^2k^2}{6} + g\mu_B B.$$

Hence, Eq. (5.3. 23) becomes

$$\left[\epsilon_k - \left(\frac{xZJ_{nm}Sa^2k^2}{6} - \frac{1}{N}xZJ_{nm} < n_1 > \sum_{k_1}\frac{k_1^2\delta^4}{36} - \frac{1}{N}xZJ_{nm} < n_2 > \sum_{k_2}\frac{k_2^2\delta^4}{36}\right)k^2\right.$$
$$\left. - \frac{\chi_k^2}{(\epsilon_k - \lambda_{-k})} - g\mu_B B\right] \ll b_k; b_k^+ \gg = \frac{1}{2\pi}. \tag{5.3. 24}$$

or

$$\left[\epsilon_k - xZJ_{nm}Sa^2\left(\frac{1}{6} - \frac{1}{SN} < n_1 > \sum_{k_1}\frac{k_1^2\delta^2}{36} - \frac{1}{SN} < n_2 > \sum_{k_2}\frac{k_2^2\delta^2}{36}\right)k^2\right.$$
$$\left. - \frac{\chi_k^2}{(\epsilon_k - \lambda_{-k})} - g\mu_B B\right] \ll b_k; b_k^+ \gg = \frac{1}{2\pi}, \tag{5.3. 25}$$

where $Z\delta^2 = 12a^2$ and $Z = 12$ for fcc lattice, hence, from the last equation we obtain the equation of motion for the Green function simplified to

$$\ll b_k; b_{k'}^{+} \gg = \frac{1}{2\pi\left[\epsilon_k - \omega_k' - \frac{\chi_k^2}{(\epsilon_k - \lambda_{-k})}\right]}, \tag{5.3. 26}$$

where ω_k' contains terms contributing to spin wave scattering, and written as

$$\omega_k' = xZJ_{nm}Sa^2\left(\frac{1}{6} - \frac{1}{SN} < n_1 > \sum_{k_1} \frac{k_1^2\delta^2}{36} - \frac{1}{SN} < n_2 > \sum_{k_2} \frac{k_2^2\delta^2}{36}\right)k^2 + g\mu_B B. \tag{5.3. 27}$$

Poles of single-particle Green functions on the real energy axis represent the elementary excitation spectrum. In real systems there is a cut along the real energy axis, and the different Fourier component of some operator in upper and lower half plane of complex values of energy give damping of elementary excitations [80].

Following Eq. (5.3. 26), poles of the Green function would now be at

$$\epsilon_k - \omega_k' + \frac{\chi_k^2}{(\epsilon_k - \lambda_{-k})} = 0. \tag{5.3. 28}$$

From Eq. (5.3. 28) we find dispersion ϵ_k of the system, that can be written as

$$\epsilon_k = \omega_k' - \frac{\chi_k^2}{(\epsilon_k - \lambda_{-k})}. \tag{5.3. 29}$$

Now, we verified that

$$\begin{aligned} -\frac{1}{SN} < n_1 > \sum_{k_1} \frac{k_1^2\delta^2}{36} - \frac{1}{SN} < n_2 > \sum_{k_2} \frac{k_2^2\delta^2}{36} &\cong -2\frac{1}{SN} < n_1 > \sum_{k_1} \frac{k_1^2\delta^2}{36} \\ &\cong -2\frac{1}{SN} < n_2 > \sum_{k_2} \frac{k_2^2\delta^2}{36} \end{aligned} \tag{5.3. 30}$$

as in reference [81], hence

$$\omega_k' \cong ZxJ_{nm}Sa^2k^2\left(\frac{1}{6} - 2\frac{1}{SN} < n_1 > \sum_{k_1} \frac{k_1^2\delta^2}{36}\right) + g\mu_B B. \tag{5.3. 31}$$

or

$$\omega_k' \cong ZxJ_{nm}Sa^2k^2\left(\frac{1}{6} - \frac{a^2}{18SN} \sum_{k_1} k_1^2 < n_1 > \right) + g\mu_B B, \tag{5.3. 32}$$

since $Z\delta^2 = 12a^2$ for fcc.

One can see that the energy is lowered by an amount proportional to k^2 and $\sum k_1^2 n_1$, which is of the form of the total spin wave energy, to lowest order. In fact,

$$\sum_{k_1} k_1^2 < n_1 > \cong U_T/D, \tag{5.3. 33}$$

where U_T is the thermal magnon energy

$$U_T = \frac{\tau^{5/2}}{4\pi^2 D^{3/2}} \int_0^{y_m} dy y^{3/2} \frac{1}{e^y - 1}. \tag{5.3. 34}$$

$y = Dk^2/\tau$. The upper limit can be taken as ∞ if we are interested in the region $\tau << \omega_{max}$. So that,

$$U_T \cong \frac{0.45\tau^{5/2}}{\pi^2 D^{3/2}}, \tag{5.3. 35}$$

where $\tau = \kappa_B T$ and $D = 2xSJa^2$. This implies that

$$\sum_{k_1} k_1^2 < n_1 > \cong \frac{0.45\tau^{5/2}}{\pi^2 D^{5/2}} = \frac{0.45\kappa_B^{5/2} T^{5/2}}{\pi^2 (2xSJ_{nm}a^2)^{5/2}}. \tag{5.3. 36}$$

Substituting Eq. (5.3. 35) into (5.3. 32), gives

$$\omega_k' \cong 2xJ_{nm}Sa^2k^2 \left(1 - \frac{a^2}{3SN} \frac{0.45\kappa_B^{5/2} T^{5/2}}{\pi^2 (2xSJ_{nm}a^2)^{5/2}}\right) + g\mu_B B. \tag{5.3. 37}$$

The last expression can be written in reduced from as,

$$\omega_k' \cong 2xJ_{nm}Sa^2(1 - \Omega_0 T^{5/2})k^2 + g\mu_B B. \tag{5.3. 38}$$

where $\Omega_0 = \frac{a^2}{3SN} \frac{0.45\kappa_B^{5/2}}{\pi^2 (2xSJ_{nm}a^2)^{5/2}}$ and N is the number of lattice sites.

For zero external field, $\mathbf{B} = 0$ Eq. (5.3. 38) can be written as

$$\omega_k' \cong 2xJ_{nm}Sa^2(1 - \Omega_0 T^{5/2})k^2 \tag{5.3. 39}$$

Substituting Eq. (5.3. 39) into (5.3. 29) we obtain solved and simplified form of ϵ_k as in Eq. (C.1. 9)(see the Appendix). Hence,

$$\epsilon_k = 0.5Ak^2 + B'. \tag{5.3. 40}$$

or

$$\epsilon_k = D'k^2 + B'. \tag{5.3. 41}$$

where $D' = xJ_{nm}Sa^2(1 - \Omega_0 T^{5/2})$ and $B' = \frac{g^2\mu_\beta^2\mu_0 S}{4V}$.

In the following sections we will write $B' = \frac{\alpha^2}{c}$, where α magnon-photon (coupling) interaction strength which depends on volume of the resonator cavity ($\alpha^2 = \frac{cg^2\mu_B^2\mu_0 S}{4V}$), hence χ_k can be written as $\chi_k = \alpha k^{1/2}$.

In Eq. (5.3. 41) variation of magnon dispersion with magnon-photon coupling constant and magnon scattering is shown. This factors are presumed to change the number of magnons in the system. When these effects are ignored there would be a possibility to recast the dispersion into its normal state value.

5.4 Correlation Function and the Number of Magnons

Here we apply the method of double-time temperature dependent Green function [80] to calculate the number of magnons excited at temperature T. This can be done starting with writing the correlation function, using Eq. (5.3. 26) and (5.3. 41) in (2.3. 20), as

$$< B(t')A(t) >= \lim_{\varepsilon\to 0} i\int_{-\infty}^{\infty} \frac{\ll A(t); B(t') \gg_{E+i\varepsilon} - \ll A(t); B(t') \gg_{E-i\varepsilon}}{e^{\beta\hbar E} - 1} e^{-iE(t-t')}dE. \tag{5.4. 1}$$

i.e.,

$$< b_{k'}^+ b_k >= \lim_{\varepsilon\to 0} i\int_{-\infty}^{\infty} \frac{\ll b_k; b_{k'}^+ \gg_{E+i\varepsilon} - \ll b_k; b_{k'}^+ \gg_{E-i\varepsilon}}{e^{\beta E} - 1} e^{-iE(t-t')}dE. \tag{5.4. 2}$$

Using the Dirac identity given by Eq. (2.3. 21), and equal time correlation, $t' = t$,

$$\begin{aligned} \ll b_k; b_k^+ \gg_{E+i\varepsilon} &= \frac{1}{2\pi[(E + i\varepsilon) - \epsilon_k]} \\ &= \frac{1}{2\pi}\left[\frac{\wp}{E - \epsilon_k} - i\pi\delta(E - \epsilon_k)\right] \end{aligned} \tag{5.4. 3}$$

and

$$\ll b_k; b_k^+ \gg_{E-i\varepsilon} = \frac{1}{2\pi[(E-i\varepsilon)-\epsilon_k]} = \frac{1}{2\pi}\left[\frac{\wp}{E-\epsilon_k} + i\pi\delta(E-\epsilon_k)\right], \tag{5.4. 4}$$

in which $\wp$ is the principal part of the integral. Hence, substituting Eq. (5.4. 3) and (5.4. 4) in to (5.4. 2) gives the number operator

$$< b_k^+ b_k > = \int_{-\infty}^{\infty} \frac{\delta(E-\epsilon_k)}{e^{\beta E}-1} dE \tag{5.4. 5}$$

where $\delta(E-\epsilon_k) = 1$ for $E = \epsilon_k$ and zero otherwise, hence,

$$< b_k^+ b_k > = \frac{1}{e^{\beta\epsilon_k}-1}. \tag{5.4. 6}$$

Substituting Eq. (5.3. 41) in to (5.4. 5),

$$< b_k^+ b_k >= \frac{1}{e^{\beta(D'k^2+B')}-1}. \tag{5.4. 7}$$

Since $< b_k^+ b_k >=< n_k >$, the mean number of spin waves with wave vector $\boldsymbol{k}$ at temperature T will be given by

$$< n_k >= \frac{1}{e^{\beta(D'k^2+B')}-1}, \tag{5.4. 8}$$

where $\beta = \frac{1}{k_B T}$. The last expression illustrates that the magnon number in a single mode is also affected by magnon-photon coupling constant and magnon scattering term.

With the help of Eq. (5.4. 8) the total number of excited magnons in all modes at temperature T, can be estimated. Therefore,

$$\sum_k < n_k > = \sum_k < b_k^+ b_k > = \sum_k \frac{1}{e^{\beta(D'k^2+B')}-1}. \tag{5.4. 9}$$

Since the system is attributed to resonate in a bulk Eq. (5.4. 9) requires integration over a space, hence

$$2\pi^2 \sum_k < n_k >= \int_0^\infty \frac{k^2}{e^{\beta(D'k^2+B')}-1} dk. \tag{5.4. 10}$$

The total number of excited magnons will, then, become (the integration is shown in the appendix, and the final result is expressed by Eq. (C.2. 8))

$$\sum_k < n_k >= 0.0586\left(\frac{k_B T}{D'}\right)^{\frac{3}{2}} - 63.449\frac{g^2\mu_\beta^2\mu_0 S k_B^{\frac{1}{2}} T^{\frac{1}{2}}}{V(xJ_{nm}Sa^2)^{\frac{3}{2}}}, \tag{5.4. 11}$$

and can also be written in terms of the coupling constant as

$$\sum_k < n_k >= \frac{1}{x^{3/2}a^3(1-\Omega_0 T^{5/2})^{3/2}}\left[\gamma T^{3/2} - \theta\alpha^2 T^{1/2}\right], \tag{5.4. 12}$$

where $\gamma = 0.0586(\frac{k_B}{J_{nm}S})^{3/2}$, and $\theta = 63.449\frac{k_B^{1/2}}{Sc(J_{nm}S)^{3/2}}$ obtained based on standard values of constants in the expression.

From Eq. (5.4. 12) one can also see that the total number of magnons can be affected by the coupling constat and the term appearing due to spin wave scattering. This last equation will be used in examining the magnetization, transition temperature and magnon specific heat of the considered system in the following sections.

5.5 Magnetization and Ferromagnetic Transition Temperature of the $(Ga, Mn)As$ DMS

Considering the famous Bloch relation and Eq. (5.4. 12) we write the temperature dependent magnetization $M(T)$, as

$$M(T) = M(0) - g\mu_B \sum_k < n_k >, \tag{5.5. 1}$$

Where $M(0) = g\mu_B nS$ is ground state magnetization or magnetization at absolute zero where all spins align parallel. This last expression, Eq. (5.5. 1), can be rewritten

as:

$$M(T) = g\mu_B nS - g\mu_B \sum_k < n_k > \\ = g\mu_B nS\left(1 - \frac{1}{nS}\sum_k < n_k > \right). \quad (5.5.\ 2)$$

Substituting Eq. (5.4. 12) into (5.5. 2),

$$M(T) = g\mu_B nS\left[1 - \frac{1}{S}\frac{1}{x^{3/2}na^3}\left(1 - \Omega_0 T^{5/2}\right)^{-3/2}\left(\gamma T^{3/2} - \theta\alpha^2 T^{1/2}\right)\right], \quad (5.5.\ 3)$$

where n is number of atoms per unit volume equal to Q/a^3 ($n = Q/a^3$) and $Q = 1, 2, 4$ for sc, bcc, fcc lattices respectively [8]. $(Ga, Mn)As$ has fcc lattice structure with $n = 4/a^3$ with lattice constant of about $a = 5.65A^0$.

Writing Eq. (5.5. 3) as the ratio of temperature dependent magnetization M(T) and zero temperature magnetization M(0) gives

$$\frac{M(T)}{M(0)} = 1 - \frac{1}{4S}\frac{1}{x^{3/2}}\left(1 - \Omega_0 T^{5/2}\right)^{-3/2}\left(\gamma T^{3/2} - \theta\alpha^2 T^{1/2}\right). \quad (5.5.\ 4)$$

We determined the ferromagnetic transition temperature T_c taking the limiting case of Eq. (5.5. 4) where $\frac{M(T)}{M(0)}$ approaches 0, i.e., for $\frac{M(T)}{M(0)} \rightsquigarrow 0$, $T \rightsquigarrow T_C$, hence, concentration of the magnetic impurity x, is related to the ferromagnetic transition temperature T_C. This can be shown following,

$$\frac{1}{4S}\frac{1}{x^{3/2}}\left(1 - \Omega_0 T_C^{5/2}\right)^{-3/2}\left(\gamma T_C^{3/2} - \theta\alpha^2 T_C^{1/2}\right) = 1, \quad (5.5.\ 5)$$

where cross multiplication gives

$$\left(1 - \Omega_0 T_C^{5/2}\right)^{-3/2}\left(T_C^{3/2} - \frac{\theta\alpha^2}{\gamma}T_C^{1/2}\right) = \frac{4S}{\gamma}x^{3/2}. \quad (5.5.\ 6)$$

This leads to the final result, that relates concentration of the impurity and the ferromagnetic transition temperature governing property of the system under study. Therefore,

$$x = \frac{1}{(1 - \Omega_0 T_C^{5/2})}\left[\frac{\gamma}{4S}T_C^{3/2} - \frac{\theta}{4S}\alpha^2 T_C^{1/2}\right]^{2/3}. \quad (5.5.\ 7)$$

5.6 Effect of photo-excitation and spin wave-scattering on magnon specific heat capacity of the $(Ga, Mn)As$ DMS

The internal energy of unit volume of the magnon gas in thermal equilibrium at temperature T in which magnon-magnon interaction is included at zero external field ($\mathbf{B} = 0$) is considered. Taking the case of $ka \ll 1$, the energy would be given by

$$U = \sum_k \epsilon_k < n_k >_T . \tag{5.6. 1}$$

Substituting Eq. (5.4. 12) into (5.6. 1),

$$\begin{aligned} U &= \sum_k \epsilon_k < n_k >_T \\ &= \sum_k \frac{\epsilon_k}{e^{\beta\epsilon_k} - 1}. \end{aligned} \tag{5.6. 2}$$

Converting the summation into integral form,

$$U = \frac{1}{2\pi^2} \int_0^\infty \frac{\epsilon_k}{e^{\beta\epsilon_k} - 1} k^2 dk, \tag{5.6. 3}$$

where the dispersion ϵ_k, is given by Eq. (5.3. 41).

Substituting Eq. (C.3. 3) in (5.6. 3)and completing the integration gives the desired solution as of Eq. (C.3. 10), hence, restoring for A and making rearrangements

$$U \cong \frac{1}{[xJ_{nm}Sa^2(1 - \Omega_0 T^{5/2})]^{3/2}} [0.0456 k_B^{5/2} T^{5/2} - 0.01465 \frac{\alpha^2 k_B^{3/2}}{c} T^{3/2}]. \tag{5.6. 4}$$

From the above expression the magnon specific heat can be calculated. Therefore,

$$\begin{aligned} C_{magn} &= \frac{\partial}{\partial T} U \\ &= \frac{\partial}{\partial T} \frac{1}{[xJ_{nm}Sa^2(1 - \Omega_0 T^{5/2})]^{3/2}} [0.0456 k_B^{5/2} T^{5/2} - 0.01465 \frac{\alpha^2 k_B^{3/2}}{c} T^{3/2}], \end{aligned} \tag{5.6. 5}$$

becomes

$$\begin{aligned} C_{magn} = &\frac{1}{(xJ_{nm}Sa^2)^{3/2}[(1 - \Omega_0 T^{5/2})]^{3/2}} \left(0.115 k_B^{5/2} T^{3/2} - 0.027 \frac{\alpha^2 k_B^{3/2}}{c} T^{1/2} \right) \\ &+ \frac{\Omega_0}{(2xJ_{nm}Sa^2)^{3/2}[(1 - \Omega_0 T^{5/2})]^{5/2}} \left(0.214 k_B^{5/2} T^4 - 0.0681 \frac{\alpha^2 k_B^{3/2}}{c} T^3 \right) \end{aligned} \tag{5.6. 6}$$

or

$$C_{magn} = \frac{1}{x^{3/2}[(1-\Omega_0 T^{5/2})]^{3/2}}\left(pT^{3/2} - r\alpha^2 T^{1/2}\right) + \frac{\Omega_0}{x^{3/2}[(1-\Omega_0 T^{5/2})]^{5/2}}\left(1.5pT^4 - 0.25r\alpha^2 T^3\right) \quad (5.6.\ 7)$$

where $p = \frac{0.325k_B^{5/2}}{(2JSa^2)^{3/2}}$ and $r = \frac{0.0621k_B^{3/2}}{c(2JSa^2)^{3/2}}$.

5.7 Result and Discussion

Following Eq. (5.5. 4), reduced magnetization vs. temperature is plotted. For better numerical estimations: the exchange integral of local magnetic moments, at different sites separated approximately by distance of $GaAs$ lattice constant ($a = 5.65A^0$), $J_{nm} = 2.3285meV$; spin of the Mn $3d$ sub-shell of an atom $S = \frac{5}{2}$; speed of light in free space $c = 3 \times 10^8 \frac{m}{s}$; the g-factor $g = 2$; the Bohr magneton $\mu_\beta = 9.2741 \times 10^{-24} J/T$; permeability of free space $\mu_0 = 4 \times 10^{-7} T.m/A$; the Boltzmann constant $k_B = 0.08625meV/K$; and the number of lattice points $N \sim 10^{28} m^{-3}$ in a unit volume are used.

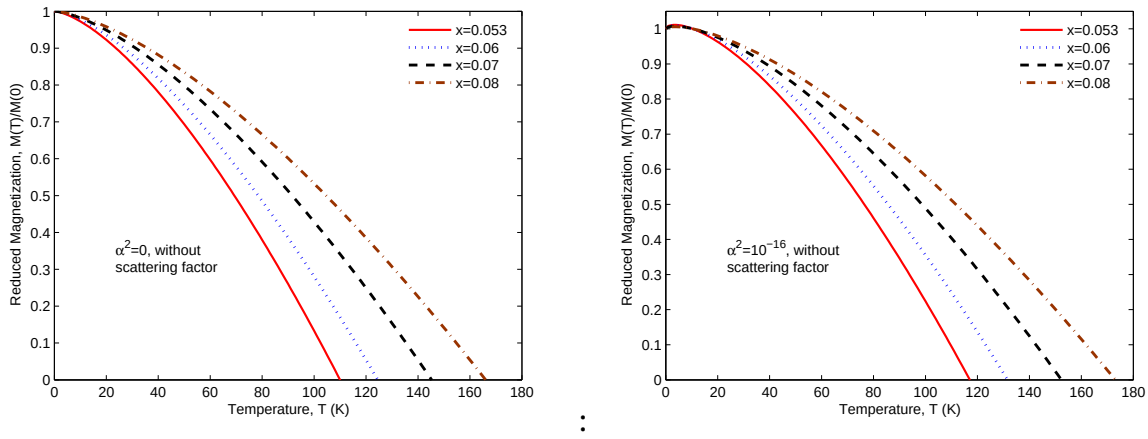

Fig. 5.1: Reduced magnetization vs temperature at impurity concentration $x = 0.053$, 0.06, 0.07 and 0.08 for magnon-photon coupling constant $\alpha^2 = 0$ (left panel) and $\alpha^2 = 10^{-16}$ (right panel) in the absence of scattering.

As shown in Figs. 5.1 and 5.2, an increase in impurity concentration increases the magnetization of the system and can be justified in comparison to the result obtained by Matsukura et al., [40] in which experimental observations are discussed without applications of light. In Fig. 5.3 the effect of magnon-photon coupling constant α, on magnetization in the absence and presence of scattering is shown. From this, one can infer that the magnetization also increases with increasing the coupling energy. Fig. 5.4 is for Mn concentration $x = 0.053$ (left panel) and $x = 0.08$ (right panel) merging plots in both panels of Fig. 5.3, and shows an enhancement of magnetization

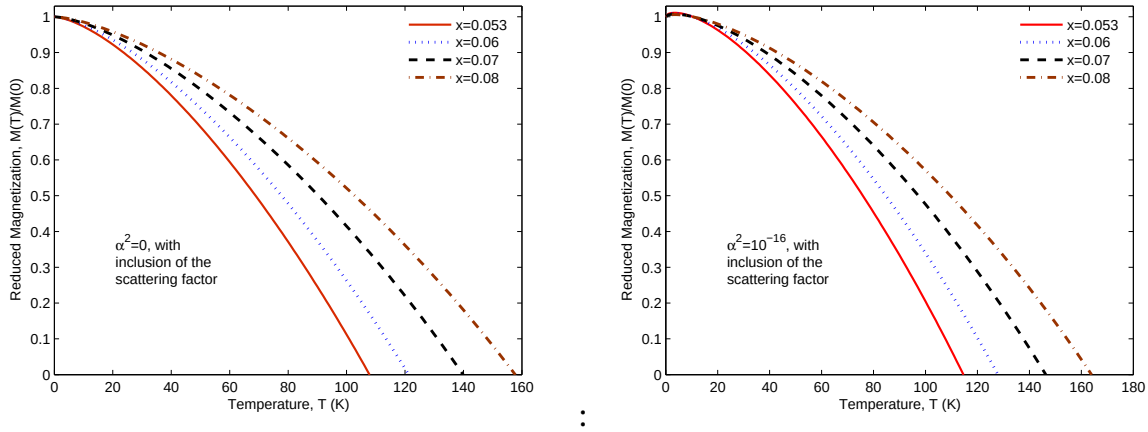

Fig. 5.2: Reduced magnetization vs temperature at impurity concentration $x = 0.053$, 0.06, 0.07 and 0.08 for magnon-photon coupling constant $\alpha^2 = 0$ (left panel) and $\alpha^2 = 10^{-16}$ (right panel) in which spin wave scattering is considered.

with increase in magnon-photon coupling constant α in contrast to what it could be on inclusion of the spin wave scattering parameter. The plots in both panels illustrate the falling of the magnetization curve below the scattering absent. It can also be seen from Eq. (5.5. 4) that the appearance of the term $T^{1/2}$ in the expression has resulted in enhancement of the magnetization in contrast to what Matsukura et al., [40] have found experimentally.

Slightly increasing of this coupling energy gives rise to gradual uplift of the magnetization. This is more pronounced for larger coupling strength yielding an unphysical increase, especially at low temperatures in which critical scrutiny of Figs. 5.3 and 5.4 reveals that there could be an upturn in the magnetization with further increase in this parameter. An increase in magnetization with magnon-photon interaction (where $\alpha^2 \sim \frac{1}{V}$) could be inferred as miniaturized size crystals are vital for the enhancement. However, with inclusion of spin wave scattering the situation is modified as temperature rises. The impurity concentrations, $x = 0.053$ [40] and $x = 0.08$ [38, 71], used frequently for plotting and comparison of results are considered due to the fact that ferromagnetic transition temperatures are experimentally reported for these values.

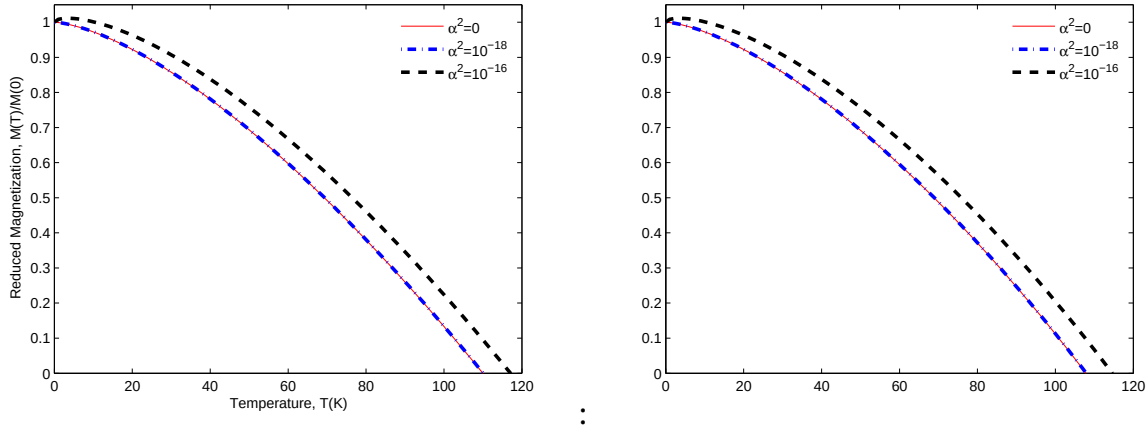

Fig. 5.3: Reduced magnetization vs. temperature for $x = 0.053$ without (left panel) and with (right panel) inclusion of spin wave scattering.

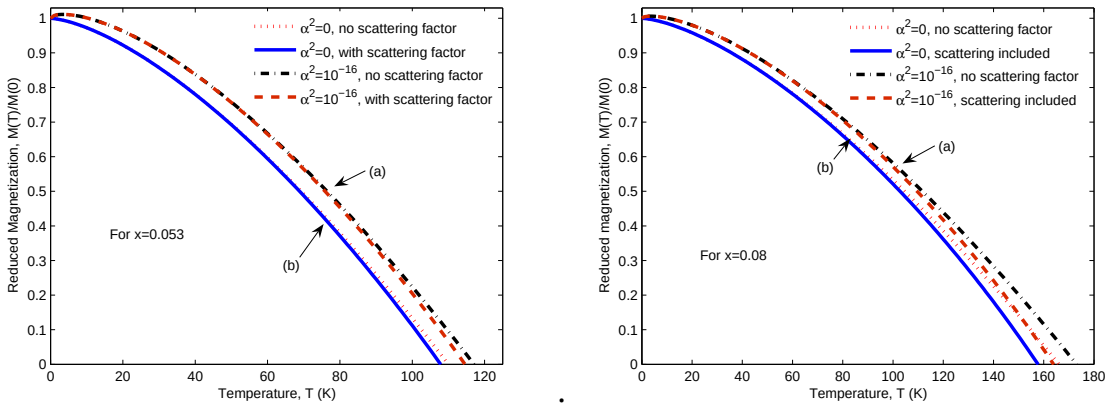

Fig. 5.4: Reduced magnetization vs. temperature when $x = 0.053$ (left panel) and $x = 0.08$ (right panel) in the absence and presence of spin wave scattering. Graphs labeled by (a) are plotted for $\alpha^2 = 10^{-16}$, and (b) for $\alpha^2 = 0$.

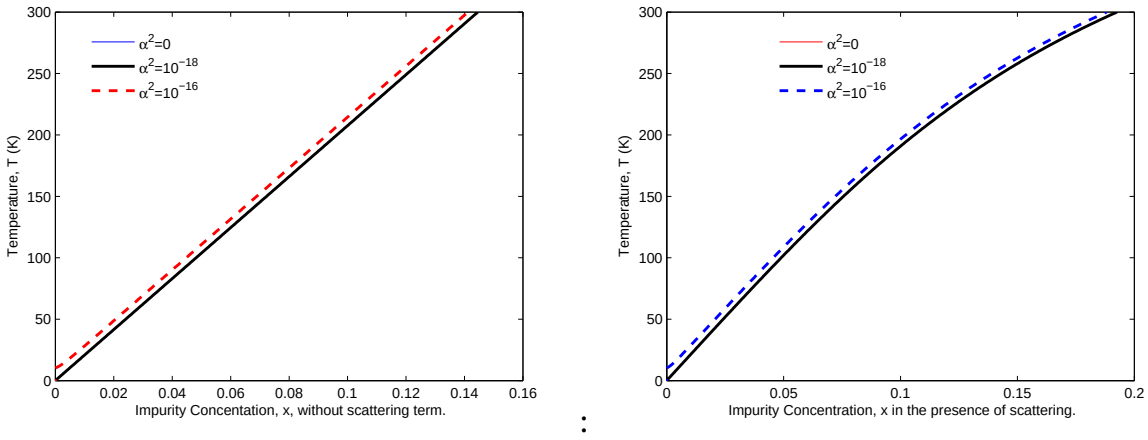

Fig. 5.5: Ferromagnetic transition temperature T_C vs. impurity concentration x, is plotted in the absence (left panel) and presence (right panel) of spin wave scattering.

The existence of ferromagnetic transition temperature in the absence of impurity concentration is indicated. This can be obtained by equating expression Eq. (5.5. 7) to zero, leading to $T_C \propto \alpha^2$. It is also reflected in Fig. 5.6, that merges plots in panels of Fig. 5.5.

It was shown in previous works [31, 40, 94] that ferromagnetic transition temperature is linearly dependent on concentration of the impurity magnetic moments in the sample. To our observation, however, this relation looks slightly altered at higher values of x, due to inclusion of magnon-photon coupling and scattering effects. Accordingly, T_C appears to increase with the coupling energy and relatively decrease with inclusion of spin wave scattering (see Fig. 5.6).

Making rough estimate gives, the values summarized in Table 5.1.

Tab. 5.1: Rough estimate of T_C with and without inclusion of the contribution of spin wave scattering and magnon-photon coupling constant α^2, for $x = 0.053$.

$\mathbf{T}_C(K)$	**Photon-Magnon coupling constant**, α^2	**Contribution of scattering**
110	0	not included
108	0	included
117	10^{-16}	not included
115	10^{-16}	included

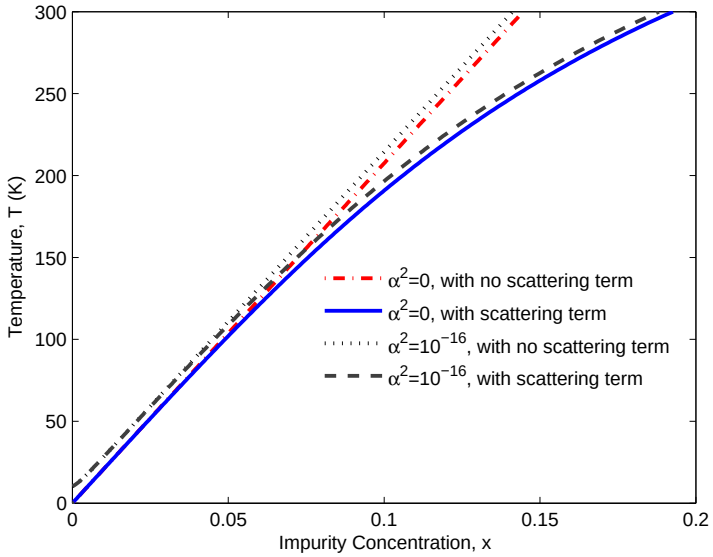

Fig. 5.6: Ferromagnetic transition temperature T_C vs. impurity concentration x

The magnon specific heat of diluted magnetic semiconductor $(Ga, Mn)As$ material is also attributed to change with volume of the optical resonator cavity in which radiation field is confined. This is explained by varying the magnon-photon coupling constant, as shown in Figs. 5.7 and 5.8, in which maximum values at $T = 400K$ are used for comparisons. One can see from these that, rise in photon-magnon coupling constant decreases the specific heat. It is explicitly shown in Fig. 5.7 that the magnon specific heat decreases with increase in magnon-photon coupling constant (left panel) and slightly increase with inclusion of the spin wave scattering factor (right panel). Similarly, Fig. 5.8 is plotted to compare magnon specific heat in the absence and presence of magnon-photon coupling energy and spin wave scattering.

Figs. 5.9 and 5.10 show the decrease in magnon specific heat with increase in magnetic impurity concentration x, and in agreement with the result obtained by Jürgen et al. [63] at lower temperatures for diluted magnetic semiconductor ferromagnetism and by Twardowski et al., [96] for the case of $Zn_{1-x}Fe_xS$ DMS; and further decrease due to the radiation field (see right panel of Fig. 5.9), but, increase with inclusion of the spin wave scattering (see Fig. 5.10).

Further Scrutiny of these plots reveal that there could be an unusual negative

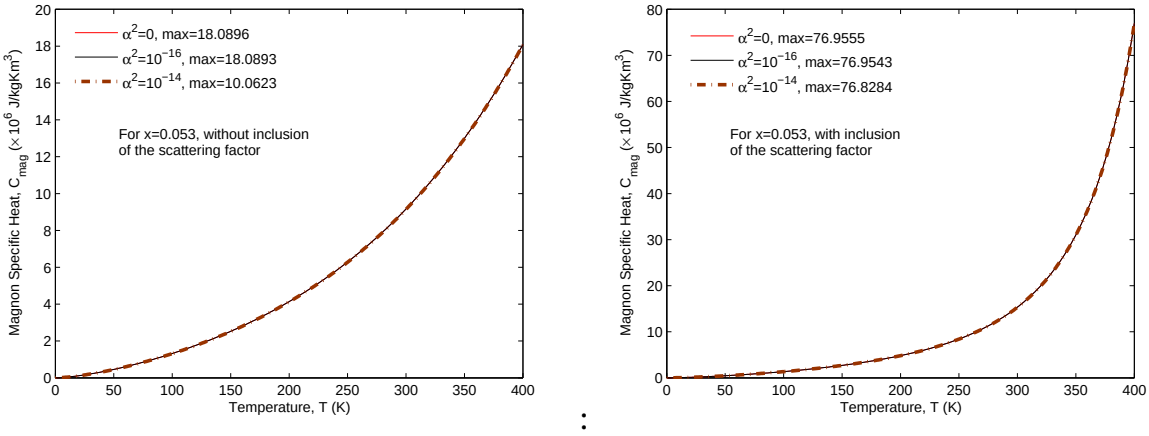

Fig. 5.7: Magnon heat capacity vs. temperature for $x = 0.053$ without (left panel) and with (right panel) inclusion of spin wave scattering factor.

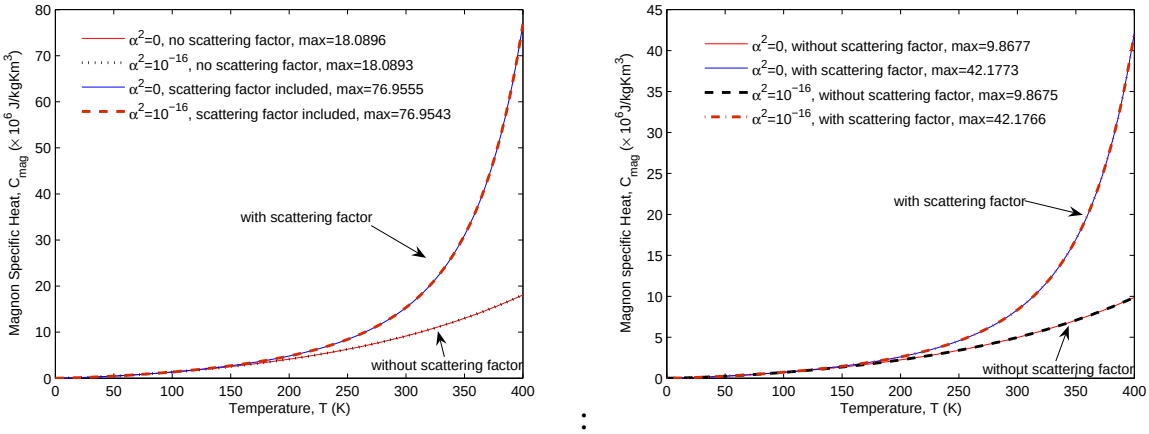

Fig. 5.8: Magnon heat capacity vs. temperature for $x = 0.053$ (left panel) and $x = 0.08$ (right panel).

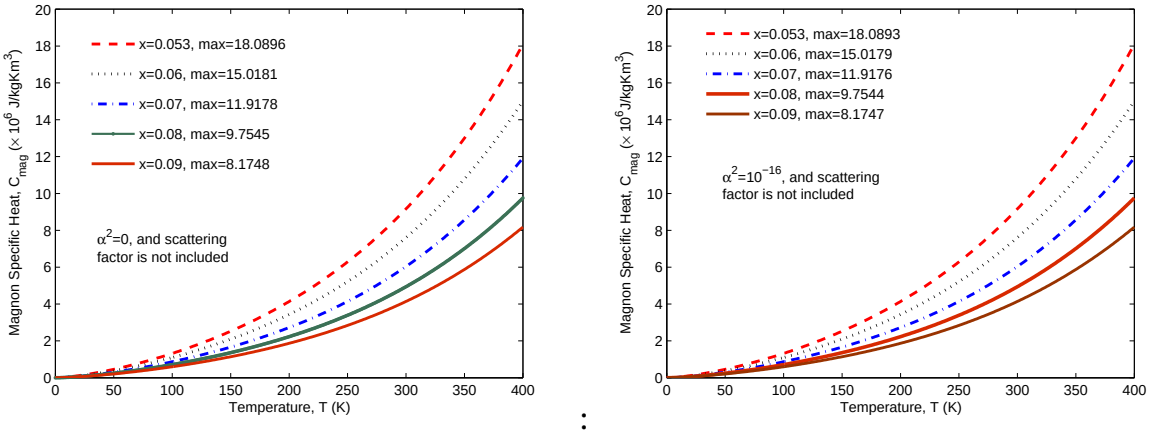

Fig. 5.9: Magnon heat capacity vs. temperature for $\alpha^2 = 0$ (left panel) and $\alpha^2 = 10^{-16}$ (right panel) without inclusion of spin wave scattering factor.

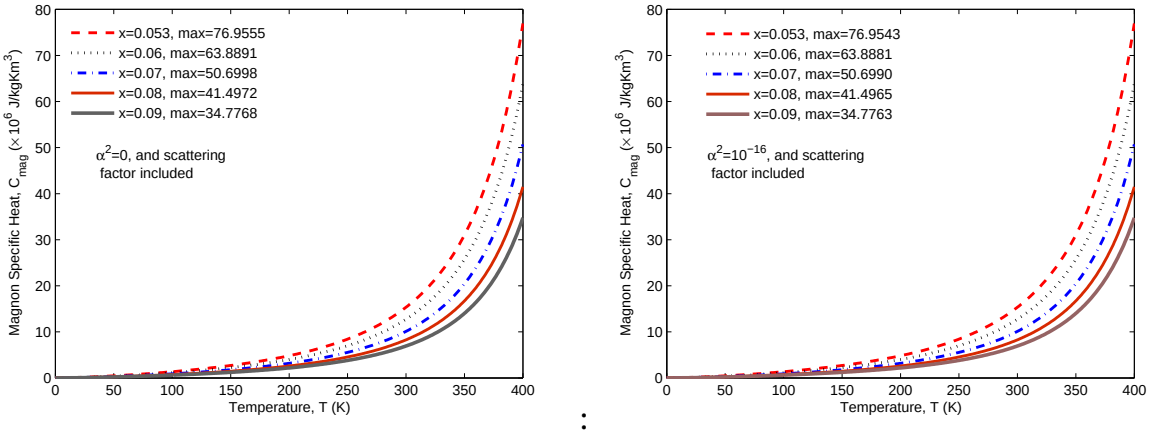

Fig. 5.10: Magnon heat capacity vs. temperature for $\alpha^2 = 0$ (left panel) and $\alpha^2 = 10^{-16}$ (right panel) with inclusion of spin wave scattering factor.

magnon specific heat at very low temperatures, for larger magnon-photon coupling energies. The appearance of this negative value is perhaps due to confinement, at very small size resulting in non-equilibrium situation and fluctuation effects in the micro-cavity. Such anomaly was also observed in experimental study of the heat capacity of $Zn_{0.98}Co_{0.02}O$ and tentatively attributed to a change in the magnetic properties of the substance [95].

Therefore, inclusion of magnon-photon interaction into the basic Hamiltonian has resulted in decreasing of the magnetic specific heat contributing to ferromagnetism of the system. However, on inclusion of the spin wave scattering the specific heat increases, even faster for higher temperatures, perhaps due to the reason given by Twardowski et al. [96] (which is typical for a Schottky-type anomaly i.e., ground state separated from the excited state by an energy gap) for the case of $Zn_{1-x}Fe_xS$. Below some temperatures there is no observed effect of spin wave scattering on the system. This could be due to the fact that at higher temperatures scattering of spin waves will become predominant resulting in reduction of magnetic ordering.

6

Summary and Conclusion

Recently observed photoinduced ferromagnetism in $(In, Mn)As$ and $(Ga, Mn)As$ diluted magnetic semiconductors is a remarkable development. Experimental studies on the materials confirmed that, excess holes created by the mechanism would promise the possibility of enhancing ferromagnetic exchange coupling and magnetization. It is from this point of view that a theoretical study of radiation induced ferromagnetism has been made starting with an interaction Hamiltonian of radiation and Mn^{2+} spins in diluted magnetic semiconductor specially $(Ga, Mn)As$.

In the first part of this work we derived an expression for the ferromagnetic coupling constant J_{nm}, starting with the Zener model from which Heisenberg type of expression is obtained, and has been made use of in Dietl model in studying diluted magnetic semiconductors. The plot shows that the exchange coupling energy has an oscillatory character and can rise to higher at a point where $F(2k_F R_{nm})$ is maximum. From this, we obtained an exchange integral that would enhance due to carrier density and increases with decrease in fermi energy indicating that ferromagnetism is carried out more by valence band system, since the fermi level is attributed to shift towards the accepter level.

In study of interaction of radiation with matter the Zeeman energy is the Hamiltonian used to describe the system. The interaction Hamiltonian has been recast into a Heisenberg type of exchange interaction. The main objective was to find the exchange coupling energy between localized spins and compare with that of carrier mediated, RKKY, indirect exchange interaction. It is suggested that the exchange coupling could be very large leading to ferromagnetism. We have also calculated and

shown its dependence on intensity of irradiated photon which would rise mode of excitation and hence enhance ferromagnetism to maximum at/ or near resonance [97]. It is possible to observe the effects in ferromagnetic and spin wave resonance experiments which are a very good probe for magnetic properties of such systems. It is shown that radiation dependent exchange coupling energy can be influenced by magnon-photon coupling constant and volume of the radiation field cavity, doing the same job as the RKKY indirect interaction. Therefore, an increase in exchange coupling energy, J_{nm}, due to increase in carriers electron/ hole concentration, as discussed in chapter three, and to frequency of the irradiated photon near resonance, as discussed in chapter four, reveals that photon irradiation would increase the concentration of the excited carriers that would mediate ferromagnetism. This implies that the role of photons is to excite carriers electrons/holes which mediate ferromagnetism. For larger Mn density in $(Ga, Mn)As$, the gradual increment of these carriers would enhance ferromagnetism; hence, T_C would rise via increase in exchange coupling energy. Due to the fact that the radiation field enters only a small skin depth, the spins in the layer experience ferromagnetic resonance and others do not. In spin wave resonance the local moments are no longer parallel inside the sample and restoring torques due to exchange interaction resulting in effects in $k \neq 0$ excitations. The ferromagnetic and spin wave resonance experiments can be used to find the above suggested spin exchange interaction.

On the other hand, we studied magnetization M(T), ferromagnetic transition temperature T_C and magnon specific heat C_{mag}, by considering the effect of photo-excitation using Green function formalism [98]. From this, unusual upturn in magnetization and negative magnon specific heat at very low temperature values for larger magnon-photon coupling constant is obtained. The phenomenon of such anomaly in magnetic specific heat has also been observed in other compounds [99]. Additionally, ferromagnetic transition temperature (T_C) in the absence of impurity concentration ($x = 0$) is indicated. These effects look pronounced in the absence of scattering. This is perhaps due to confinement at very small size resulting in non-equilibrium

situation and fluctuation effects in the micro-cavity. Both magnetization and ferromagnetic transition temperature are shown to enhance in the presence of radiation and shown to decrease with inclusion of scattering at higher temperature values. As the temperature increases the heat capacity increases, surpassing that of the magnon scattering absent. This shows that photon irradiation would enhance magnetization where as the scattering effects do not.

Therefore, if T_C of the DMS can be increased at will there is a possibility of utilizing the system under consideration for spintronic purpose at room temperature.

Bibliography

[1] H. Ohno, Science **281**, 951 (1998).

[2] T. Dietl, H. Ohno, F. Matsukura, J. Cibert, and D. Ferrand, science **287**, 1019 (2000).

[3] H. Ohno, F. Matsukura, and Y. Ohno, 2002, *Semiconductor Spin Electronics*, General report, Cutting edge1.

[4] I. $\check{Z}$utić, J. Fabian, and S. Das Sarma, Rev. Mod. Phys. **76**, 323 (2004)

[5] C. Timm, J. Phys: Condens. Matter **15**, R1865 (2003).

[6] http://www.fz-juelich.de/nic-series/volume39.

[7] M. J. Steven, A. L. Smirl, R. D. R . Bhat, A. Najmaie, J. E. Sipe, and H. M. van Driel, Phys. Rev. Lett. **90**, 136603 (2003).

[8] C. Kittel, 1986, *Introduction to Solid State Physics*, 6^{th} ed, (John Wiley and sons, New York).

[9] D. A. NEAMEN, 1992, *Semiconductor Physics and Devices*: *Basic principles*, (Richard D. Irwin, INC., University of New Mexico).

[10] M. N. Baibich, J. M. Broto, A. Fert, F. Nguyen van Dau, and F. Pettroff, Phys. Lett. **61**, 2472 (1988).

[11] G. Binasch, P. Grunberg, F. Saurenbach and W. Zinn, Phys. Rev. **B 39**, 4828 (1989).

[12] C. Chappert, A. Fert, and F. N. Van Dau, Nature Materials **6**, 813 (2007).

[13] S. A. Wolf, J. Supperconductivity: Incorporating Novel Magnetism **13**, 195 (2000).

[14] S. Koshihara, A. Oiwa, M. Hirasawa, S. Katsumoto, Y. Iye, C. Urano, H. Takagi and H. Munekata, Phys. Rev. Lett. **78**, 4617 (1997).

[15] H. Munekata, T. Abe, S. Kushihara, A. Oiwa, M. Hirasawa, S. Katsumoto, Y. Iye, C. Urano and H. Takagi, J. Appl. Phys. **81**, 4862 (1997).

[16] A. Oiwa, Y. Mitsumori, R. Moriya, T. stupinski, and H. Munekata; Phys. Rev. Lett. **88**, 137202 (2002).

[17] C. Zener, Phys. Rev. **82**, 403 (1956).

[18] C. Zener, Phys. Rev. **81**, 440 (1956).

[19] B. T. Matthias, R. M. Bozorth, and J. H. Van Vleck, Phys. Rev. Lett. **7**, 160 (1961).

[20] A. Mauger and C. Godart, Phys. Rep. **141**, 51 (1986).

[21] T. Kasuya and A. Yanase, Rev.mod.Phy. **40**, 684 (1968).

[22] H. Munekata, H. Ohno, S. Von Molnar, Armin Segm$\ddot{u}$ller L. L. Chang, and L. Esaki Phys. Rev. Lett. **63**, 1849 (1989).

[23] J. K. Furdyna; J. Appl. Phys. 64, R29 (1988).

[24] M. Dinu, I. Miotkowski, and D. D. Nolte, Phys. Rev. B **58**, 10435, (1998-II).

[25] H. Ohno, J. Magn. Magn. Mater. **200**, 110 (1999).

[26] S. Sun, H. Lin, Cond-mat/0303328, 2003.

[27] S. R. Eric Yang and A. H. McDonald, Phys. Rev. B **67**, 155202 (2003).

[28] H. Ohno, A. Shen, F. Matsukura, A. Oiwa, A. Endo, S. Hatsumoto, and Y. lye, Appl. Phys. Lett. **69**(3) (1996).

[29] B. Lee, T. Jungwirth, and A. H. MacDonald, Cond-matt/0203081, 2002.

[30] N. W. Ashcroft, and N. D. Mermin, 2001, *Solid state Physics*, (Thomson learning, Inc., cornell university, USA).

[31] M. Berciu, and R. N. Bhatt, Phys. Rev. Lett. **87**, 107203 (2001).

[32] Mubeen and Mubeen, 2004, *Material Science*, 2^{nd} ed., (Khanna , Delhi).

[33] X. Liu, and J. K. Furdyna, J. Phys: Condens. Matter **18**, R245 (2006) .

[34] M. P. Kennett, 2002, Ph.D dessertation, Princeton university.

[35] T. Jungwirth, Jairo Sinova, J. Kučera and A. H. MacDonald, Curr. Appl. Phys. **3**, 461 (2003).

[36] J. K. Furdyna, and J. Kossut(Eds), 1988, *Semiconductor and Semimetals*, **25**, (Academic press, New York).

[37] S. Rodrizuez, and A. K. Ramdas, Pure and Appl. Chem., **59**, 1269 (1987).

[38] S. Das Sarma, E. H. Hwang, and A. Kaminski, Phys. Rev. B **67**, 155201 (2003).

[39] A. Haury, A. Wasiela, A. Arnoult, J. Cibert, S. Tatarenko, T. Dietl, and Y. Merle d'Aubigne, Phys. Rev. Lett. **79**, 511 (1997).

[40] F. Matsukura, H. Ohno, A. Shen, and Y. Sugawara, Phys. Rev. B **57**, R2037 (1998).

[41] A. Van Esch, L. Van Bockstal, J. De Boeck, G. Verbanck, A. S. van Steenbergen, P. J. Wellmann, B. Grietens, R. Bogaerts, F. Herlach, and G. Borghs , Phys. Rev. B **56**, 13103 (1997-II).

[42] J. Kudrnovsky, I. Turek, V. Drchal, F. Maca, P. Weinberger, and P. Bruno, Phys. Rev. B **69**, 115208 (2004).

[43] S. Sanvito, N. A. Hill; J. Mag. Mag. Materials **238**, 252 (2002).

[44] R. N. Bhatt, Mona Berciu, Malcolm P. Kennett, and Xin Wan, J. Sup. Inco. Nov. Mag. **15**, 71 (2002).

[45] H. Ohno, H. Munekata, T. Penney, S. Von Molnar, and L. L. Chang Phys. Rev. Lett. V. **68**, 2664 (1992).

[46] S. C. Itaya, Y. Ymamoto and H. Hori, in *Proceedings of the* 27^{th} *International Conference on the Physics of Semiconductors*, Flagstaff, Arizona, 2004, edited by J. Menéndez and G. Van de Walle (Melville, New York, 2005), **772**, part A, p-355.

[47] T. Dietl, J. Cibert, P. Kossacki, D. Ferrand, S. Tatarenko, A. Wasiela, Y. Merle d'Aubigne', F. Matsukura, N. Akiba, and H. Ohino, Physica E **7**, 967 (2000).

[48] T. Dietl, H. Ohno and F. Matsukura, Phys. Rev. B **63**, 195205 (2001)

[49] T. Dietl, F. Matsukura and H. Ohno, cond-mat/0109245, 2001.

[50] T. Story, R. R. Galazka, R. B. Frankel and P. A. Wolff; Phys. Rev. Lett. **56**, 777 (1986).

[51] M. Gesh, K. Kusakabe, H. Tsukamato and N. Suzuki, in *proceedings of the* 27^{th} *International Conference on the Physics of Semiconductors*, Flagstaff, Arizona, 2004, edited by J. Menéndez and G. Van de Walle (Melville, New York, 2005), **772**, part A, pp-327.

[52] M. Seike, K. Kommochi, K. Sato, A. Yanase and H. Katayama-Yoshida, in *Proceedings of the* 27^{th} *International Conference on the Physics of Semiconductors*, Flagstaff, Arizona, 2004, edited by J. Menéndez and G. Van de Walle (Melville, New York, 2005), **772**, part A, pp-317.

[53] T. Jungwith, Jairo Sinova, J. Mašek, J. Kučera, A. H. MacDonald, Rev. Mod. Phys. **78**, 809 (2006).

[54] A. O. E. Animalu, 1977, *Intermediate Quanum Theary of Crystalline Solids*, (Englewood cliff, N. J., Printice-Hall, New Jersey).

[55] O. W. Anderson, Phys. Rev. **79**, 350 (1950).

[56] M. A. Scarpula, Yu K. M., Walukiewicz W., Dubon O. D. *Carrier Concentration Dependencies of Magnetization* and *Transport in* $Ga_{1-x}Mn_x)As$ Berkeley, CA94720 (unpublished).

[57] K. S. Burch, D. D. Awschalom and D. N. Basov, cond-mat.mtrl-sci, 2008.

[58] J. De Boeck, R. Oesterholt, A. Van Esh, H. Bender, C. Bruynseraede, C. Van Hoof, and G. Borghs, Appl. Phys. Lett. **68** (19) (1996).

[59] T. Hayashi, M. Tanaka, T. Nishinaga, and H. Shimada, J. Appl. Phys. 81, 4865 (1997).

[60] J. Mašek, J. Kudrnovsk$y$, and F. M$a$ca Phys. Rev. B **67**, 153203 (2003).

[61] K. Y. Wang, R. P. Campion, K. W. Edmonds, M. Sawicki, T. Dietl, C. T. Foxon, and B. L. Gallagher, in *Proceedings of the* 27^{th} *International Conference on the Physics of Semiconductors*, Flagstaff, Arizona, 2004, edited by J. Menéndez and G. Van de Walle (Melville, New York, 2005), **772**, part A, pp-333.

[62] V. K. Dugaev, V. I. Litvinov, J. Barnas, A. H. Slobodskyy, W. Dobrowolskyi and M. Vieira, J. Supper., **16** (1), (2003).

[63] J. K$\ddot{o}$nig, H. H. Lin and A. H. MacDonald, Phys. Rev. Lett. 84, 5628 (2000).

[64] B. Le , Xvier Cartoix$\grave{a}$, Nandini Trivedi, and Richard M. Martin, Phys. Rev. B**76**, 155208 (2007).

[65] T. Jungwrth, K. Y. Wang, J. Mašek, K. W. Edmonds, J$\ddot{u}$rgen K$\ddot{o}$nig, Jairo Sinova, M. Polini, N. A. Goncharuk, A. H. MacDonald, M. Sawicki, A. W. Rushforth, R. P. Campion, L. X. Zhao, C. T. Foxon, and B. L. Gallagher, Phys. Rev. B **72**, 165204 (2005).

[66] A. Kaminski, V. M. Galitski, and S. Das Sarma, Phys. Rev. B **70**, 115216 (2004).

[67] G. Bouzerar, J. Kudrnovsky, and P. Bruno, Phys. Rev. B **68**, 205311 (2003).

[68] M. Sawicki, European School of Magnetism: *New Experimental Approaches to Magnetism-Constanta*, 2005.

[69] C. Zhou, M. P. Kennett, M. Beriu, and R. N. Bhatt, Cond-mat/0310322 (2003).

[70] M. Berciu and R. N. Bhatt, Phys. Rev. B **66**, 085207 (2002).

[71] G. Bouzerar, EPL, **79**, 57007 (2007).

[72] J. Ferna'ndez-Rossier, c. Piermarocchi, P. Chen, A. H. MacDonald, and L. J. Sham; Phys. Rev. Lett. **93**, 127201 (2004).

[73] H. Munekata, in *Proceedings of the* 27^{th} *International Conference on the Physics of Semiconductors*, Flagstaff, Arizona, 2004, edited by J. Menéndez and G. Van de Walle (Melville, New York, 2005), **772**, part A, p-307.

[74] C. Piermarocchi, pochung chen, L. J. Sham, and D. G. Steel, Phys. Rev. Lett.**89**, 167402 (2002).

[75] G. Tuttle, H. Kroemer, and J. H. English, J. Appl. Phys. 65, 5239 (1989).

[76] T. Dietl, F. Matsukura and H. Ohno, Phys. Rev. B **66**, 033203 (2002).

[77] C. Timm and A. II. MacDonald, Cond-mat/0405484 (2004).

[78] Kashimura, F. Minami and H. Munekata, Phys. Rev. B **69**, 033203 (2004).

[79] A. S. Chakravarty, 1980, *Introduction to the Magnetic properties of solids*, (John Wiley & Son, Calcutta, India).

[80] D. N. Zubarev, Sov. Phys. Usp. **3**, 320 (1960).

[81] C. Kittel, 1987, *Quantum Theory of Solids*, 2nd ed., (Johin Wiley and Sons, Inc., University of California).

[82] M. E. Lines, Phys. Rev. **135**, A1336 (1964).

[83] H. B. Callen, Phys. Rev. **130**, 890 (1963).

[84] C. G. Montgomery, J. I. Krugler and R. M. Stubbs, Phys. Rev. Lett. **25**, 669(1970).

[85] T. Kasuya, Prog. Theoret. Phys. **16**, 45 (1956).

[86] A. H. Mitchell, Phys. Rev. **105**, 1439 (1957).

[87] K. Yosida, Phys. Rev. **106**(5), 893 (1957)

[88] K. P. Sinha and N. Kumar, 1980, *Interaction in Magnetically Ordered Solids*, (Oxford University Press).

[89] D. J. Priour and S. Das Sarma, Phys. Rev. B **73**, 165203 (2006).

[90] D. C. Look, J. Appl. Phys. **70**, 3148 (1991).

[91] S. T. B. Goennenwein, T. Graf, T. Wassner, M. S. Brandt, M. Stutzmann, J. B. Philipp, R.Gross, M. Krieger, K. Z$\ddot{u}$rn, P. Ziemann, A. Koeder, S. Frank, W. Schoch, and A. Waag, Appl. Phys. Lett. **82**(5), 730 (2003).

[92] A. Auerbach, 1994, *Interacting Electrons and Quantum Magnetism*, (Springer, New York).

[93] M. Sperl, A. Singh, U. Wurstbauer, S. K. Das, A. Sharma, M. Hirmer, W. Nolting, C. H. Back, W. Wegscheider, and G. Bayreuther, Phys. Rev. B **77**, 125212 (2008).

[94] S. A. Tarasenko, Phys. Rev. B**72**, 113302 (2005).

[95] K. S. Gavrichev, A. V. Tyurin, M. A. Ryumin, A. V. Khoroshilov, G. D. Nipan, V. A. Ketsko, T. N. Koltsova, I. Yu. Pinus, G. A. Buzanov, and N. A. Votinova, Russian Journal of Inorganic Chemistry, **54** (1), 1 (2009)

[96] A. Twardowski, H. J. M. Swagten, W. J. M. de Jonge and M. Demianiuk, Phys. Rev. B **44**, 2220 (1991).

[97] Chernet Amente and P. Singh, 2009, *Photo-induced Ferromagnetism in Diluted Magnetic Semiconductor (Ga,Mn)As*, a paper presented on MMSETLSA-2009, Department of Physics, Allahabad university, (Allahabad, India).

[98] Chernet Amente and P. Singh, 2009, *Photo-excitation Enhanced Magnetization of the Diluted Magnetic Semiconductor* (Ga_{1-x}, Mn_x)*As*, a paper presented on MMSETLSA-2009, Department of Physics, Allahabad university, (Allahabad, India).

[99] M. Schmidt, R. Kusche, T. Hippler, J. Donges, W. Kronmüller, B. vonIssendorff, and H. Haberland, Phy. Rev. Lett. **86**, 1191 (2001).

APPENDIX

A

Appendix

A.1 Evaluation of Cauchy Principal value

From Eq. (3.2. 18),

$$\int_0^\infty d^3k' \frac{e^{-i\mathbf{k}'\cdot\mathbf{R}_{nm}}}{k^2-k'^2} = \int_0^{2\pi} d\varphi \int_0^\pi sin\theta d\theta \int_0^\infty dk' k'^2 \frac{e^{-i\mathbf{k}'\cdot\mathbf{R}_{nm}}}{k^2-k'^2} \tag{A.1. 1}$$

or

$$\int_0^\infty d^3k' \frac{e^{-i\mathbf{k}'\cdot\mathbf{R}_{nm}}}{k^2-k'^2} = 2\pi \int_0^\pi sin\theta d\theta \int_0^\infty dk' k'^2 \frac{e^{-ik'R_{nm}cos\theta}}{k^2-k'^2}. \tag{A.1. 2}$$

Let $t = cos\theta$. By differentiation, $dt = -sin\theta d\theta$. This leads to

$$\begin{aligned}\int_0^\infty d^3k' \frac{e^{-i\mathbf{k}'\cdot\mathbf{R}_{nm}}}{k^2-k'^2} &= 2\pi \int_{-1}^1 dt \int_0^\infty dk' k'^2 \frac{e^{-ik'R_{nm}t}}{k^2-k'^2} \\ &= \frac{-2\pi}{iR_{nm}}\left[\int_0^\infty dk' k' \frac{e^{-ik'R_{nm}}}{k^2-k'^2} - \int_0^\infty dk' k' \frac{e^{ik'R_{nm}}}{k^2-k'^2}\right].\end{aligned} \tag{A.1. 3}$$

To solve this equation we require Cauchy Principal value $\wp$, contour integration. Let $\rho = k'R_{nm}$, $k' = \rho/R_{nm}$ and $d\rho = dk'R_{nm}$; and $\sigma = kR_{nm}$, $k = \sigma/R_{nm}$. Substituting into Eq. (A.1. 3),

$$\begin{aligned}\int_0^\infty d^3k' \frac{e^{-i\mathbf{k}'\cdot\mathbf{R}_{nm}}}{k^2-k'^2} &= \frac{-2\pi}{iR_{nm}}\wp\left[\int_0^\infty d(\rho/R_{nm})(\rho/R_{nm}) \frac{e^{-i\rho}}{(\sigma/R_{nm})^2-(\rho/R_{nm})^2}\right. \\ &\quad \left. - \int_0^\infty d(\rho/R_{nm})(\rho/R_{nm}) \frac{e^{i\rho}}{(\sigma/R_{nm})^2-(\rho/R_{nm})^2}\right] \\ &= \frac{-2\pi}{iR_{nm}}\wp\left[\int_0^\infty d\rho\rho \frac{e^{-i\rho}}{\sigma^2-\rho^2} - \int_0^\infty d\rho\rho \frac{e^{i\rho}}{\sigma^2-\rho^2}\right].\end{aligned} \tag{A.1. 4}$$

This can be written in a simplified form as,

$$\int_0^\infty d^3k' \frac{e^{-i\mathbf{k}'\cdot\mathbf{R}_{nm}}}{k^2-k'^2} = \frac{-2\pi}{iR_{nm}}\wp[I_1+I_2]. \tag{A.1. 5}$$

For the integral I_1 the exponent is negative and we complete the contour by an infinite semicircle in the lower half-plan, where

$$I_1 = \int_0^\infty d\rho\rho \frac{e^{-i\rho}}{\sigma^2-\rho^2} = -\frac{1}{2}\int_{-\infty}^\infty d\rho\rho \frac{e^{-i\rho}}{(\rho-\sigma)(\rho+\sigma)} \tag{A.1. 6}$$

and can be written as

$$I_1 = -\frac{1}{2} lim_{\rho\to\infty}\left[\int_\Gamma d\rho\rho \frac{e^{-i\rho}}{\sigma^2-\rho^2} + \int_\rho^{-\rho} d\rho\rho \frac{e^{-i\rho}}{(\rho-\sigma)(\rho+\sigma)}\right]. \tag{A.1. 7}$$

But the first term in the right hand side of Eq. (A.1. 7) is zero by **Jordan's Lemma**, where $1/\rho \to 0$ as $\rho \to \infty$. Hence,

$$I_1 = \frac{1}{2} lim_{\rho\to\infty}\int_{-\rho}^{\rho} d\rho\rho \frac{e^{-i\rho}}{(\rho-\sigma)(\rho+\sigma)}. \tag{A.1. 8}$$

Considering poles at, $\rho=\sigma$ and $\rho=-\sigma$,

$$\begin{aligned} I_1 &= \frac{2\pi i}{2}\Sigma R^- \\ &= (\pi i) lim_{\rho=\sigma}(\rho-\sigma)\rho\frac{e^{-i\rho}}{(\rho-\sigma)(\rho+\sigma)} + (\pi i) lim_{\rho=-\sigma}(\rho+\sigma)\rho\frac{e^{-i\rho}}{(\rho-\sigma)(\rho+\sigma)}. \end{aligned} \tag{A.1. 9}$$

This implies that,

$$I_1 = \pi i\sigma\frac{e^{-i\sigma}}{(2\sigma)} + \pi i(-\sigma)\frac{e^{i\sigma}}{(-2\sigma)} \tag{A.1. 10}$$

or

$$I_1 = \pi i[\frac{e^{-i\sigma}}{2} + \frac{e^{i\sigma}}{2}]. \tag{A.1. 11}$$

Which becomes,

$$I_1 = \pi i cos\sigma = \pi i cosk R_{nm}. \tag{A.1. 12}$$

Similarly solving for integral I_2, where the exponent is positive and requiring completing the contour by an infinite semicircle in the upper half-plan,

$$I_2 = \pi i cos\sigma = \pi i cosk R_{nm}. \tag{A.1. 13}$$

Substituting Eq. (A.1. 12) and (A.1. 13) into Eq. (A.1. 5),

$$\int_0^\infty d^3k' \frac{e^{-i\mathbf{k}'\cdot\mathbf{R}_{nm}}}{k^2 - k'^2} = \frac{-2\pi}{iR_{nm}} \wp[2\pi i cosk R_{nm}], \tag{A.1. 14}$$

where the principal value of the last equation is

$$\wp[2\pi i cosk R_{nm}] = \frac{1}{2} 2[\pi i cosk R_{nm}] = \pi i cosk R_{nm}. \tag{A.1. 15}$$

A.2 Integrating on fermi surface

Eq. (3.2. 24) will be integrated as follows:

Let $t = cos\theta$ and $dt = -sin\theta d\theta$ as before.

$$E^{(2)} = -\frac{2\pi m^* 4x J^2}{(2\pi)^3 (4\pi R_{nm}) N^2} \sum_{nm} \int_0^{k_F} dk k^2 cosk R_{nm} \int_{-1}^{1} dt e^{ikR_{nm}t} \mathbf{S}_n \cdot \mathbf{S}_m, \tag{A.2. 1}$$

which can be written as

$$E^{(2)} = -\frac{2\pi m^* 4x J^2}{(2\pi)^3 4\pi R_{nm} N^2} \sum_{nm} \int_0^{k_F} dk \frac{k^2}{ikR_{nm}} cosk R_{nm} \left[e^{ikR_{nm}} - e^{-ikR_{nm}} \right] \mathbf{S}_n \cdot \mathbf{S}_m. \tag{A.2. 2}$$

The last expression is simplified to

$$E^{(2)} = -\frac{4m^* x J^2}{R_{nm}^2 N^2 (2\pi)^3} \sum_{nm} \int_0^{k_F} dk k (cosk R_{nm} sink R_{nm}) \mathbf{S}_n \cdot \mathbf{S}_m. \tag{A.2. 3}$$

But $cosk R_{nm} sink R_{nm} = \frac{1}{2} sin2k R_{nm}$.

This implies that

$$E^{(2)} = -\frac{4m^* x J^2}{2R_{nm}^2 N^2 (2\pi)^3} \sum_{nm} \int_0^{k_F} dk [k sin(2k R_{nm})] \mathbf{S}_n \cdot \mathbf{S}_m. \tag{A.2. 4}$$

Let $y = 2kR_{nm}$ and $dy = 2R_{nm}dk$. Eq. (A.2. 4) becomes

$$E^{(2)} = -\frac{4m^* x J^2}{8R_{nm}^4 N^2 (2\pi)^3} \sum_{nm} \int_0^{2k_F R_{nm}} dy\, y sin y \mathbf{S}_n \cdot \mathbf{S}_m \tag{A.2. 5}$$

or

$$E^{(2)} = \frac{4m^* x J^2}{8R_{nm}^4 N^2 (2\pi)^3} \sum_{nm} (ycosy - siny) \mathbf{S}_n \cdot \mathbf{S}_m, \tag{A.2. 6}$$

Where $\int ysinydy = siny - ycosy$.

A.3 The Curie Temperature, T_c

The Magnetization

Assuming that the orbital angular momentum is zero ($\mathbf{L} = 0$, the phenomena of the quenching of orbital angular momentum), energy of a system in a magnetic field **H** is

$$E = -\mu \cdot \mathbf{H} \tag{A.3. 1}$$

or

$$E = -g\mu_B m_S H, \tag{A.3. 2}$$

where m_S is spin quantum number and **H** is total effective field.

On the other hand, the resultant magnetization for density of Mn_{Ga} in $(Ga_{1-x}Mn_x)As$ N_{Mn}, is given by

$$M = N_{Mn} g\mu_B \frac{\sum_{-S}^{+S} m_S e^{\frac{g\mu_B m_S H}{k_B T}}}{\sum_{-S}^{+S} e^{\frac{g\mu_B m_S H}{k_B T}}} \tag{A.3. 3}$$

which can be simplified to

$$M = N_{Mn} \mu_m B_S \left(\frac{\mu_m H}{k_B T} \right) \tag{A.3. 4}$$

where $B_S(\frac{\mu_m H}{k_B T})$ is the Brillouin function, and $\mu_m = g\mu_B S$.

Let $x = \frac{\mu_m H}{k_B T}$, hence, (A.3. 4) will be written as

$$B_S(x) = \frac{2S+1}{2S} coth \frac{2S+1}{2S} x - \frac{1}{2S} coth \frac{x}{2S}. \tag{A.3. 5}$$

Remark: For $y \ll 1$,

$$cothy = \frac{1}{y} + \frac{y}{3} - \frac{y^3}{3} + \dots . \tag{A.3. 6}$$

When $y = \frac{2S+1}{2S}x$,

$$coth\left(\frac{2S+1}{2S}x\right) = \frac{2S}{(2S+1)x} + \frac{2S+1}{3(2S)}x. \tag{A.3. 7}$$

when $y = \frac{x}{2S}$,

$$coth\left(\frac{x}{2S}\right) = \frac{2S}{x} + \frac{x}{3(2S)} \tag{A.3. 8}$$

Substituting Eq. (A.3. 7) and (A.3. 8) in to Eq. (A.3. 5),

$$B_S(x) = \frac{2S+1}{2S}\left(\frac{2S}{(2S+1)x} + \frac{2S+1}{3(2S)}x\right) - \frac{1}{2S}\left(\frac{2S}{x} + \frac{x}{3(2S)}\right). \tag{A.3. 9}$$

Considering extreme case where $x << 1$,

$$B_S(x) = \frac{x}{3S}(S+1). \tag{A.3. 10}$$

Substituting Eq. (A.3. 10) in (A.3. 4),

$$M = \frac{N_{Mn}\mu_m^2}{3Sk_BT}(S+1)H \tag{A.3. 11}$$

or

$$M = \frac{N_{Mn}g^2\mu_B^2}{3k_BT}S(S+1)H. \tag{A.3. 12}$$

The Susceptibility

The interionic forces are not necessarily magnetic; in fact, they are electrostatic in nature, giving rise to "exchange" interactions, which are generally responsible for the development of the internal field. The total effective field, therefore, is the sum of the applied magnetic field (H_{app}) and the internal field (H_{int}). Thus,

$$H = H_{app} + H_{int}. \tag{A.3. 13}$$

Substituting the last Eq. (A.3. 13) into (A.3. 12),

$$M = \frac{N_{Mn} g^2 \mu_B^2}{3 k_B T} S(S+1)(H_{app} + H_{int}), \tag{A.3. 14}$$

Where $H_{int} = \gamma M$, and γ is the molecular field constant which upon substituting into Eq. (A.3. 14) gives,

$$M = \frac{N_{Mn} g^2 \mu_B^2}{3 k_B T} S(S+1)(H_{app} + \gamma M). \tag{A.3. 15}$$

From the last expression we can find the susceptibility χ as the ratio of magnetization and the applied field,

$$\begin{aligned} \chi &= \frac{M}{H_{app}} \\ &= \frac{N_{Mn} g^2 \mu_B^2}{3 k_B T} S(S+1) \left(\frac{H_{app}}{H_{app}} + \gamma \frac{M}{H_{app}} \right) \\ &= \frac{C}{T}(1 + \gamma\chi), \end{aligned} \tag{A.3. 16}$$

where

$$C = \frac{N_{Mn} g^2 \mu_B^2 S(S+1)}{3 k_B} \tag{A.3. 17}$$

is the so called Curie constant. From Eq. (A.3. 16) the susceptibility could be obtained, hence,

$$\chi = \frac{C}{T - \gamma C}. \tag{A.3. 18}$$

From the last expression,

$$\gamma C = T_C \tag{A.3. 19}$$

is the Weiss constant and it is from which we find the transition temperature T_c knowing the molecular field constant γ.

The Molecular Field Constant, γ

Consider two interacting atoms or ions. Their resultant exchange energy is determined by the resultant spin moments of the ions, S_n and S_m, if localized at sites n and m. Following Heisenberg exchange Hamiltonian

$$E_{ex} = -\sum_{n \neq m} J_{nm} < \mathbf{S}_n \cdot \mathbf{S}_m >, \tag{A.3. 20}$$

where J_{nm} is an average exchange integral for the overlapping ions.

In the nearest neighbor (n.n) approximation, if the n^{th} magnetic ion interacts equally with each of Z nearest neighbors, situated at the m^{th} site with spin moments S_m, the total exchange energy is given by

$$E_{ex} = -J_{nm} \sum_{m}^{Z} < \mathbf{S}_n \cdot \mathbf{S}_m >, \tag{A.3. 21}$$

where the summation is over Z neighbors.

If **p** is the dipole moment of the Z neighbors, then, assuming that only the spin contributes to the magnetic moments, we have

$$\mathbf{p} = g\mu_B \sum_{m}^{Z} \mathbf{S}_m, \tag{A.3. 22}$$

which gives,

$$\sum_{m}^{Z} S_m = \frac{\mathbf{p}}{g\mu_B} \tag{A.3. 23}$$

where g is the landé g-factor, which is assumed to be the same for all Z neighbors.

Substituting Eq. (A.3. 22) into Eq. (A.3. 21), we have

$$E_{ex} = \frac{-J_{nm}}{g\mu_B} < \mathbf{S}_n \cdot \mathbf{p} > . \tag{A.3. 24}$$

Let the magnetic moment of the n^{th} ion be

$$\mu_n = g\mu_B \mathbf{S}_n, \tag{A.3. 25}$$

hence,

$$\mathbf{S}_n = \frac{\mu_n}{g\mu_B}. \tag{A.3. 26}$$

Substituting Eq. (A.3. 26) in (A.3. 24),

$$E_{ex} = \frac{-J_{nm}}{g\mu_B}\frac{1}{g\mu_B} < \mu_n \cdot \mathbf{p} > . \tag{A.3. 27}$$

The intensity of magnetization **M**, in which all N magnetic lattice points in the sample are likely occupied by impurity ions is given by

$$M = \frac{N\overline{p}}{Z}, \tag{A.3. 28}$$

where $\overline{p}$ is the average of **p** over all groups of Z ions in unit volume.

Assuming no fluctuation of **p** from point to point, we may replace $\overline{p}$ by **p** and thus have

$$M = \frac{N\mathbf{p}}{Z} \tag{A.3. 29}$$

or

$$\mathbf{p} = \frac{Z\mathbf{M}}{N}. \tag{A.3. 30}$$

$$\begin{aligned} E_{ex} &= \frac{-J_{nm}}{g^2\mu_B^2} < \mu_n \cdot \mathbf{p} > \\ &= \frac{-ZJ_{nm}}{Ng^2\mu_B^2} < \mu_n \cdot \mathbf{M} > . \end{aligned} \tag{A.3. 31}$$

Following (A.3. 2),

$$\mathbf{E}_{ex} = -\mu_n.\mathbf{H}_{int} \tag{A.3. 32}$$

and

$$\mathbf{H}_{int} = \gamma\mathbf{M}, \tag{A.3. 33}$$

so that eq. (A.3. 31) becomes,

$$\mathbf{E}_{ex} = -\mu_n\gamma\mathbf{M} = \frac{-ZJ_{nm}}{Ng^2\mu_B^2} < \mu_n \cdot \mathbf{M} >, \tag{A.3. 34}$$

which implies that

$$\gamma = \frac{ZJ_{nm}}{Ng^2\mu_B^2}, \tag{A.3. 35}$$

which is the required molecular field constant.

B

Appendix

B.1 Interaction of radiation with magnons

Expression (4.2. 3) can be written in terms of the Holstien-Primakoff transformation from the atomic creation and annihilation operators a_i^+, a_i with the Fourier transforms to the magnon variables b_k^+ and b_k. Replacing the spin with boson creation and annihilation operators is required in transforming the spin problem to a many-body interaction. The significance of using fourier variables arises due to the fact that spin deviations are not localized to a particular site but propagates throughout the lattice. Now this spin operator will be written as

$$S_x = \sqrt{\frac{S}{2N}} \sum_{m,k} \left(b_k e^{-i\mathbf{k}\cdot\mathbf{r}_m} + b_k^+ e^{i\mathbf{k}\cdot\mathbf{r}_m} \right), \tag{B.1. 1}$$

where for spins at site m,

$$S^+ \cong (2S)^{\frac{1}{2}} a_m = \left(\frac{2S}{N}\right)^{\frac{1}{2}} \sum_k e^{-i\mathbf{k}\cdot\mathbf{r}_m} b_k \tag{B.1. 2}$$

and

$$S^- \cong (2S)^{\frac{1}{2}} a_m^+ = \left(\frac{2S}{N}\right)^{\frac{1}{2}} \sum_k e^{i\mathbf{k}\cdot\mathbf{r}_m} b_k^+. \tag{B.1. 3}$$

Substituting Eq. (4.2. 2) and (B.1. 1) into Eq. (4.2. 1),

$$H_I = ig\mu_B \sum_{m,q,k} \left(\frac{S\hbar c}{4N\mu_0 qV}\right)^{\frac{1}{2}} (\mathbf{q}\times\hat{\mathbf{e}_q})\left(\hat{d}_q e^{i\mathbf{q}\cdot\mathbf{r}_m} - \hat{d_q}^{+} e^{-i\mathbf{q}\cdot\mathbf{r}_m}\right)\left(b_k e^{-\mathbf{k}\cdot\mathbf{r}_m} + b_k^{+} e^{i\mathbf{k}.\mathbf{r}_m}\right), \tag{B.1. 4}$$

which is the energy of interaction of the system. Making rearrangements,

$$\begin{aligned} H_I = ig\mu_B \sum_{m,q,k} \left(\frac{S\hbar c}{4N\mu_0 qV}\right)^{\frac{1}{2}} (\mathbf{q}\times\hat{\mathbf{e}_q})\Big[d_q b_k e^{-i(\mathbf{k}-\mathbf{q})\cdot\mathbf{r}_m} \\ - d_q^{+} b_k e^{-i(\mathbf{k}+\mathbf{q})\cdot\mathbf{r}_m} + d_q b_k^{+} e^{i(\mathbf{k}+\mathbf{q})\cdot\mathbf{r}_m} - d_q^{+} b_k^{+} e^{i(\mathbf{k}-\mathbf{q})\cdot\mathbf{r}_m}\Big]. \end{aligned} \tag{B.1. 5}$$

The first and the last terms in Eq. (B.1. 5) are ignored assuming that photon and magnon can not be created or destroyed at the same time. Therefore, the interaction Hamiltonian will became

$$H_I = ig\mu_B \sum_{m,q,k} \left(\frac{S\hbar c}{4N\mu_0 qV}\right)^{\frac{1}{2}} (\mathbf{q}\times\hat{\mathbf{e}_q})\left[d_q b_k^{+} e^{i(\mathbf{k}+\mathbf{q})\cdot\mathbf{r}_m} - d_q^{+} b_k e^{-i(\mathbf{k}+\mathbf{q})\cdot\mathbf{r}_m}\right] \tag{B.1. 6}$$

Following the transversality condition, $|\mathbf{q}\times\hat{\mathbf{e}}| = q$. Hence, Eq. (B.1. 6) will be written $(\hbar = 1)$ as,

$$H_I = ig\mu_B \sum_{q,k} \left(\frac{Scq}{4\mu_0 V}\right)^{\frac{1}{2}} \left[d_q b_k^{+}\delta(\mathbf{k}+\mathbf{q}) - d_q^{+} b_k \delta(\mathbf{k}+\mathbf{q})\right]. \tag{B.1. 7}$$

The $\delta(\mathbf{k}+\mathbf{q}) = 1$ when $\mathbf{q} = -\mathbf{k}$ and zero otherwise which shows that the magnon and the photon propagate in opposite directions where there be a resonance. However, the last expression has no hermitian conjugate and fall short of describing the photon-magnon interaction energy. Therefore, taking one of the terms in the right hand side gives required standard model. Hence, considering the positive contribution of the last expression only, Eq. (B.1. 7) reduces to

$$H_I = \sum_k \chi_k \left[d_{-k}^{+} b_k + h.c\right], \tag{B.1. 8}$$

where $\chi_k = g\mu_B\left(\frac{\mu_0 Sck}{4V}\right)^{\frac{1}{2}}$ is the momentum dependent coupling constant responsible for the changes that may result during the interaction process. This final result, Eq. (B.1. 8), will be the interaction Hamiltonian used in **chapter 5**.

C

Appendix

C.1 Magnon Dispersion

Solving for ϵ_k and making rearrangements Eq. (5.3. 29) gives

$$\epsilon_k = \frac{\lambda_{-k} + \omega'_k}{2} \pm \frac{1}{2}\sqrt{\lambda^2_{-k} + \omega'^2_k + 4\chi^2_k - 2\lambda_{-k}\omega'_k}. \tag{C.1. 1}$$

However, for $\omega'^2_k - 2\lambda_{-k}\omega'_k << \lambda^2_{-k} + 4\chi^2_k$, Eq. (C.1. 1) reduces to

$$\epsilon_k \cong \frac{\lambda_{-k} + \omega_k{}'}{2} \pm \frac{1}{2}\sqrt{\lambda^2_{-k} + 4\chi^2_k}. \tag{C.1. 2}$$

Restoring ω'_k, λ_{-k} and χ_k,

$$\epsilon_k = \frac{-ck + x2JSa^2(1 - \Omega_0 T^{5/2})k^2}{2} \pm \frac{1}{2}\sqrt{c^2k^2 + \frac{g^2\mu_\beta^2\mu_0 Sck}{V}}. \tag{C.1. 3}$$

where

$$\Omega_0 = \frac{a^2}{3SN}\frac{0.45\kappa_B^{5/2}}{\pi^2(2xSJ_{nm}a^2)^{5/2}}$$

and N is the number of lattice sites

It is usual and seek of convenience to consider the sum, so that

$$\epsilon_k = \frac{-ck + x2JSa^2(1 - \Omega_0 T^{5/2})k^2}{2} + \frac{1}{2}\sqrt{c^2k^2 + \frac{g^2\mu_\beta^2\mu_0 Sck}{V}} \tag{C.1. 4}$$

Let us make denotations, $A = 2xJSa^2(1-\Omega_0 T^{5/2})$, and $B = \frac{g^2\mu_\beta^2\mu_0 S}{Vc}$. Therefore, from the last equation,

$$\epsilon_k = \frac{1}{2}(Ak^2 - ck + c\sqrt{k^2+Bk}). \tag{C.1. 5}$$

The term under radical can be written as,

$$\sqrt{k^2+Bk} = \sqrt{\left(k+\frac{B}{2}\right)^2 - \frac{B^2}{4}}, \tag{C.1. 6}$$

where the term $\frac{B^2}{4}$ is so small that we can neglect. Hence, Eq. C.1. 6 becomes,

$$\sqrt{k^2+Bk} \cong \sqrt{\left(k+\frac{B}{2}\right)^2} = k+\frac{B}{2}. \tag{C.1. 7}$$

Substituting Eq. (C.1. 7) into (C.1. 5)

$$\epsilon_k \simeq \frac{1}{2}Ak^2 + \frac{cB}{4}, \tag{C.1. 8}$$

and finally,

$$\epsilon_k \simeq D'k^2 + B'. \tag{C.1. 9}$$

where $D' = 0.5A$ and $B' = \frac{cB}{4}$

C.2 Calculating total number of magnons

To complete the integration in expression Eq. (5.4. 10) it requires making denotation for the terms in the exponential of the denominator.

Let

$$u = D'\beta k^2 + \beta B'. \tag{C.2. 1}$$

$du = 2D'\beta k dk$, where $k^2 = \frac{1}{D'\beta}(u-\beta B')$ and $k = [\frac{1}{D'\beta}(u-\beta B')]^{\frac{1}{2}}$

Substituting the last expressions into Eq. (5.4. 10),

$$2\pi^2 \sum_k < n_k >= \frac{1}{2(D'\beta)^{\frac{3}{2}}} \int_{-\beta B'}^{\infty} \frac{(u-\beta B')^{\frac{1}{2}}}{e^u - 1} du, \tag{C.2. 2}$$

which i.e,

$$2\pi^2 \sum_k < n_k >= \frac{1}{2(D'\beta)^{\frac{3}{2}}} \int_{-\beta B'}^{0} \frac{(u - \frac{\beta B'}{2})^{\frac{1}{2}}}{e^u - 1} du + \frac{1}{2(D'\beta)^{\frac{3}{2}}} \int_0^{\infty} \frac{(u - \beta B')^{\frac{1}{2}}}{e^u - 1} du. \quad \text{(C.2. 3)}$$

Since the contribution from the first term of the right hand side of the last expression is negligible we work out with

$$2\pi^2 \sum_k < n_k >= \frac{1}{2(D'\beta)^{\frac{3}{2}}} \int_0^{\infty} \frac{(u - \beta B')^{\frac{1}{2}}}{e^u - 1} du. \quad \text{(C.2. 4)}$$

Expanding the term in the numerator $(u - \beta B')^{\frac{1}{2}}$ where $\beta B'$ is very small,

$$\begin{aligned} f\bigg(u + (-\beta B')\bigg) &= \bigg(u - \beta B'\bigg)^{\frac{1}{2}} \\ &= f(u) - \beta B' f'(u) + \frac{1}{2!}\bigg(-\beta B'\bigg)^2 f''(u) + \frac{1}{3!}\bigg(-\beta B'\bigg)^3 f'''(u) \\ &+ \frac{1}{4!}\bigg(-\beta B'\bigg)^4 f''''(u) + ..., \end{aligned} \quad \text{(C.2. 5)}$$

or

$$f\bigg(u - \beta B'\bigg) = u^{\frac{1}{2}} - \beta B' u^{\frac{-1}{2}} - \frac{1}{8}(\beta B')^2 u^{\frac{-3}{2}} - \frac{1}{16}(\beta B')^3 u^{\frac{-5}{2}} - \dots . \quad \text{(C.2. 6)}$$

Substituting the first two terms of the Eq. (C.2. 6) into (C.2. 4),

$$\sum_k < n_k >= \frac{1}{4\pi^2 (D'\beta)^{\frac{3}{2}}} \int_0^{\infty} \frac{u^{\frac{1}{2}}}{e^u - 1} du - \frac{\beta B'}{4\pi^2} \frac{1}{(D'\beta)^{\frac{3}{2}}} \int_0^{\infty} \frac{u^{\frac{-1}{2}}}{e^u - 1} du. \quad \text{(C.2. 7)}$$

The indefinite integrals are taken approximately, as $\int_0^{\infty} \frac{u^{\frac{1}{2}}}{e^u - 1} du \simeq 2.3134$ and $\int_0^{\infty} \frac{u^{\frac{-1}{2}}}{e^u - 1} du \simeq 3542.3$, so that Eq. (C.2. 7) can be written as

$$\sum_k < n_k >= \frac{1}{4\pi^2 (D'\beta)^{\frac{3}{2}}} \times 2.3134 - \frac{\beta B'}{4\pi^2} \frac{1}{(D'\beta)^{\frac{3}{2}}} \times 3542.3. \quad \text{(C.2. 8)}$$

NB: The integrals are solved based on the general expression given by

$$\int_0^{\infty} \frac{x^{n-1}}{e^x - 1} dx = \Gamma(n)\bigg(\frac{1}{1^n} + \frac{1}{2^n} + \frac{1}{3^n} + ...\bigg), \quad \text{(C.2. 9)}$$

where $\Gamma(n)$ is a Gamma function, n is $\frac{3}{2}$ and $\frac{1}{2}$ for each of expressions in (C.2. 7), respectively.

C.3 Calculation of Magnon Energy

The integration in expression Eq. (5.6. 3) is completed starting with differentiating Eq. (C.1. 9) with respect to k. Hence,

$$d\epsilon_k = 2D'kdk \tag{C.3. 1}$$

and

$$dk = \frac{d\epsilon_k}{2D'[\frac{1}{D'}(\epsilon_k - B')]^{\frac{1}{2}}}, \tag{C.3. 2}$$

where

$$k = \left[\frac{1}{D'}\left(\epsilon_k - B^{'}\right)\right]^{\frac{1}{2}}. \tag{C.3. 3}$$

Using the last expression we can find the internal energy of the magnon system as

$$U = \frac{1}{4\pi^2 D'^{3/2}} \int_0^\infty \frac{\epsilon_k(\epsilon_k - B^{'})^{1/2}}{e^{\beta\epsilon_k} - 1} d\epsilon_k. \tag{C.3. 4}$$

Expanding the term $(\epsilon_k - B^{'})^{1/2}$ where $B^{'}$ is very small as indicated above,

$$\left(\epsilon_k - B^{'}\right)^{1/2} = \epsilon_k^{1/2} - \frac{1}{2}B'\epsilon_k^{-1/2} - \dots . \tag{C.3. 5}$$

Taking the first two terms of the expansion and substituting into Eq. (C.3. 4),

$$\begin{aligned} U &= \frac{1}{4\pi^2 D'^{3/2}} \int_0^\infty \frac{\epsilon_k(\epsilon_k^{1/2} - \frac{1}{2}B'\epsilon_k^{-1/2})}{e^{\beta\epsilon_k} - 1} d\epsilon_k \\ &= \frac{1}{4\pi^2 D'^{3/2}} \left[\int_0^\infty \frac{\epsilon_k^{3/2}}{e^{\beta\epsilon_k} - 1} d\epsilon_k - \frac{B'}{2}\int_0^\infty \frac{\epsilon_k^{1/2}}{e^{\beta\epsilon_k} - 1} d\epsilon_k\right]. \end{aligned} \tag{C.3. 6}$$

Let $y = \beta\epsilon_k \Rightarrow \epsilon_k = \frac{1}{\beta}y$. Substituting in Eq. (C.3. 6)

$$U = \frac{1}{4\pi^2 D'^{3/2}\beta^{5/2}} \int_0^\infty \frac{y^{3/2}}{e^y - 1} dy - \frac{B'}{16\pi^2 D'^{3/2}\beta^{3/2}} \int_0^\infty \frac{y_k^{1/2}}{e^y - 1} dy, \tag{C.3. 7}$$

where,

$$\int_0^\infty \frac{y^{3/2}}{e^y-1}dy \simeq 1.7995367 \qquad (a)$$

and

$$\int_0^\infty \frac{y^{1/2}}{e^y-1}dy \simeq 2.3134. \qquad (b)$$

Therefore,

$$U = \frac{1.7995367}{4\pi^2 D'^{3/2}\beta^{5/2}} - \frac{B'(2.3134)}{16\pi^2 D'^{3/2}\beta^{3/2}}, \qquad \text{(C.3. 8)}$$

in which $\beta = \frac{1}{k_B T}$,

substituting for β in Eq. (C.3. 8),

$$\begin{aligned} U &= \frac{1.7995367 k_B^{5/2} T^{5/2}}{4\pi^2 D'^{3/2}} - \frac{\frac{g^2\mu_B^2 S}{2\mu_0 V}(2\times 2.3134)k_B^{3/2}T^{3/2}}{32\pi^2 D'^{3/2}} \\ &= \frac{\sqrt{2}\times 0.0912 k_B^{5/2} T^{5/2}}{A^{3/2}} - \frac{\frac{g^2\mu_B^2 S}{\mu_0 V}(\sqrt{2}\times 0.01465)k_B^{3/2}T^{3/2}}{A^{3/2}}. \end{aligned} \qquad \text{(C.3. 9)}$$

Finally, in terms of the light-matter coupling constant α,

$$\begin{aligned} U &= \frac{1.7995367 k_B^{5/2} T^{5/2}}{4\pi^2 D'^{3/2}} - \frac{\frac{g^2\mu_B^2 S}{2\mu_0 V}(2\times 2.3134)k_B^{3/2}T^{3/2}}{32\pi^2 D'^{3/2}} \\ &= \frac{0.0456 k_B^{5/2} T^{5/2}}{D'^{3/2}} - \frac{\alpha^2(0.01465)k_B^{3/2}T^{3/2}}{cD'^{3/2}}. \end{aligned} \qquad \text{(C.3. 10)}$$

DECLARATION

I hereby declare that this PhD dissertation is my original work and has not been presented for a degree in any other universities, and that all sources of material used for the dissertation have been duly acknowledged.

Name: Chernet Amente

Signature: ———————————

This PhD dissertation has been submitted to for examination with my approval as university advisor.

Name: Professor P. Singh

Signature: ———————————

Place and date of submission:

Department of Physics

Addis Ababa University

October 2010